



Title	Nuclear magnetic resonance studies on structure and properties of paramagnetic metal ion-polyglutamic acid complex
Author(s)	HIRAOKI, TOSHIFUMI
Citation	北海道大学. 博士(理学) 甲第1368号
Issue Date	1979-03-24
Doc URL	http://hdl.handle.net/2115/29718
Type	theses (doctoral)
File Information	thesis.pdf



[Instructions for use](#)

NUCLEAR MAGNETIC RESONANCE STUDIES
ON
STRUCTURE AND PROPERTIES OF PARAMAGNETIC
METAL ION—POLYGLUTAMIC ACID COMPLEX

TOSHIFUMI HIRAOKI

DISSERTATION
FOR
THE DEGREE OF DOCTOR OF SCIENCE

FACULTY OF SCIENCE
HOKKAIDO UNIVERSITY
SAPPORO, JAPAN

November 1978

CONTENTS

ABSTRACT	iii
Acknowledgements	v
Symbols and Abbreviations	vi
CHAPTER I. Introduction	1
CHAPTER II. Basic Concepts of NMR Parameters	6
CHAPTER III. ¹³ C Nuclear Magnetic Relaxation of Poly(D-glutamic acid)	16
CHAPTER IV. Cu(II)-Poly(D-glutamic acid) Complex	41
CHAPTER V. Mn(II)-Poly(D-glutamic acid) Complex	59
CHAPTER VI. Co(II)- and Ni(II)-Poly(D-glutamic acid) Complexes	80
CHAPTER VII. Conclusion	93

ABSTRACT

^{13}C and water proton nuclear magnetic resonance methods were applied to elucidate the structure and dynamics of the complex of poly(D-glutamic acid) (PGA) and paramagnetic ions (Cu(II), Mn(II), Co(II), and Ni(II)). Chemical shift, spin-lattice relaxation time (T_1), spin-spin relaxation time (T_2), and the nuclear Overhauser enhancement (NOE) of ligand of the complex were measured as functions of pH and temperature.

Molecular motion and the conformation of PGA in the absence of a paramagnetic ion were first investigated by measuring chemical shift, T_1 , and NOE of ^{13}C nuclei. The correlation time of tumbling motion of C_α obtained from T_1 and NOE decreases from 2.8 nsec to 0.65 nsec with the helix-to-coil transition, as a result of the onset of rapid segmental motion. There is a progressive increase in T_1 and NOE of the side chain carbons as going away from the backbone. The correlation time deduced from T_1 indicates that the end of the side chain undergoes more rapid internal reorientation than others in all pH region studied.

Relaxation rates of C_γ and C_δ of PGA and water proton are enhanced by the addition of Cu(II) in the pH region of 4.5 to 8, indicating that carboxyl groups of side chain and water molecules bind to Cu(II). On the other hand, above pH 9 the paramagnetic effects on ^{13}C and water proton NMR were not observed, indicating that the carboxyl group of PGA and water molecules are excluded from Cu(II), and that Cu(II) probably binds to nitrogen atoms of the backbone.

Addition of Mn(II) also caused the enhancement of relaxation rates for C_γ and C_δ carbons and water proton at neutral pH, indicating that carboxyl groups and water proton bind to Mn(II). The number of water molecules in the first coordination sphere of Mn(II) bound to PGA, hyperfine coupling constant of Mn(II)- ^1H , the correlation time, and the activation energies of tumbling motion and exchange for water molecules of the complex were evaluated and compared with those for the hexaquo Mn(II). With decreasing pH, Mn(II) is released from the carboxyl groups and PGA changes its conformation from coil to helix.

Water proton relaxation enhancement reflects the conformational change (the helix-coil transition) of PGA in the case of Mn(II), while it does not in the case of Cu(II). In both complexes of Cu(II) and Mn(II) the spin-lattice relaxation of ^{13}C nuclei caused by the unpaired

electron spin is due to the dipolar interaction, the paramagnetic contribution to ^{13}C spin-spin relaxation is primarily the scalar interaction. The distance between the metal ion and each carbon atom in the ligand was evaluated from the dipolar relaxation term.

In the cases of Co(II) and Ni(II) complexes significant paramagnetic shift and broadening were observed for C_δ , C_γ , and C_β carbons, indicating that metal ions bind to carboxyl groups. Paramagnetic shifts of both complexes show the temperature dependence opposite to Curie's law. This result can be explained in terms of the chemical equilibrium shifting to the direction of formation of the complex.

Acknowledgements

The research works described in this thesis have been made at Polymer Physics Laboratory, Department of Polymer Science, Faculty of Science, Hokkaido University.

I would like to take this opportunity to mention some of many people without whose help this thesis would never have materialized.

It is a genuine pleasure to acknowledge the help of Professor Kunio Hikichi. His advise, encouragement, and interest have helped me immeasurable in seeing this work through. I would like to express my gratitude for suggestion and encouragement received from Professor Motozo Kaneko and Dr. Akihiro Tsutsumi. I also thank other members of Polymer Physics Laboratory, Dr. Norio Matsushima, Dr. Yuji Yamashita, M. Masatoshi Osanai, M. Naoki Sasaki, M. Naoki Higuchi, and B. Shin-ichi Shiwa for valuable discussions.

In addition, I am grateful to Dr. Sigeo Mori of Ajinomoto Co. for kindly providing poly(γ -methyl D-glutamate), to Mr. Sigezo Shimokawa and Mr. Eiji Yamada of NMR Laboratory of Faculty of Engineering for help with operating a Bruker SXP spectrometer, to Professor Michio Yoneyama for help with CD measurements, to Professor Isao Sekikawa of the Research Institute of Immunological Science for giving me the opportunity to use an NMR spectrometer for a preliminary work, to Glass Shop members of Faculty of Science for help with the onerous task of the experimental equipments, and to Miss Toshiko Ōhno and Miss Hiroko Katō for secretarial assistance.

This work was supported in part by a research fellowship from the Japan Society for the Promotion of Science.

Finally, this list would be glaringly incomplete without mentioning my family, whose patience, understanding, and encouragement have helped me to make this work possible.

Sapporo

November 8th, 1978

Toshifumi Hiraoki

Symbols and Abbreviation

The following symbols may appear without explanation in certain parts.

Roman Symbols

A	hyperfine coupling constant
a, b	half lengths of major and minor axes of ellipsoid
D_a, D_b	rotational diffusion constants of major and minor axes of ellipsoid
E_R	activation energy of rotation
E_M	activation energy of chemical exchange
f	concentration ratio of paramagnetic ion to ligand
g	electronic g factor
$g_{ }, g_{\perp}$	components of g along the z axis and the xy-plane
\hbar	Planck's constant divided by 2π
I	I nuclear spin or spin quantum number
$J(\omega)$	spectral density at frequency ω
K	1024 (referring to computer memory) or temperature in Kelvin
K_d	dissociation constant
k	Boltzmann constant
m	unit length of peptide
n	degree of polymerization or number of binding sites per residue
r_o	radius of an equivalent rigid sphere
r	distance
S	spin quantum number
T	absolute temperature
T_1	spin-lattice relaxation time
T_2	spin-spin relaxation time
T_{1o}, T_{2o}	relaxation times of the unbound site
T_{1M}, T_{2M}	relaxation times of the bound site
T_{1p}, T_{2p}	paramagnetic contributions to the relaxation times

Greek Symbols

β	Bohr magneton
$\gamma_I, \gamma_C, \gamma_H$	gyromagnetic ratios of nucleus I, ^{13}C , and proton
δ	chemical shift
ϵ^*	water-proton relaxation enhancement factor
η	viscosity of solvent

θ	angle
$\Delta\nu$	line width
$\Delta\nu_p$	line width contribution due to presence of paramagnetic ion
ρ	axial ratio
$\Delta\sigma_p$	chemical shift due to presence of paramagnetic ion
τ	correlation time
τ_c	dipolar correlation time
τ_{cl}	see Chapter III, eq 3.10
τ_e	scalar correlation time
τ_{eff}	effective correlation time
τ_{int}	correlation time of internal reorientation
τ_M	chemical exchange lifetime
τ_s	electron-spin relaxation time
τ_A, τ_B, τ_C	correlation time (see Chapter III, eq 3.9)
ϕ	angle
ψ	angle
ω	Larmor frequency
$\omega_C, \omega_H, \omega_I, \omega_S$	Larmor frequencies of ^{13}C , proton, nucleus I, and electron.
$\Delta\omega$	observed paramagnetic shift
$\Delta\omega_M$	chemical shift in bound site

Abbreviation

IR	Inversion recovery
NOE	Nuclear Overhauser enhancement
PGA	Poly(D-glutamic acid)
SR	Saturation recovery
TMS	Tetramethylsilane

LITTLE and PIQUANT

CHAPTER I

Introduction

Metal ions participate as essential constituents in many faces of biological structure and functions.¹ Metal ions are frequently involved in production of the highly organized structures. The coordinative properties of metal ions are commonly utilized to bring together two or more reacting components for purpose of biochemical catalysis.

Transition metal ions are characterized by having partially filled d-orbitals. The characteristic electronic configurations of transition metals impart to them chemical properties favoring their biological functions. First, transition elements generally have more than one relatively stable valence state. Thus these metal ions may function in oxidation-reduction processes by undergoing reversible valency changes. Second, metal ions generally form strong complexes only with anions or with the negative end of dipolar molecules, but many transition metal ions, particularly in their lower valencies, can bind O₂, which is an electrically neutral and symmetric molecule. This becomes possible because of the peculiar electronic structure of these ions as well as of O₂. Finally, the complex forming properties of metal ions are profoundly influenced by the chemical nature and spatial arrangement of the ligands, so that a given metal may show a surprising versatility in function.

Polypeptides have been investigated as protein models suitable for examining characteristics of the secondary structure without the complications arising from tertiary structure. Their structures and properties have been studied extensively by many physico-chemical techniques.² Structural features (e.g., α -helix, β -form, random-coil, etc.,) first recognized in synthetic polypeptides were later found to be important elements of protein structure.

The interaction of metal ions with polypeptides has been studied by many physico-chemical techniques.³ Such complexes can be considered as useful models in order to understand the way of action of metalloproteins. Metal ion-polypeptide interaction necessarily differs from those of metal ions with amino acids and small peptides to the extent that the α -NH₂ and α -COOH of polypeptide chains are separated covalently by a number of intervening residues. These interactions also differ because of the

influence of peptide chain conformation which may block reaction at potential metal-binding sites or which may place amino acid side-chains which are distant in sequence in suitable position to form a complex.

Nuclear magnetic resonance (NMR) spectroscopy has been developed during the last 30 years. NMR spectroscopy is unique and a direct observation technique among spectroscopic methods, sharing with X-ray crystallography the ability to yield experimental parameters concerning individual atoms within a molecule. Information relevant to electronic as well as molecular structure, to molecular motion, and to intermolecular interactions can be provided by analyzing NMR parameters such as chemical shift, spin-lattice relaxation time (T_1), spin-spin relaxation time (T_2), and the nuclear Overhauser enhancement (NOE).⁴ Nuclei with non-zero spin that are present in molecules are suitable for this purpose in principle at least: ^1H , ^2D , ^{13}C , ^{14}N , ^{15}N , ^{17}O , ^{23}Na , ^{31}P , etc.

In cases where the metal ion involved in a system is paramagnetic, the presence of the metal ion would be expected to affect the characteristics of NMR of solvent and ligand molecules in the neighborhood of paramagnetic probes. Principle manifestations would be the reduction of nuclear relaxation times and NOE and the introduction of chemical shift displacement. When a ligand (e.g., water or substrate) bound to the paramagnetic ion (or near the ion) is the macromolecule, the relaxation times of nuclei in the ligand will decrease. The magnitude of the decrease depends on the distance of the nucleus from the paramagnetic center, the stoichiometry of the binding, the motional freedom of the ligand, and the time of the ligand's residence in the sphere influence of the paramagnetic center. In some cases kinetic data (ligand exchange rate) and structural information (coordination schemes, number of water ligands, interatomic distance) may be deduced from the magnitude of observed NMR parameters.

The possibilities of obtaining structural and kinetic information in biological system from nuclear relaxation effects caused by paramagnetic ions were first realized for water proton with some metal complexes of DNA by Eisinger, et al.⁵; the binding of several transition metal ions to DNA gave a large enhancement in water relaxation rates in the solvent water. A similar enhancement phenomenon was observed in binary and ternary complexes of proteins with manganese ion and substrates by Cohn and Leigh.⁶ It has been possible to obtain binding parameters and even

to propose various schemes of enzyme mechanisms.⁷ Many subsequent applications of paramagnetic ions in biological system have been presented in several reviews and monographs.⁷⁻¹¹ Little NMR study has been made of the interaction of homopolypeptides with the metal ions,^{12,13} although it would be expected that the results obtained give unequivocal answer compared with the enzyme.

High-resolution ^1H NMR in paramagnetic system encounters certain inherent limitations. First, the relatively narrow range of chemical shifts of protons may combine with the broad lines often found in paramagnetic species to give seriously overlapping proton lines. This situation may prevent one from extracting the separate relaxation parameters for individual proton transition especially when large molecules are studied. Second, protons generally are strongly spin coupled to other magnetic nuclei in the molecules, especially other protons, through the hyperfine interaction and this may unduly complicate the extraction of parameters. Third, protons are often at the periphery in most complexes leading to proton metal distances which are relatively long compared with the corresponding distances between the metal ion and the heavier atoms of the ligand such as C, N, or O. This tends to decrease the contribution of the paramagnetic ion to the relaxation and amplifies the inaccuracies arising from paramagnetic ions in neighboring molecules, particularly when dealing with small ligand molecules and high concentrations of the paramagnetic ions. Finally, in most cases only upper limits of the nuclei-metal distances have been estimated because information on the effect of chemical exchange on the relaxation process is often lacking. As far as water protons are concerned, these difficulties have reduced since water proton having large sensitivity is readily observable.

If ^{13}C nuclei are used, these disadvantages can be eliminated or significantly reduced. The greater chemical shift range for ^{13}C tends to eliminate overlapping lines. Furthermore, proton decoupling usually collapses spin-spin multiplets to singlets leaving the relaxation of the ^{13}C nuclei. ^{13}C nuclei are generally closer to the paramagnetic center than protons and therefore affected greatly.

In this thesis ^{13}C and water proton nuclear magnetic resonance studies for the interaction of several paramagnetic transition ions with poly(D-glutamic acid) (PGA) in aqueous solution were made in order to obtain

fundamental information concerning the relationship between the structure and the dynamics of the complex. Chemical shift, T_1 , T_2 , and NOE of ligand and solvent molecules for the complex were investigated as functions of pH and temperature. Since PGA undergoes the coil-to-helix transition in aqueous solution when pH is lowered,¹⁴ PGA is suitable for studying the relation of the conformational change and metal ions. Paramagnetic ions used in this study are Cu(II), Mn(II), Co(II), and Ni(II). Cu(II) and Mn(II) whose electron-spin relaxation time is relatively long are used as relaxation probes, and Co(II) and Ni(II) whose electron-spin relaxation time is short are used as shift probes.⁸⁻¹¹

Before presenting and discussing experimental results, it will be useful to present briefly the basic concepts of NMR parameters in paramagnetic system which is pertinent to this study. These are described in Chapter II. Chapter III deals with the relationship between molecular motion and conformations of PGA in the absence of paramagnetic ions. Chapter IV is concerned with the Cu(II)-PGA interaction and Chapter V with the Mn(II)-PGA interaction. In Chapter VI the interaction of Co(II) and Ni(II) with PGA is described. Conclusions are summarized in Chapter VII.

REFERENCES

1. G. L. Eichhorn, Ed., "Inorganic Biochemistry", Vol.1 and 2, Elsevier, Amsterdam, 1973.
2. G. D. Fasman, Ed., "Poly- α -amino acids", Marcel Dekker, New York, N.Y., 1967.
3. M. Hatano and T. Nozawa, "Metal-Ions in Biological Systems", Vol. 5, H. Sigel, Ed., Marcel Dekker, 1976, p245, and references therein quoted.
4. A. Abragam, "The Principles of Nuclear Magnetism", Clarendon Press, Oxford, 1961.
5. J. Eisinger, R. G. Shulman, and B. M. Szymansky, J. Chem. Phys., 36, 1721(1962).
6. M. Cohn and J. R. Leigh, Nature, 193, 1037(1962).
7. A. S. Mildvan and M. Cohn, Adv. Enzymol., 33, 1(1970).
8. R. A. Dwek, "Nuclear Magnetic Resonance in Biochemistry", Clarendon Press, Oxford, 1973, chapters 9-11.
9. W. D. Phillips, "NMR of Paramagnetic Molecules", G. N. La Mar, W. D. Horrocks, Jr., and R. H. Holm, Eds., Academic Press, New York, N.Y., 1973, chapter 11.
10. T. J. James, "Nuclear Magnetic Resonance in Biochemistry", Academic Press, New York, N.Y., 1976, chapter 6.
11. K. Wüthrich, "NMR in Biological Research", North-Holland, Amsterdam, 1976, chapter 6.
12. O. Iwaki, K. Hikichi, M. Kaneko, S. Shimizu, and T. Maruyama, Polymer J., 4, 623(1973).
13. R. E. Wasylshen and J. S. Cohen, J. Amer. Chem. Soc., 99, 2480(1977).
14. P. Doty, A. Wada, J. T. Yang, and E. R. Blout, J. Polymer Sci., 23, 851(1957).

CHAPTER II

Basic Concepts of NMR parameters

When a resonance has been resolved and assigned, it may be possible to derive from it the desired structural and dynamic information. In this chapter we define the observable parameters such as chemical shift, spin-lattice relaxation time, spin-spin relaxation time, and the nuclear Overhauser enhancement, which are pertinent to this study in the NMR measurements.

Chemical Shift

The resonance condition for a given nucleus depends not only on the nature of the nucleus but also on its electronic environment. For nuclei of the same isotope, the difference in the resonance condition with chemical environments leads to the concept of a chemical shift. The chemical shift has its origin in the magnetic shielding or screening of the nucleus produced by electrons around it: (1) local diamagnetic effects, (2) diamagnetic and paramagnetic effects from neighboring atoms or ions, (3) effects from interatomic currents. Solvent as well as such specific interactions as molecular association, complex formation, and hydrogen bonding, will also affect chemical shifts.

Chemical shifts in paramagnetic system often largely shift from their corresponding resonance positions in diamagnetic complexes. These shifts arise from the presence of unpaired electrons and can be expressed as the sum of two parts, the contact shift and the pseudo-contact shift. These effects are caused by the interactions of nuclei with the unpaired electron spin.

The contact shift results from the direct interaction of delocalized unpaired electron with nucleus. The delocalization of the unpaired electron spin density provides overlap with the s-orbital of the resonating atom. This electron spin density is usually transmitted through chemical bonds to the nucleus. The shift of nucleus I, $\Delta\omega_M$, is given by¹

$$\frac{\Delta\omega_M}{\omega_I} = - \left(\frac{A}{\hbar} \right) \frac{g\beta S(S+1)}{3kT\gamma_I}, \quad (2.1)$$

where ω_I is the nuclear Larmor angular frequency, A the hyperfine coupling constant between the paramagnetic electron and the observed nuclei, \hbar Planck's constant divided by 2π , g the electronic g factor, β the Bohr magneton, S the electron spin quantum number, γ_I the gyromagnetic ratio of nucleus I , k the Boltzmann constant, and T the absolute temperature. This shift will be proportional to the unpaired electron spin density.

The pseudo-contact (dipolar) shift results from the dipolar interaction between nucleus and electron spin. On the assumption that the g tensor of electron spin is axially symmetric, this shift is given by²

$$\frac{\Delta\omega_M}{\omega_I} = - \frac{\beta^2 S(S+1) (3\cos^2\theta - 1)}{27kr^3} (g_{\parallel} - g_{\perp})(g_{\parallel} + 2g_{\perp}), \quad (2.2)$$

where r is the distance between the metal ion and the nucleus, and θ is the angle between r and the principle axis of symmetry of the complex. The pseudo-contact shift will be determined by the geometry of the complex and the principle values of the g tensor. It is therefore apparent that the pseudo-contact shift can provide valuable information about the orientation and the distance if $(3\cos^2\theta - 1)$ term is separated from r^3 term in eq 2.2. On the other hand the contact shift provides information about the electronic structure of the complex.

Spin-Lattice Relaxation Time and Spin-Spin Relaxation Time

Nuclei in the applied static magnetic field are distributed among the energy levels according to the Boltzmann distribution in equilibrium. If this distribution is disturbed by some means, the nuclear spin system tends to return to its equilibrium with its surrounding ("lattice") by a first-order relaxation process characterized by a time constant T_1 , the spin-lattice relaxation time. There is also another process that causes the nuclear spins to come to equilibrium with each other, having a characteristic time constant T_2 , the spin-spin relaxation time.

The origin of the spin relaxation process is the interaction of the nuclear spin system with fluctuating local fields. These fluctuating

fields are made by neighboring nuclei and the fluctuation is governed by motions of molecules. If the fluctuating magnetic fields have components of the Larmor frequency, they can induce the transition between energy levels and therefore cause spin relaxation. Since the range of relevant frequencies is in the MHz region, fast motions such as electronic motions and molecular vibrations are going to be insufficient and of little important. Brownian motion (rotational and diffusional) is important here, as well as certain molecular torsional and rotational motions. The Brownian tumbling motion of the molecule is mainly determined by the random molecular collisions in solution, which cause the direction and rate of the rotational and translational motions to vary in a random fashion with time. Molecular collisions during a certain period of time cause the molecules to lose the memory their foregoing motional history.

A number of different physical interactions have been found to be important in coupling the nuclei to the lattice and hence providing a link through which energy between these two systems can be exchanged. These processes are: (1) magnetic dipole-dipole interaction, (2) scalar coupling interaction, (3) electric quadrupole interaction, (4) chemical shift anisotropy, and (5) spin-rotation interaction. In general, any mechanism which gives rise to fluctuating magnetic fields at a nucleus is a possible relaxation mechanism. For any given system, the observed relaxation times will result from contributions by various different relaxation mechanisms. To relate the observed relaxation times with the molecular properties, one will therefore have to devise means by which the relative importance of the different mechanism can be established. All mechanisms leading to T_1 relaxation also lead to T_2 relaxation. More detailed and quantitative discussions of all relaxation mechanisms are referred to the text by Abragam.³

Since a magnetic moment of an electron spin is about 2600 (or 650) times greater than that of ^{13}C (or ^1H), the randomly fluctuating magnetic field due to a paramagnetic ion usually dominates the spin relaxations of nuclei in its neighborhood. As described above, there are two types of electron-nucleus interactions that contribute to the relaxation times of nuclei bound near a paramagnetic sites: the first is the electron-nucleus dipolar interaction which depends on the molecular geometry, the second is the nucleus-electron scalar coupling via the Fermi contact interaction

which depends on the electron spin density at the nucleus. Solomon derived equations for the dipolar interaction,⁴ and Bloembergen added the terms entailing scalar interaction for nuclei in solutions containing paramagnetic ions.¹

The contribution of the electron spin to relaxation times of nuclei located near a paramagnetic center is given by

$$\begin{aligned} \frac{1}{T_{1M}} = & \frac{2}{15} \frac{\gamma_I^2 g^2 \beta^2 S(S+1)}{r^6} \left(\frac{3\tau_c}{1 + \omega_I^2 \tau_c^2} + \frac{7\tau_c}{1 + \omega_S^2 \tau_c^2} \right) \\ & + \frac{2S(S+1)}{3} \left(\frac{A}{\hbar} \right)^2 \left(\frac{\tau_e}{1 + \omega_S^2 \tau_e^2} \right), \end{aligned} \quad (2.3)$$

$$\begin{aligned} \frac{1}{T_{2M}} = & \frac{1}{15} \frac{\gamma_I^2 g^2 \beta^2 S(S+1)}{r^6} \left(4\tau_c + \frac{3\tau_c}{1 + \omega_I^2 \tau_c^2} + \frac{13\tau_c}{1 + \omega_S^2 \tau_c^2} \right) \\ & + \frac{S(S+1)}{3} \left(\frac{A}{\hbar} \right)^2 \left(\tau_e + \frac{\tau_e}{1 + \omega_S^2 \tau_e^2} \right), \end{aligned} \quad (2.4)$$

where ω_S and ω_I are electronic and nuclear angular Larmor frequencies, and other symbols are described before. The first term in both equations arises from the dipolar interaction between the electron spin S and the nuclear spin I . This interaction is characterized by a correlation time τ_c . The second term arises from modulation of the scalar interaction which is characterized by a correlation time τ_e . Scalar interaction requires a finite electronspin density at the nucleus.

The correlation times in the Solomon-Bloembergen equations (eq 2.3 and 2.4) are defined by

$$\tau_c^{-1} = \tau_R^{-1} + \tau_M^{-1} + \tau_s^{-1}, \quad (2.5)$$

$$\tau_e^{-1} = \tau_M^{-1} + \tau_s^{-1}, \quad (2.6)$$

where τ_R is the rotational correlation time of the complex, τ_s is the electron-spin relaxation time, and τ_M is the mean life time of a nucleus in the bound site. A value of τ_c is thus determined by the fastest rate process, i.e., the shortest τ value. The temperature dependences of τ_R and τ_M are given by the Arrhenius expression,

$$\tau_R = \tau_R^\circ \exp(E_R/RT) \quad , \quad (2.7)$$

$$\tau_M = \tau_M^\circ \exp(E_M/RT) \quad , \quad (2.8)$$

where E_R and E_M are the activation energy of rotational motion and the chemical exchange. The temperature dependence of τ_s was given by Bloembergen and Morgan.⁵

For the aquo complexes of paramagnetic ions such as Mn(II) and Cu(II), τ_e is sufficiently long (10^{-8} - 10^{-9} sec) and $\tau_M, \tau_s > \tau_R \simeq 10^{-11}$ sec at room temperature,⁶ so that $\omega_S^2 \tau_e^2 \gg 1$, $\omega_I^2 \tau_c^2 \ll 1$ at the magnetic field used in this work (1.4 and 2.1 Tesla). Then eq 2.3 and 2.4 reduce to

$$\frac{1}{T_{1M}} = \frac{2}{15} \frac{\gamma_I^2 g^2 \beta^2 S(S+1)}{r^6} \frac{3\tau_c}{1 + \omega_I^2 \tau_c^2} \quad , \quad (2.9)$$

$$\begin{aligned} \frac{1}{T_{2M}} = & \frac{1}{15} \frac{\gamma_I^2 g^2 \beta^2 S(S+1)}{r^6} \left(4\tau_c + \frac{3\tau_c}{1 + \omega_I^2 \tau_c^2} \right) \\ & + \frac{S(S+1)}{3} \left(\frac{A}{\pi} \right)^2 \tau_e \quad . \end{aligned} \quad (2.10)$$

Here, it will be convenient to tabulate the Larmor frequencies of proton, ^{13}C , and electron in the field used in this work. These are shown in Table II-I.

Table II-I. Larmor angular frequencies of proton,
¹³C, and electron in rad/sec

field (Tesla)	ω_H	ω_C	ω_S
1.4	3.77×10^8	9.48×10^7	2.48×10^{11}
2.1	5.66×10^8	1.42×10^8	3.71×10^{11}

Nuclear Overhauser Enhancement

The nuclear Overhauser enhancement (NOE) is a more subtle double irradiation effect and intimately linked to the spin-lattice relaxation. Nuclei B at resonance is irradiated with a strong rf field while another A is monitored with a non-saturating rf field. To have continuous resonance absorption the nuclei must give up this energy to the lattice. The lattice provides a fluctuating component at the Larmor frequency which causes the nuclei to relax back to the equilibrium. When dipolar interaction is the dominant mechanism for transfer of energy from nuclei A to the lattice, it is possible by irradiation of nuclei B to increase the intensity of A. This effect is called as the NOE.

If the dipolar interaction with ^1H is the dominant relaxation mechanism, a three times enhancement of ^{13}C intensities may be observed in proton decoupled ^{13}C NMR spectra (see Chapter III, Figure III-9). When paramagnetic ion is present, NOE is efficiently quenched. This arises from the fact that not only the ^{13}C - ^1H dipolar interaction but also the ^{13}C -electron interaction contribute to the relaxation mechanism in the paramagnetic complex.⁷

Chemical Exchange

In order to observe the signal from the nuclei in the ligand, it becomes necessary, in most instances, to observe the resonance signal of a solution with a low concentration of the paramagnetic ion relative to the ligand to avoid inordinate line broadening. In addition, a temperature must be selected to give a ligand exchange rate between the coordination sphere and the bulk solution which is sufficiently fast on the NMR time scale to average the spectral features of the complex with those of the unbound ligand. Under these conditions, the observed paramagnetic shift $\Delta\omega$ is given by⁶

$$\Delta\omega = \frac{fq\Delta\omega_M}{\left(1 + \frac{\tau_M}{T_{2M}}\right)^2 + \tau_M^2 \Delta\omega_M^2}, \quad (2.11)$$

where f is the concentration ratio of paramagnetic ion to ligand in solution and q is the number of ligands in the first coordination sphere of a paramagnetic ion. The value of $\Delta\omega_M$ has its origin in either the contact or the pseudo-contact interactions, or possibly both.

The temperature dependence of $\Delta\omega$ arises from that of τ_M and $\Delta\omega_M$; the former is proportional to the reciprocal of temperature (eq 2.1 and 2.2) and the latter is given by the Arrhenius relationship (eq 2.8).

If the observed relaxation times in the presence of chemical exchange are T_1 and T_2 , the contribution of the paramagnetic ion to these times T_{1p} and T_{2p} may be expressed as^{6,8}

$$\frac{1}{T_{1p}} = \frac{1}{T_1} - \frac{1}{T_{1o}} = \frac{fq}{T_{1M} + \tau_M}, \quad (2.12)$$

$$\frac{1}{T_{2p}} = \frac{1}{T_2} - \frac{1}{T_{2o}} = \frac{fq}{\tau_M} \frac{\frac{1}{T_{2M}} \left(\frac{1}{T_{2M}} + \frac{1}{\tau_M} \right) + \Delta\omega_M^2}{\left(\frac{1}{T_{2M}} + \frac{1}{\tau_M} \right)^2 + \Delta\omega_M^2}, \quad (2.13)$$

where T_{io} ($i=1,2$) is the relaxation time in the unbound site or in the absence of paramagnetic ions. Since in the case of Cu(II) and Mn(II) complexes the conditions of $\Delta\omega_M^2 \ll (T_{2M} \tau_M)^{-1}$ almost hold at room temperature, eq 2.13 reduces to

$$\frac{1}{T_{2p}} = \frac{fq}{T_{2M} + \tau_M}, \quad (2.14)$$

In such a case, eq 2.12 and 2.14 have the same form.

In order to interpret the structure and dynamic properties of the complex one would like to be able to determine the values, or at least range, of q , r , τ_R , τ_M , and τ_S from the observed relaxation times. The observed values of relaxation times are functions of the following variables, f , q , T_{1M} , T_{2M} , r , τ_R , τ_M , and τ_S . To disentangle the values of the different parameters from T_{1p} and T_{2p} , these are two variables at our disposal: namely, temperature and frequency. A few simplifications of eq 2.12 and 2.13 (or 2.14) may be formulated under some conditions.^{6,9,10}

Water Proton Relaxation Enhancement

The relaxation rates of the solvent water protons in the presence of the paramagnetic ion may increase when the metal ion such as Mn(II) and Cu(II) is bound to a macromolecule of which tumbling motions are slow compared with those of the aquo complex of the paramagnetic ion. The main reason for the enhancement of relaxation rate relative to the aquo complex is the change in the correlation time τ_c . For paramagnetic ions whose τ_s is relatively long, τ_c of the aquo complex is determined by τ_R . On the other hand τ_c of the complex of macromolecule may be τ_R , or if the tumbling motion is too slow, τ_s or τ_M may become the relevant τ_c . In any case the new τ_c is longer than that of the aquo complex.

The enhancement of the water proton relaxation rate, which is the ratio of the paramagnetic contributions to the relaxation rate in the presence and the absence of macromolecules, is defined by,¹¹

$$\epsilon^* = \frac{1/T_{1p}^*}{1/T_{1p}} \quad , \quad (2.15)$$

where the asterisk indicates the presence of macromolecule.

REFERENCES

1. N. Bloembergen, J. Chem. Phys., 27, 572(1957).
2. R. J. Kurland and B. R. McGarrey, J. Magn. Resonance, 2, 286(1970).
3. A. Abragam, "The Principle of Nuclear Magnetism", Clarendon Press, Oxford, 1961, chapter 8.
4. I. Solomon, Phys. Rev., 99, 559(1955).
5. N. Bloembergen and L. O. Morgan, J. Chem. Phys., 34, 842(1961).
6. T. J. Swift and R. E. Connick, *ibid.*, 37, 307(1962).
7. R. Freeman, K. G. R. Pachler, and G. N. La Mar, *ibid.*, 55, 4586(1971).
8. Z. Luz and S. Meiboom, *ibid.*, 40, 2686(1964).
9. R. A. Dwek, "Nuclear Magnetic Resonance in Biochemistry", Clarendon Press, Oxford, 1973, chapter 9.
10. T. J. James, "Nuclear Magnetic Resonance in Biochemistry", Academic Press, New York, N.Y., 1976, chapter 6.
11. J. Eisinger, R. G. Shulman, and B. M. Szymansky, J. Chem. Phys., 36, 1721(1962).

CHAPTER III

¹³C Nuclear Magnetic Resonance of Poly(D-glutamic acid)

The conformational transition of a polypeptide in solution has been extensively studied both experimentally and theoretically,¹ including nuclear magnetic resonance (NMR) spectroscopy² which can monitor individual atoms in a molecule. So far, the approach to the conformational study of polypeptide by NMR was to observe the change in chemical shift caused by the conformational transition. The observed change in the chemical shift was interpreted empirically by reference to the results of other measurements, i.e., optical rotatory dispersion, circular dichroism, intrinsic viscosity, etc.

In addition to chemical shift, nuclear magnetic relaxation times provide useful information about the conformational transition of a molecule. Spin-lattice relaxation time (T_1), spin-spin relaxation time (T_2), and the nuclear Overhauser enhancement (NOE) are sensitive functions of the correlation time of reorientational motion of internuclear vector.³⁻⁶ Thus, these NMR parameters are useful to estimate the correlation time of molecular motion.

There are a few ¹³C nuclear magnetic relaxation studies on homopolypeptides; poly(γ -benzyl L-glutamate),^{7,8} poly(L-lysine),⁹ poly(L-proline),¹⁰ poly(L-hydroxyproline).¹⁰ It is well known that poly(D-glutamic acid) undergoes the coil-to-helix transition in an aqueous solution when the pH is lowered. In this chapter we will present the results of ¹³C NMR studies on poly(D-glutamic acid) in aqueous solution carried out to obtain information the relationship between molecular motions and the conformation. The chemical shift, T_1 , T_2 , and NOE of the backbone and side chain carbons were measured as functions of pH.

EXPERIMENTAL

Sodium salt of poly(D-glutamic acid) (PGA) used in this work was prepared by alkaline hydrolysis of poly(γ -methyl D-glutamate) provided by Ajinomoto Co. After exhaustive dialysis against distilled water and passing through a Chelex-100 (Bio-Rad) column to remove paramagnetic impurities, PGA was lyophilized to a powder. The degree of polymerization was determined to be 260 from the intrinsic viscosity measured in 0.2 M NaCl solution at pH 7.1 and at 298 K, using an Ubbelohde type viscometer.¹¹

PGA solutions were prepared at a residual concentration of 0.67 M in 99.8% D₂O obtained from Commissariat a l'Energie Atomique (CEA) and in distilled and deionized H₂O. Adjustments of pH were made with 1 N NaOD and DCl obtained from Merck. The pH was measured on a Hitachi-Horiba M-7 pH meter equipped with a combination micro-electrode (3 mm ϕ). The pH values reported here are direct meter readings without correction for any deuterium isotope effect. PGA solutions were pipetted into 10-mm micro-sample tubes obtained from Sigemi Standard Co. Ltd. and in some cases Teflon plugs were used to prevent solution vortexing due to sample spinning. In all instances the sample volume was restricted to 0.6-0.8 ml, insuring that the entire sample lies within the volume of the transmitter-receiver coil. Although higher sensitivity resulted when larger volumes were employed, the H₁ homogeneity over the sample was degraded. Since measured values of T₁ of all the carbons were less than about 2 sec, no attempt was made to remove oxygen gas dissolved in the solution.

Natural-abundance proton-decoupled ¹³C NMR spectra were obtained at 15.04 MHz using a JEOL FX-60Q Fourier transform spectrometer with a digital quadrature phase detector and with a JEC-980B computer. The deuterium resonance of the solvent D₂O was used as the field-frequency lock signal. All measurements were done at a temperature of 300 K. The chemical shift reported in this work were measured relative to the resonance of internal dioxane and corrected to tetramethylsilane (TMS) by the relation of $\delta_{\text{TMS}} = \delta_{\text{dioxane}} + 67.86 \text{ ppm}$.¹² Spectral widths of 3002 Hz with 8 K data points and 1500 Hz with 4 K data points were used.

Spin-lattice relaxation times (T₁) of protonated carbons were measured by the inversion recovery (IR) method,^{13,14} using a pulse

sequence of $180^\circ\text{-}\tau\text{-}90^\circ\text{-T}$ where τ is a variable delay time and T is at least five times longer than the longest T_1 to be measured. T_1 of nonprotonated carbons was measured by the saturation recovery (SR) method,^{15,16} using a pulse sequence of $90^\circ\text{-HS,}\tau\text{-}90^\circ\text{-T,HS}$ where HS is a homogeneity spoiling pulse. The T_1 values were calculated for the IR method from $\ln(M_0 - M_\tau) = \ln 2M_0 - (\tau/T_1)$, and for the SR method from $\ln(M_0 - M_\tau) = \ln M_0 - (\tau/T_1)$, where M_0 and M_τ are the line intensities of delay times ∞ and τ , respectively. In practice M_0 was determined by the condition of $\tau \gg 5T_1$. Since $\ln(M_0 - M_\tau)$ is a linear function of τ , least-squares analysis of 12-17 data yields T_1 .

Spin-spin relaxation time (T_2) was estimated from the measured line width $\Delta\nu$ at half height assuming a Lorentzian line shape and the relation of $1/T_2 = \pi\Delta\nu$. The line width was obtained from expanded spectra of each resonance and corrected for digital broadening.

The NOE was determined for protonated carbons by the comparison with the intensities of fully decoupled and gated decoupled spectra obtained by gating the decoupling power on only for the time during which the free induction decay was accumulated. In the gated decoupling measurements the 90° pulse repetition time and the off-time of decoupling were at least twenty and ten times, respectively, of the measured T_1 for the carbon under consideration.^{17,18}

RESULTS AND DISCUSSION

Chemical Shift

The proton-decoupled ^{13}C NMR spectra of PGA at pH 4.9 and 7.5 are shown in Figure III-1. The assignment of all peaks follows from that of Lyerla, et al.¹⁹ It is apparent that the line widths of all resonances are broader at pH 4.9 than at pH 7.5.

Figure III-2 shows the effect of pH on the chemical shifts of PGA in the pH range of 4.8 to 10.1. Since PGA strongly aggregates in the lower pH region at concentrations studied here,²⁰ measurements were made only above pH 4.8, at which pH PGA will be a partial helix in consideration of deuterium effect on pH measurements.²¹ Below pH 4.8 where white precipitates came out in the solution, it was very difficult to observe resonances.

When pH increases, the α -carbon (C_α) and the peptide carbonyl (C') resonances move upfield by about 2 ppm, while the β -carbon (C_β), the γ -carbon (C_γ), and the side chain carboxyl carbon (C_δ) resonances move downfield by comparable amounts. Keim, et al., have shown that all ^{13}C resonances of glutamic acid incorporated as central residue of a linear pentapeptide Gly-Gly-Glu-Gly-Gly, not forming a helix, move downfield by 1-3 ppm with increasing pH.²² ^{13}C NMR studies on some homopolypeptides in aqueous and non-aqueous solutions indicate that upfield shifts of C_α and C' resonances are accompanied by the transition from helix to coil.^{7,9,19,23,24} Our results therefore indicate that the shifts of C_α and C' resonances are due mainly to the opening of the hydrogen bond of PGA, and that the behavior of C_β , C_γ , and C_δ resonances reflect primarily the ionization of the carboxyl group of the side chain. These results are in good agreement with those of Lyerla, et al.,¹⁹ except for the difference between D and L enantiomers.

T_1 , T_2 , and NOE

Figure III-3 shows proton-decoupled partially relaxed Fourier transform spectra²⁵ of protonated carbons. Figure III-4 shows proton-decoupled saturation recovery spectra of C_δ and C' carbons. The pH dependence of T_1 for each carbon is shown in Figure III-5. For C_α , C_β , and C_γ carbons NT_1 values are plotted, where N is the number of protons directly bound to the carbon atom, and for C_δ and C' carbons simply T_1 values are plotted.

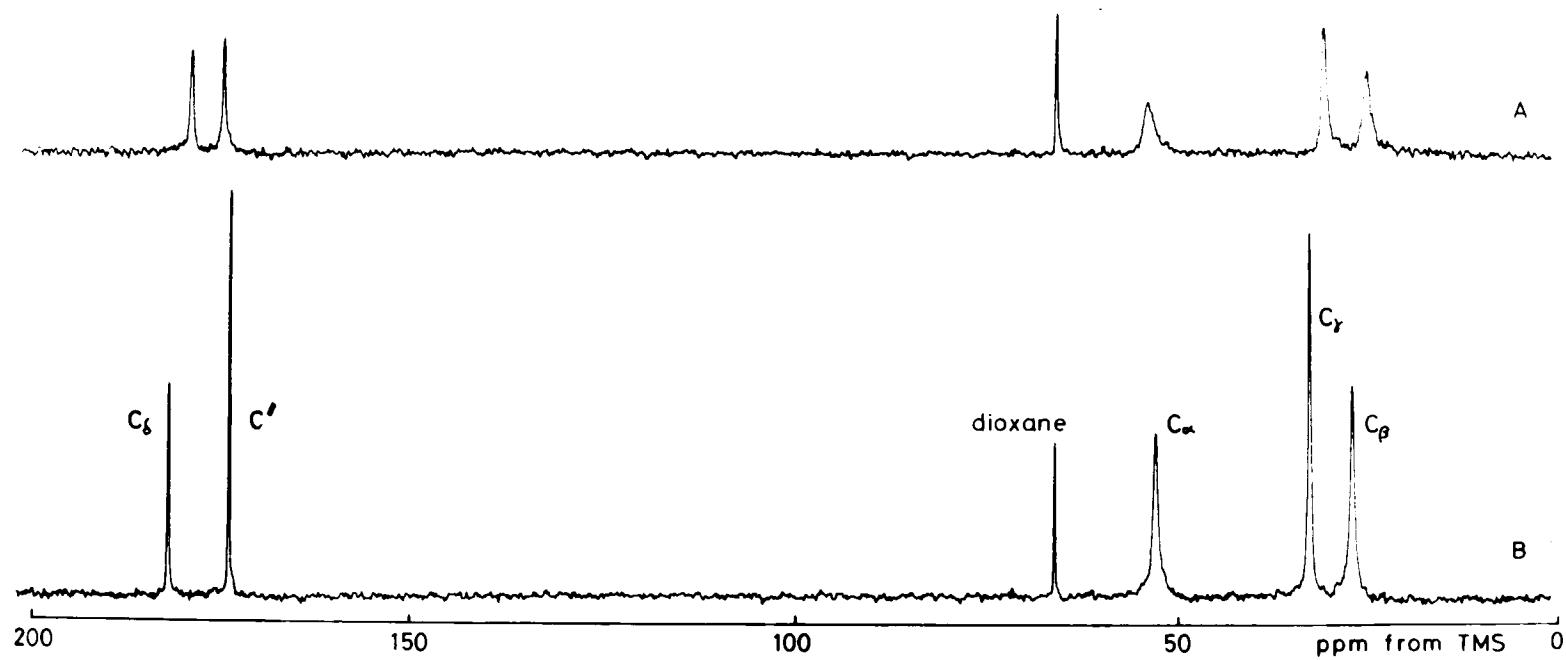


Figure III-1. Natural-abundance proton-decoupled ^{13}C Fourier transform NMR spectra of PGA at two pH's: (A) pH 4.9, 14,000 scans; (B) pH 7.5, 10,000 scans. Repetition time of 90° pulses is 1.5 sec. Chemical shift scale in ppm from TMS.

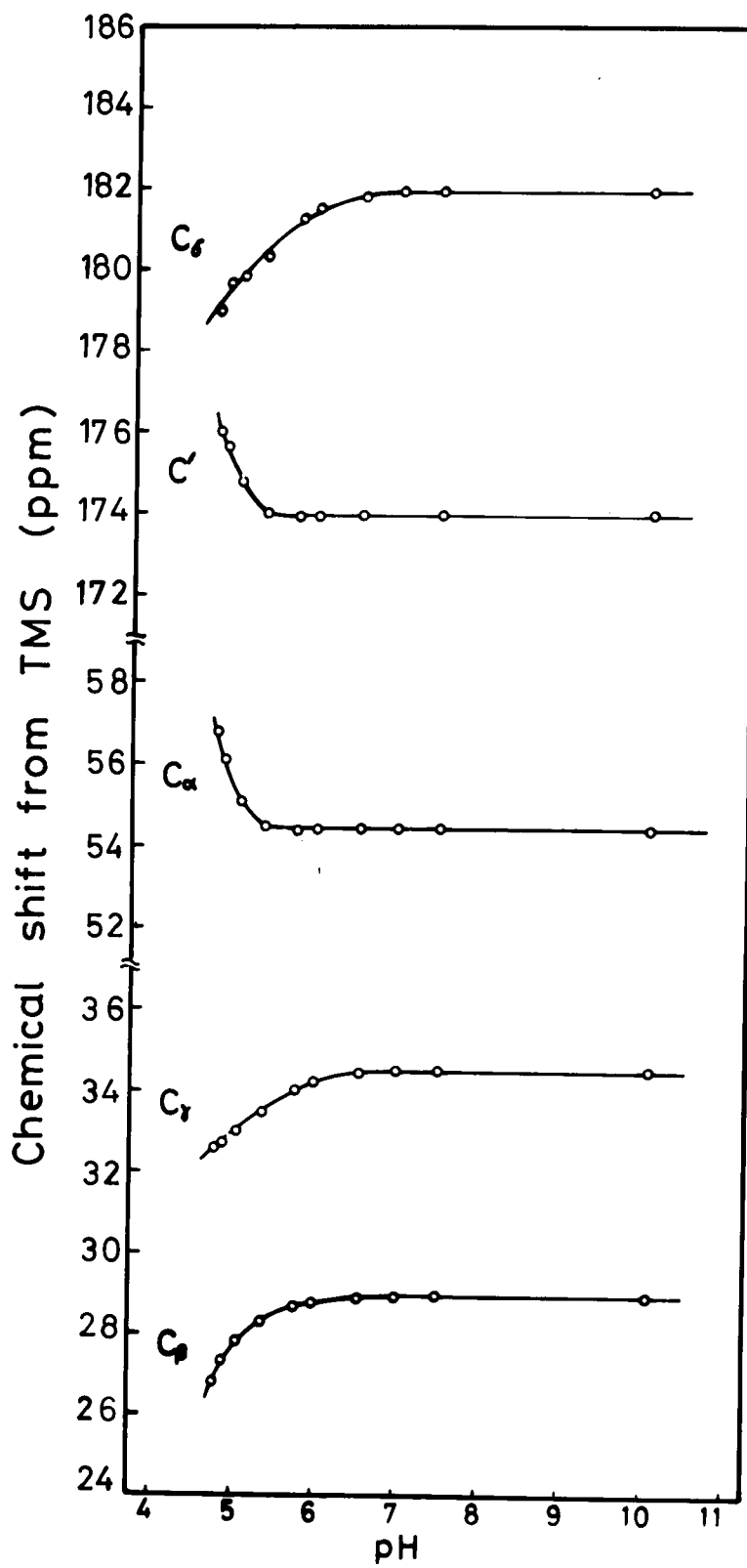


Figure III-2. pH dependence of chemical shift of PGA.

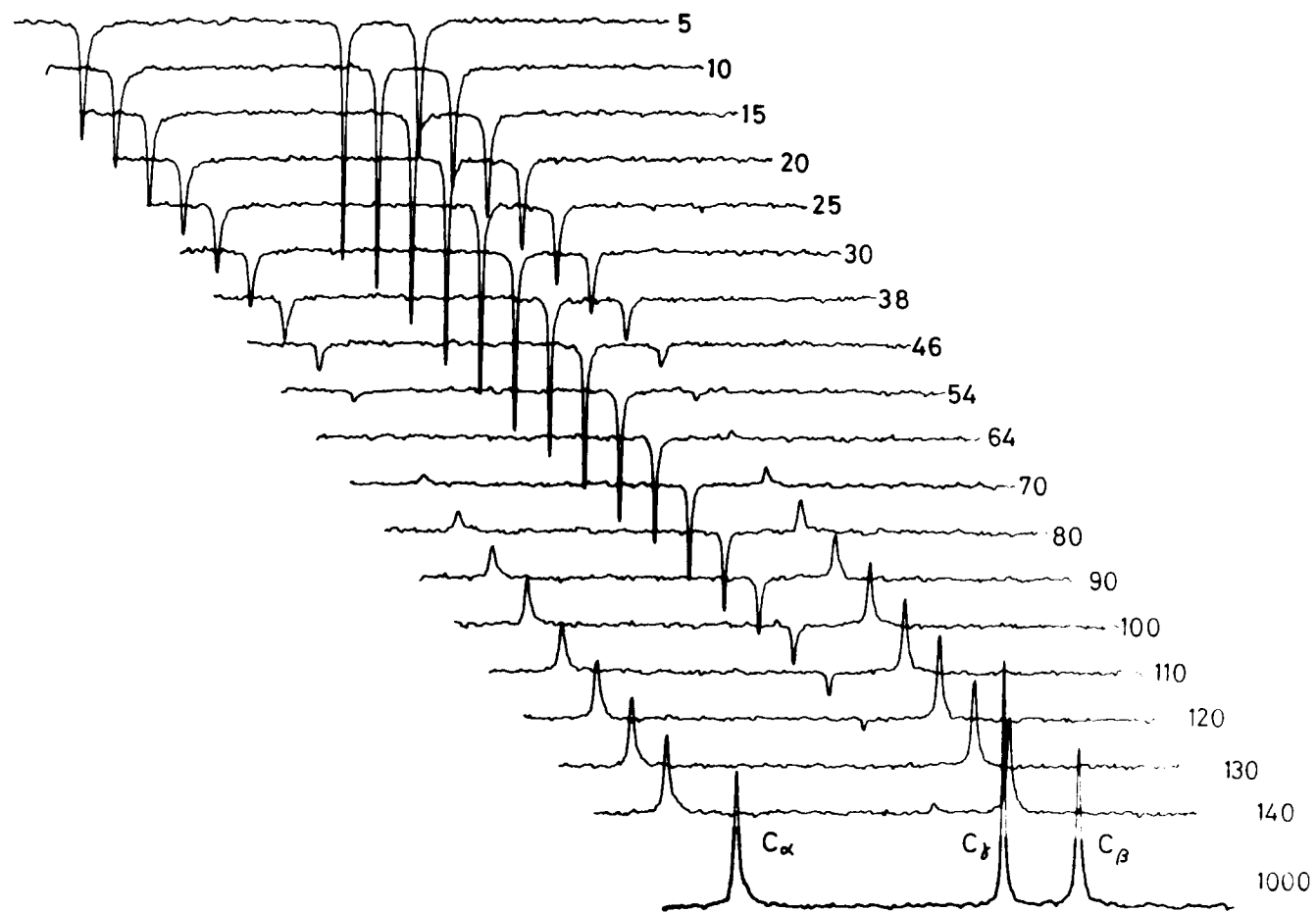


Figure III-3. ^{13}C partially relaxed Fourier transform NMR spectra for protonated carbons of PGA at pH 7.5. Each spectrum is the result of 2,500 scans with a waiting time of 1.5 sec. The delay time is shown at the right of each spectrum in milliseconds.

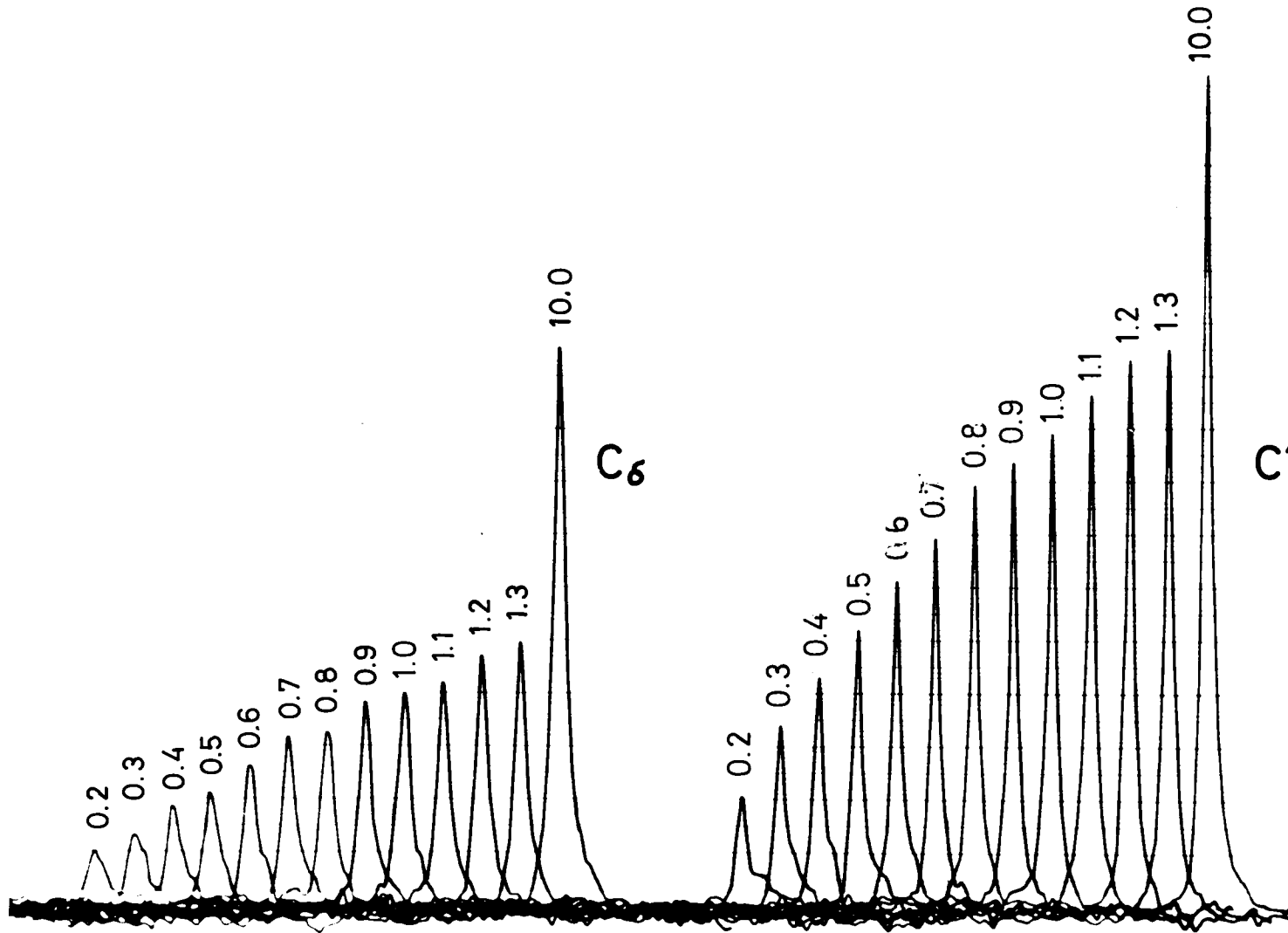


Figure III-4. ^{13}C saturation recovery Fourier transform NMR spectra of C_δ and C' carbons at pH 5.3. Each spectrum is the result of 2048 scans with a waiting time of 1.86 sec. The delay time is shown at the top of each spectrum in seconds.

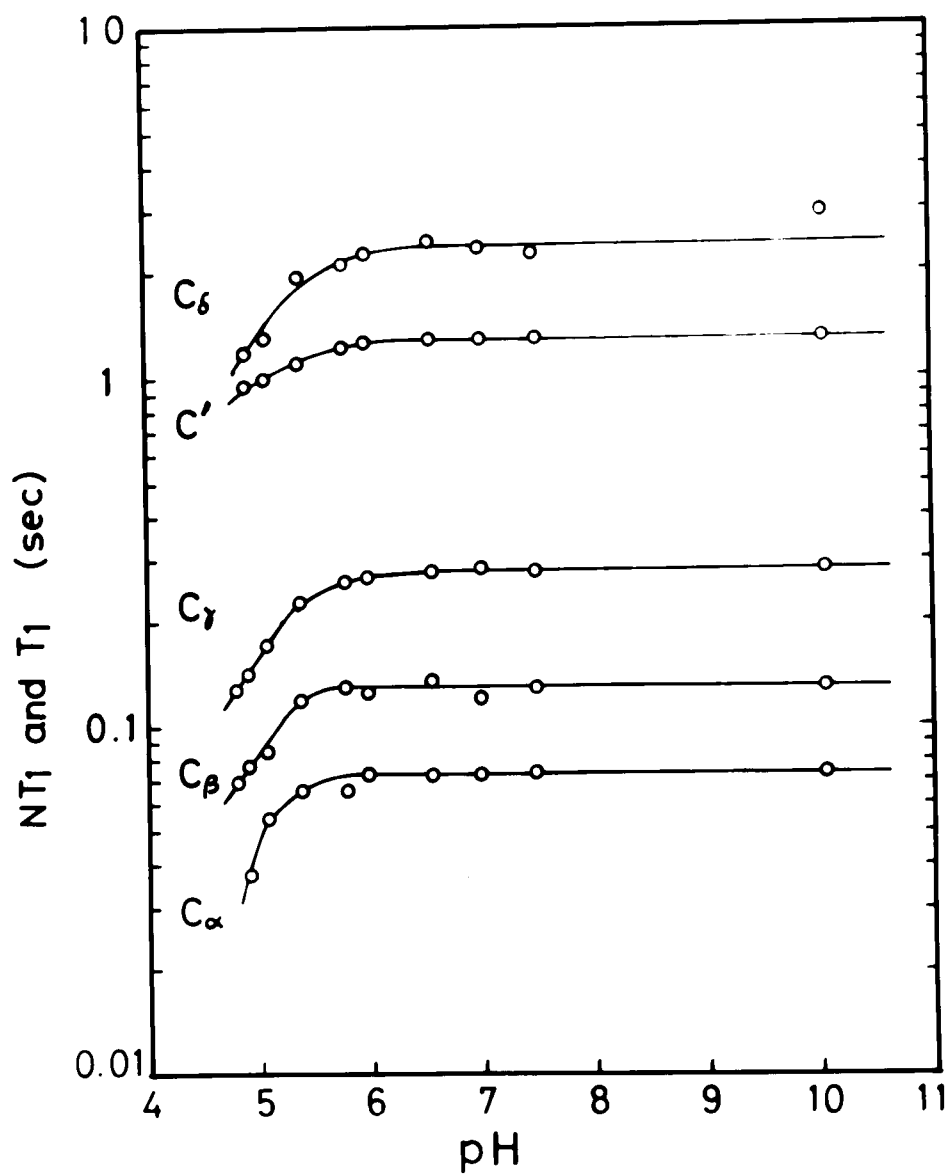


Figure III-5. pH dependence of NT_1 values of C_α , C_β , and C_γ carbons, and T_1 values of C_δ and C' carbons. N is the number of protons directly bound to the carbon.

In the region above pH 6, T_1 values of all carbons do not vary with pH, while with decreasing pH below 6 T_1 values decrease sharply. The pH dependence of T_1 values is very similar to that of the chemical shift as shown in Figure III-2. NOE and the line width are plotted against pH in Figure III-6 and III-7, respectively. These results suggest that the correlation time of tumbling motion becomes longer in conjunction with the coil-to-helix transition.

When analyzing the values of relaxation times for a diamagnetic system studied in this work, one must consider three possible relaxation mechanisms as described in Chapter II: namely, chemical shift anisotropy, spin-rotation, and ^{13}C - ^1H dipole-dipole interactions. Relaxation arising from chemical shift anisotropy is important only at very high field strengths.²⁶ The spin-rotation relaxation mechanism can contribute significantly to ^{13}C relaxation in very small molecules, but can be confidently ignored when dealing with large molecules.²⁶ The dominant mechanism for protonated carbons is the ^{13}C - ^1H dipole-dipole interaction which is modulated by reorientational motions of macromolecules.^{5,6}

The effectiveness of this relaxation mechanism is inversely proportional to the sixth power of r which is the distance between ^{13}C and ^1H nuclei. The value of r^{-6} is about sixty times greater for directly bonded C-H group ($r=1.08 \text{ \AA}$) than for the closest nonbonded C-H interaction ($r=2.16 \text{ \AA}$). As a result, one must consider only the ^{13}C - ^1H dipolar relaxation mechanism for protonated carbons. If the details of reorientation of ^{13}C - ^1H internuclear vector are known, it is possible to present expressions of T_1 , T_2 , and NOE in terms of correlation times of reorientational motions. Here, we assume that a simplified model of isotropic motion with a single effective correlation time (τ_{eff}) can describe the main feature of the nuclear relaxation. Then, T_1 , T_2 , and NOE are given by^{3,5},

$$\frac{1}{T_1} = \frac{N}{20} \frac{\pi^2 \gamma_C^2 \gamma_H^2}{r^6} \{J(\omega_H - \omega_C) + 3J(\omega_C) + 6J(\omega_C + \omega_H)\}, \quad (3.1)$$

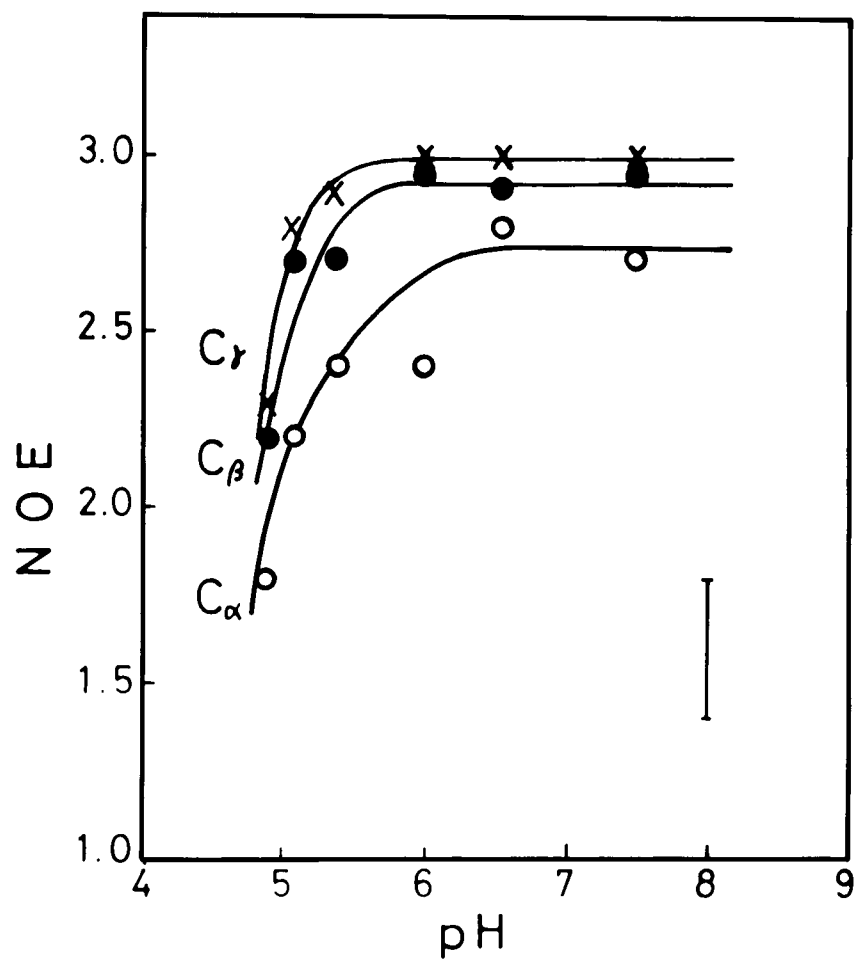


Figure III-6. pH dependence of NOE of protonated carbons.
I means error bar.

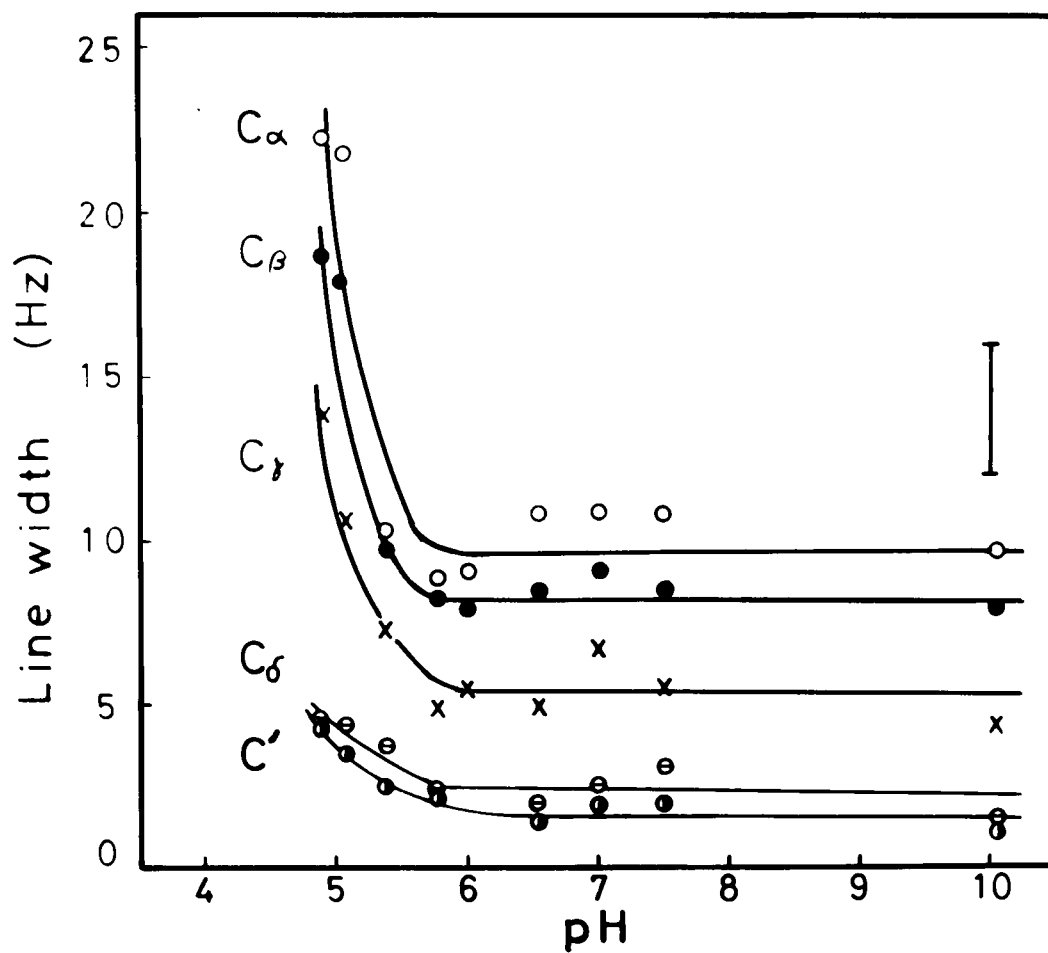


Figure III-7. pH dependence of line width of PGA.
 I means error bar.

$$\frac{1}{T_2} = \frac{N}{40} \frac{\hbar^2 \gamma_C^2 \gamma_H^2}{r^6} \{J(\omega_H - \omega_C) + 3J(\omega_C) + 6J(\omega_C + \omega_H) + 4J(0) + 6J(\omega_H)\}, \quad (3.2)$$

and

$$\text{NOE} = 1 + \frac{\gamma_H}{\gamma_C} \frac{6J(\omega_H + \omega_C) - J(\omega_H - \omega_C)}{J(\omega_H - \omega_C) + 3J(\omega_C) + 6J(\omega_H + \omega_C)}, \quad (3.3)$$

and the spectral density is given by

$$J(\omega) = 2 \tau_{\text{eff}} / (1 + \omega^2 \tau_{\text{eff}}^2), \quad (3.4)$$

where γ_C and γ_H are the gyromagnetic ratios of ^{13}C and ^1H , respectively, r is the distance between ^{13}C and ^1H nuclei, and ω_C and ω_H are the angular resonance frequencies of ^{13}C and ^1H nuclei, respectively.

In Figure III-8 are shown the theoretical ^{13}C NT_1 and NT_2 values (at 1.4 Tesla) against eq 3.1 and 3.2. From the measured T_1 and T_2 values one can, in principle, extract rotational correlation times. In practice, T_2 values are difficult to measure. Moreover, even though accurate T_1 can be obtained, the interpretation can be clouded by the fact that T_1 is not a monotonous function as shown in Figure III-8. In Figure III-9 is shown the theoretical NOE value as a function of τ_{eff} , using eq 3.3. It is noted that the NOE is independent of the number of directly attached protons and of the distance r .⁷ Figure III-9 predicts the maximum NOE of 2.998 when ^{13}C relaxation is purely dipolar and when the rotational reorientation is sufficiently fast to satisfy the "extreme narrowing" conditions

$$(\omega_C + \omega_H)^2 \tau_{\text{eff}}^2 \ll 1. \quad (3.5)$$

Even if the relaxation is purely dipolar, less than the full NOE is expected when eq 3.5 is not satisfied. In the limit of very slow rotation, defined by

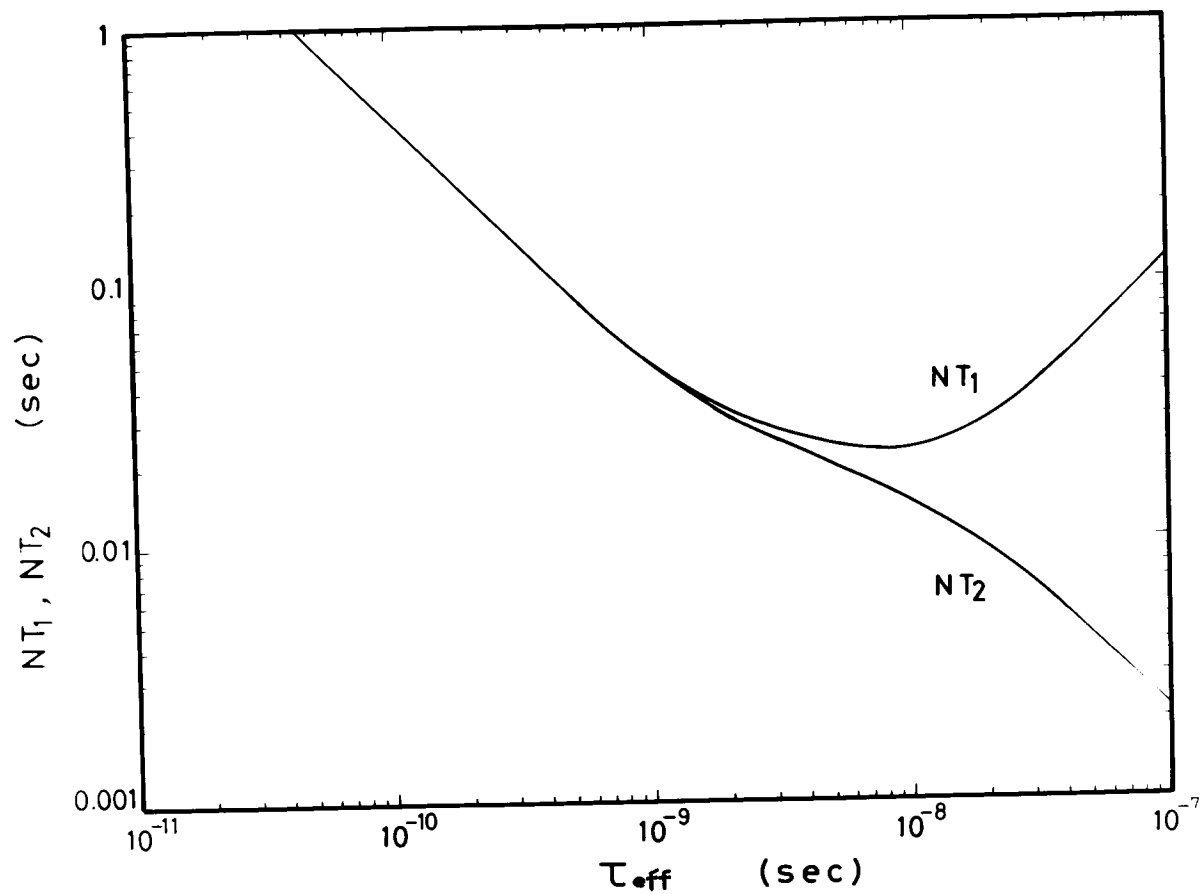


Figure III-8. Log-log plot of NT_1 and NT_2 vs. τ_{eff} at 1.4 Tesla for ^{13}C spin relaxation by a dipolar interaction with N protons 1.08 Å apart (typical C-H bond distance) under the conditions of isotropic rotational reorientation and complete proton decoupling.

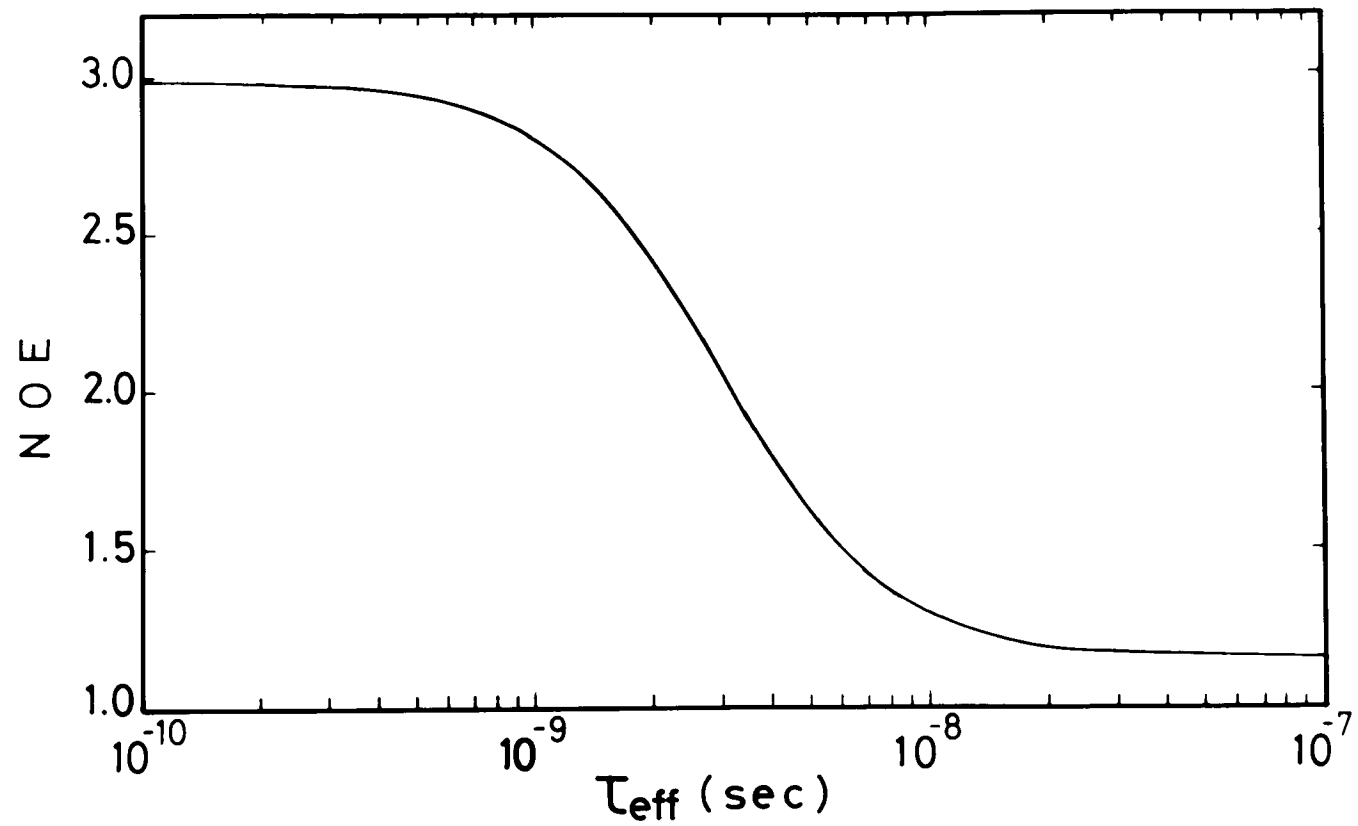


Figure III-9. Semilog plot of NOE vs. τ_{eff} . See caption of Figure III-8 for other details.

$$(\omega_C + \omega_H)^2 \tau_{\text{eff}}^2 \gg 1, \quad (3.6)$$

the NOE will be only 1.153.⁷ In practice, it is desirable to obtain first the two solutions for τ_{eff} from T_1 measurements, and then to choose between the two values on the basis of the NOE values since NOE is a monotonous function.

C_α carbon

At pH 7.5 a measured NOE of 2.7 ± 0.2 is maximal as shown in Figure III-6, and is in the region where NOE is no longer a sensitive function of the correlation time. This leads to two important consequences that the nuclear relaxation of C_α is determined only by ^{13}C - ^1H dipolar interaction, and that extreme narrowing conditions (eq 3.5) are fulfilled. Using eq 3.1 under extreme narrowing conditions, T_1 value of 73 msec measured at pH 7.5 ^{gives} $\tau_{\text{eff}} = 0.65$ nsec with an assumption of the ^{13}C - ^1H distance $r = 1.08 \text{ \AA}$.

If we assume the polypeptide in the coil state as an equivalent rigid sphere, the correlation time of overall tumbling motion (τ_{coil}) is given by³

$$\tau_{\text{coil}} = 4\pi\eta r_o^3 / 3kT, \quad (3.7)$$

where η is the viscosity of the solvent and r_o is the radius of the sphere. The value of r_o may be approximated by the radius of gyration of a freely jointed chain of n units of length m , i.e., $m\sqrt{n/6}$. Using the degree of polymerization of 260 as n , m of 3.8 \AA ,²⁷ and η of 10.5 mP for D_2O at 300 K,²⁸ we obtain a correlation time of 17 nsec from eq 3.7. It should be noted that this calculated value is a lower limit, since the excluded volume effect is not taken into account for r_o and polymer chains are subject to entanglements. The actual value of the correlation time for overall tumbling motion would be therefore greater than the calculated value of 17 nsec. The effective correlation time measured at pH 7.5 where the polypeptide is in the coil state is significantly smaller than the calculated value for overall tumbling motion. This suggests that the correlation time of C_α is determined by local segmental motions of the backbone rather than by overall motion of the molecule. It is found

that the effective correlation time obtained here is in good agreement with those of poly(γ -benzyl L-glutamate)⁸ and of poly(L-lysine)⁹ in the coil state at room temperature.

Using the τ_{eff} obtained from T_1 , we calculated NOE and T_2 from eq 3.2 and 3.3. The results are shown in Table III-I. The calculated NOE is consistent with the measured one. On the other hand, the calculated T_2 is two times greater than the one estimated from the line width.

At pH 4.9 the observed value of T_1 is 38 msec and the NOE is 1.8 ± 0.2 . The combination of T_1 and NOE values yields $\tau_{\text{eff}} = 2.8$ nsec. It turns out that under these conditions the approximation of the extreme narrowing is not valid for C_α . This pH region is the helix region for PGA. Thus, it is quite probable that the longer effective correlation time at pH 4.9 than at pH 7.5 is the consequence of slower segmental motions of the molecules in the helix region.

It has been supposed that a helical PGA molecule in solution behaves like a rigid prolate ellipsoid²⁹ undergoing rotational diffusion characterized by two rotational diffusion constants. These are designated as D_a and D_b for rotation about the major axis and rotation about an axis perpendicular to the major axis, respectively. The dimensions of the ellipsoid, a (the major semi-axis) and b (the minor semi-axis), were each assumed to be half the length of the helix and to have an average radius of gyration of $\frac{1}{2}$ Λ_{PGA} ^{the helix} in solution. Here, we assume the diameter of the solvated helix to be 15 \AA ,²⁹ and the length of a peptide residue to be 1.5 \AA . For a highly prolate ellipsoid with an axial ratio ($\rho = b/a$) much less than unity, D_a and D_b are shown by³⁰

$$D_a = \frac{3kT}{16\pi\eta ab^2} \quad , \quad (3.8)$$

$$D_b = \frac{3kT}{16\pi\eta a^3} \left\{ 2 \ln\left(\frac{2}{\rho}\right) - 1 \right\} \quad , \quad (3.9)$$

and the spectral density is given by⁴

$$J(\omega) = \frac{2A\tau_A}{1 + \omega^2 \tau_A^2} + \frac{2B\tau_B}{1 + \omega^2 \tau_B^2} + \frac{2C\tau_C}{1 + \omega^2 \tau_C^2} \quad , \quad (3.9)$$

Table III-1. Comparison of measured NOE and T_2 values of C_α carbon in the helix and the coil states with the values calculated using τ_{eff} estimated from measured T_1

	pH	
	4.9	7.5
measured T_1 (msec)	38	73
measured τ_{eff} (nsec)	2.8*	0.65
measured NOE	1.8	2.7
calculated NOE	2.1	2.9
measured T_2 (msec)	16	37
calculated T_2 (msec)	13	72

* This value was obtained from the combination of T_1 and NOE values.

where $A=(3\cos^2\theta-1)^2/4$, $\tau_A^{-1}=6D_b$, $B=3\sin^2\theta\cos^2\theta$, $\tau_B^{-1}=D_a + 5D_b$, $C=3\sin^4\theta/4$, and $\tau_C^{-1}=4D_a + 2D_b$, where θ is the angle between the C_α -H internuclear vector and the major axis of ellipsoid.

For the PGA helix used here, a value of \underline{a} is estimated to be 195 Å from the degree of polymerization and \underline{b} to be 7.5 Å from a radius of the solvated helix.²⁹ The angle θ is calculated to be 65° from the coordinates of the α -helix.³¹ Using these parameters we obtained $\tau_A=766$ nsec, $\tau_B=44.3$ nsec, and $\tau_C=11.6$ nsec. Equations 3.1, 3.3, and 3.9 with these correlation times yield a value of T_1 of 33 nsec and a value of NOE of 1.2. It is inferred from the combination of T_1 and NOE that the effective correlation time of the C_α -H vector fixed to the ellipsoid is 23 nsec, which is greater than the correlation time of T_1 minimum.

The correlation times of overall motion of the molecule calculated on the assumption of a rigid ellipsoid are apparently longer than the measured correlation time. This suggests that the tumbling motion of the C_α -H vector is not only overall tumbling motion but also involves appreciable local segmental motion of the backbone. This is clear from the fact that at pH 4.9 PGA is a partial helix as mentioned above. Using the effective correlation time of 2.8 nsec estimated from T_1 and NOE we can calculate the values of NOE and T_2 , which are in reasonable agreement with measured values as shown in Table III-I.

When going from helix to coil with increasing pH, T_1 and NOE increase, and the line width decreases. All these observations are consistent with a decrease in τ_{eff} , which is caused by the onset of the fast segmental motion of the polymer backbone.

C_α and C_β carbons

In all pH region studied, as one goes away from C_α of the backbone to C_γ of the side chain, there is a progressive increase in NT_1 values and also in NOE as shown in Figure III-5 and III-6. This increase in NT_1 and NOE is due to the decrease in the correlation time of motion in the sequence of C_α , C_β , and C_γ . These results indicate that C_β and C_γ carbons of the side chain undergo internal reorientation. Such internal reorientation will be possible even in the helix state, since the side chains of PGA are located at the surface of the helix. Internal reorientation of the side chain has been reported for esters of poly(glutamic acid) in non-aqueous solution.^{7,8,32}

Under the extreme narrowing conditions, the spin-lattice relaxation time of a protonated carbon, undergoing internal reorientation as well as isotropic overall reorientation, is given by⁴

$$\frac{1}{NT_1} = \frac{\hbar^2 \gamma_C^2 \gamma_H^2}{r^6} \tau_{cl} \left\{ A + \frac{B\tau_{int}}{\tau_{int} + \tau_{cl}} + \frac{C\tau_{int}}{\tau_{int} + 4\tau_{cl}} \right\},$$

with

$$A = (3\cos^2\psi - 1)^2/4, \quad B = 3\sin^2\psi\cos^2\psi, \quad C = 3\sin^4\psi/4, \quad (3.10)$$

where τ_{int} is the correlation time of internal reorientation, τ_{cl} is the correlation time for reorientation of the axis of internal reorientation, and ψ is the angle between the C-H internuclear vector and the axis of internal reorientation. For C_β carbon, the internal rotation about the $C_\alpha-C_\beta$ bond is allowed, and ψ is a tetrahedral angle. If the correlation time of the axis is assumed to be equal to the effective correlation time for C_α , τ_{int} for C_β can be calculated from eq 3.10. The correlation time for internal reorientation for C_γ was calculated by assuming that τ_{cl} for C_γ is the effective correlation time for C_β which is estimated from eq 3.1 under extreme narrowing limit. The results are summarized in Table III-2 at pH 5.1 and 7.5. It is found that the effective correlation time progressively decreases in the order of C_α , C_β , and C_γ . The correlation time of internal reorientation also shows a similar trend. It is seen that the internal motion of C_γ carbon is about three times faster than that of C_β carbon. These results suggest that the end of the side chain undergoes more rapid motions than others even in the helix state. This added degree of motional freedom is also convinced from the fact of the larger NOE observed for C_γ carbon as compared with C_α carbon. It is also seen that the internal motion of C_β and C_γ carbons are about two times slower at pH 5.1 than at 7.5, suggesting that the internal motions of the side chain carbons in the helix state are more hindered than they are in the coil state.

Table III-2. Effective correlation time (τ_{eff}) and correlation time of internal reorientation (τ_{int}) in nsec

pH	C_{α}	C_{β}		C_{γ}	
	τ_{eff}	τ_{eff}	τ_{int}	τ_{eff}	τ_{int}
5.1	0.96	0.53	2.7	0.26	0.94
7.5	0.65	0.35	1.5	0.16	0.55

C' carbon

Figure III-4 indicates that the T_1 value of the peptide C' carbon is an order of magnitude greater than that of C_α carbon. This is due to the fact that there is no proton directly bonded to C' carbon. The same situation is found for C_δ carbon.

We measured the spin-lattice relaxation time of C' carbon in both D_2O and H_2O at neutral pH to identify neighboring nuclei which greatly contribute to the relaxation of C' carbon. It was found that C' carbon relaxes more rapidly in H_2O than in D_2O . Results are shown in Table III-3. The measured T_1 value is longer in D_2O than in H_2O by 50%. It is reasonable to assume that the main contribution to the T_1 value of C' is the dipolar interaction with directly bonded nitrogen (^{14}N), α -proton which is two bonds removed, and an amide proton, also two bonds removed. The amide proton is readily exchanged with deuterium in a D_2O solution. Therefore, the longer relaxation time in D_2O is due to the exchange of a proton for deuterium of the amide group. Because the gyromagnetic ratio of deuterium (γ_D) is smaller than of proton (γ_H), the ^{13}C - 2D dipolar relaxation is less effective compared to the ^{13}C - 1H dipolar relaxation.

In order to confirm this consideration we calculated the distance between C' carbon and the amide proton. Under the extreme narrowing limit (eq 3.5), the distance r will be given by

$$\left(\frac{1}{T_1}\right)_{H_2O} - \left(\frac{1}{T_1}\right)_{D_2O} = \frac{\hbar^2 \gamma_C^2 \gamma_H^2}{r^6} \tau \left\{ 1 - \frac{I_D(I_D+1) \gamma_D^2}{I_H(I_H+1) \gamma_H^2} \right\} \quad (3.11)$$

where τ is the correlation time of C' carbon, I_D and I_H are the spin quantum numbers of deuterium and proton, respectively. Assuming that τ of C' carbon is identical to the correlation time of C_α carbon and using the measured T_1 values in H_2O and D_2O , the resulting distance is 1.98 Å. This value is in good agreement with the value of 2.04 Å calculated from bond distance and angle³³ in spite of rough assumption.

Table III-3. Comparison of T_1 value of C' carbon in H_2O and D_2O in the coil state at 300 K

	pH 7.5 in H_2O	pH 7.5 in D_2O *
T_1 (sec)	0.88	1.28

* Direct meter reading in D_2O solution.

REFERENCES

1. G. D. Fasman, Ed., "Poly- α -amino acids", Marcel Dekker, New York, N. Y., 1967.
2. F. A. Bovey, J. Polymer Sci., Macromolecular Reviews, 9, 1(1974).
3. A. Abragam. "The Principles of Nuclear Magnetism", Clarendon Press, Oxford, 1961, chapter 8.
4. D. E. Woessner, J. Chem. Phys., 37, 647(1962).
5. A. Allerhand, D. Doddrell, and R. Komoroski, *ibid*, 55, 189(1971).
6. J. Schaefer and D. F. S. Natusch, Macromolecules, 5, 416(1972).
7. L. Paolillo, T. Tancredi, P. A. Temussi, E. Trivellone, E. M. Bradbury, and C. Crane-Robinson, J. Chem. Soc., Chem. Commun., 335(1972).
8. A. Allerhand and E. Oldfield, Biochemistry, 12, 3428(1973).
9. H. Saito and I. C. P. Smith, Arch. Biochem, Biophys., 158, 154(1973).
10. D. A. Torchia and J. R. Lyerla, Jr., Biopolymers, 13, 97(1974).
11. A. Wada, Mol. Phys., 3, 409(1960).
12. E. Oldfield, R. S. Norton, and A. Allerhand, J. Biol. Chem., 250, 6381(1975).
13. R. L. Vold, J. S. Waugh, M. P. Klein, and D. E. Phelps, J. Chem. Phys., 48, 3831(1968).
14. R. Freeman and H. D. W. Hill, *ibid*, 54, 3367(1970).
15. J. L. Markley, W. J. Horsley, and M. P. Klein, *ibid*, 55, 3604(1971).
16. G. G. McDonald and J. S. Leigh, Jr., J. Magn. Reson., 9, 358(1973).
17. K. F. Kuhlman, D. M. Grant, and R. K. Harris, J. Chem. Phys., 52, 3439(1970).
18. S. J. Opella, D. J. Nelson, and O. Jardetzky, *ibid.*, 64, 2533(1976).
19. J. R. Lyerla, Jr., B. H. Barber, and M. H. Freedman, Can. J. Biochem., 51, 460(1973).
20. J. Y. Cassim and J. T. Yang, Biochem. Biophys. Res. Commun., 26, 58(1967).
21. P. K. Glasoe and F. A. Long, J. Phys. Chem., 64, 188(1960).
22. P. Keim, R. A. Vigna, J. S. Morrow, R. C. Marshall, and F. R. N. Gurd, J. Biol. Chem., 248, 7811(1973).
23. G. Boccalon, A. S. Verdini, and G. Giacometti, J. Amer. Chem. Soc., 94, 3639(1972).
24. Y. Suzuki, Y. Inoue, and R. Chujo, Biopolymers, 16, 2521(1977).
25. A. Allerhand, D. Doddrell, V. Glushko, D. W. Cochran, E. Wenkert, D. J. Lawson, and F. R. N. Gurd, J. Amer. Chem. Soc., 93, 544(1971).

26. T. C. Farrar and E. D. Becker, "Pulse and Fourier Transform NMR", Academic Press, New York, N. Y., 1971, chapter 4.
27. D. A. Brant and P. J. Flory, J. Amer. Chem. Soc., 87, 2791(1965).
28. The Chemical Society of Japan, Ed., "Kagaku Binran", Maruzen Co., Tokyo, 1960, p71.
29. D. K. Schiffer and A. Holtzer, Biopolymers, 13, 853(1974).
30. F. Perrin, J. Phys. Radium, 5, 497(1934).
31. R. D. B. Fraser and T. P. MacRae, "Conformation in Fibrous Proteins", Academic Press, New York, N. Y., 1973, p181.
32. N. Tsuchihashi, T. Enomoto, M. Hatano, and J. Sohma, Polymer, 18, 857(1977).
33. G. N. Ramachandran and V. Sasisekharan, Advan. Protein Chem., 23, 283(1968).

CHAPTER IV

Cu(II)-Poly(D-glutamic acid) Complex

Copper carries out its various physiological functions in association with specific proteins, like most metals that play a role in living cells.^{1,2} It is well known that Cu(II) forms the strongest complex with most ligands among all divalent ions as shown in the Irving-Williams series.³ Since Cu(II) has one less electron than can be accommodated in the five d-orbitals, it has one unpaired electron in all mono-nuclear complexes. The complexes are therefore paramagnetic and characterized by a spin of 1/2 ($S=1/2$). The Cu(II) ion often has a coordination number of four with the ligands arranged at the corners of a planar-square. In some cases there are two additional ligands bound more weakly and with their valence bonds directly perpendicular to the plane of the square.

Copper complexes of polypeptides have been investigated in detail from the point of views of the structural properties and the catalytic activities.⁴⁻¹² Poly(glutamic acid) (PGA) forms a complex with Cu(II), the nature of which has been examined by a variety of physico-chemical techniques.¹⁰⁻¹² It has been suggested for Cu(II)-PGA complex that ligands which are coordinated to Cu(II) are the carboxyl groups as well as the peptide nitrogens in acid solution and the nitrogen atoms in alkaline solution.¹⁰⁻¹² There are a few NMR studies on the interaction of the paramagnetic metal ion with homopolypeptides.^{13,14} In the Cu(II)-poly(L-histidine) complex at acid pH, NMR relaxations of protons of the imidazole ring become much more faster, showing that Cu(II) binds imidazole nitrogen atoms.

As well as ligand nuclei, the relaxation rate of water proton of aqueous solution of the paramagnetic complex also provides useful information about structure and dynamics in the proximity of the metal ion.

In this chapter we will describe the results of ¹³C nuclear magnetic relaxation times of Cu(II)-PGA complex in aqueous solution measured as functions of temperature and pH in order to obtain further information concerning the relationship between the structure and the dynamics of

the complex. Water proton relaxation times were also measured.

EXPERIMENTAL

PGA was prepared as described in the previous chapter. Analytical grade anhydrous copper(II) chloride from Nakarai Chemicals was used without further purification. Solutions for ^{13}C and ^1H NMR measurements were prepared with D_2O (99.8%) obtained from CEA and with redistilled and deionized H_2O , respectively. Aliquots of CuCl_2 solution were added to PGA solution to prepare the complex, and the resulting solution was stirred for a sufficiently long period. Adjustments of pH were made with NaOH and HCl solutions. The pH was measured on a Hitachi-Horiba M-7 pH meter equipped with a combination micro-electrode (3 mm ϕ) (Nisshin Rika Co.). The pH values reported here are direct meter reading.

Natural-abundance proton-decoupled ^{13}C NMR spectra were obtained at 15.04 MHz using a JEOL FX-60Q spectrometer. All measurements were carried out at controlled temperatures using a JEOL temperature control unit. Temperature was calibrated with a thermometer before and after each measurement. Dioxane used as an internal standard because of the unlikelihood of its competition with PGA residues and solvent molecules in entering the first coordination sphere of the metal ion.¹⁵ Chemical shifts reported here were corrected to TMS. Spin-lattice relaxation time (T_1) was measured by two methods. The IR method^{16,17} was adopted for protonated carbons in metal-free solution and all carbons in complex solution. The SR method^{18,19} was applied to non-protonated carbons in metal-free solutions. Spin-spin relaxation time (T_2) was estimated from measured line width $\Delta\nu$ using the relation of $1/T_2 = \pi\Delta\nu$. T_1 of water proton was measured on the JEOL FX-60Q spectrometer at 60 MHz by the IR method.^{17,18} The 90° pulse was 10 μsec for ^{13}C and 35 μsec for ^1H . Details of measurements are referred to the previous chapter.

RESULTS AND DISCUSSION

Effects of Cu(II)

The effects of adding Cu(II) on ^{13}C NMR spectra of PGA are shown in Figure IV-1 at pH 7.4 and at 300 K. This figure illustrates the selective broadening of ^{13}C resonances. On progressive addition of Cu(II), C_γ and C_δ resonances of side chain particularly show broadening, while C_α , C_β , and C' resonances were not affected at Cu(II) concentration studied. Paramagnetic broadenings $\Delta\nu_p$ for C_γ and C_δ resonances shown in Figure IV-2 are proportional to f . These observations indicate that Cu(II) specifically interacts with the carboxyl group of the side chain of PGA.

T_{1p} and T_{2p} of C_γ and C_δ carbons

It was found that values of $1/T_{1p}$ and $1/T_{2p}$ for C_γ and C_δ carbons increase with increasing Cu(II) concentration. On the other hand, T_1 and T_2 values of other carbons except for C_γ and C_δ do not vary with the addition of Cu(II).

Figure IV-3 shows $1/fT_{1p}$ and $1/fT_{2p}$ for C_γ and C_δ carbons as a function of the reciprocal of temperature at pH 7.4. It is apparent that both of relaxation rates decrease with increasing temperature. These results indicate that T_{1p} and T_{2p} are controlled by T_{1M} and T_{2M} , respectively, rather than τ_M , that is, $T_{1M}, T_{2M} \gg \tau_M$ in eq 2.12 and 2.14 (fast exchange). Therefore, it follows

$$\frac{1}{T_{1p}} = \frac{fq}{T_{1M}} = \frac{2fq}{15} \frac{\gamma_I^2 g^2 \beta^2 S(S+1)}{r^6} \frac{3\tau_c}{1 + \omega_I^2 \tau_c^2}, \quad (4.1)$$

$$\begin{aligned} \frac{1}{T_{2p}} = \frac{fq}{T_{2M}} = \frac{fq}{15} \frac{\gamma_I^2 g^2 \beta^2 S(S+1)}{r^6} & \left(4\tau_c + \frac{3\tau_c}{1 + \omega_I^2 \tau_c^2} \right) \\ & + \frac{fqS(S+1)}{3} \left(\frac{A}{\pi} \right)^2 \tau_e. \end{aligned} \quad (4.2)$$

The relation of $T_{1p}/T_{2p} \gg 1$ holds in all temperature range studied, indicating that the scalar relaxation is dominant in T_{2M} , while T_{1M} is dominated by the dipolar relaxation. The paramagnetic broadening in the present case does not therefore show the dependence of r^{-6} in eq 4.2.

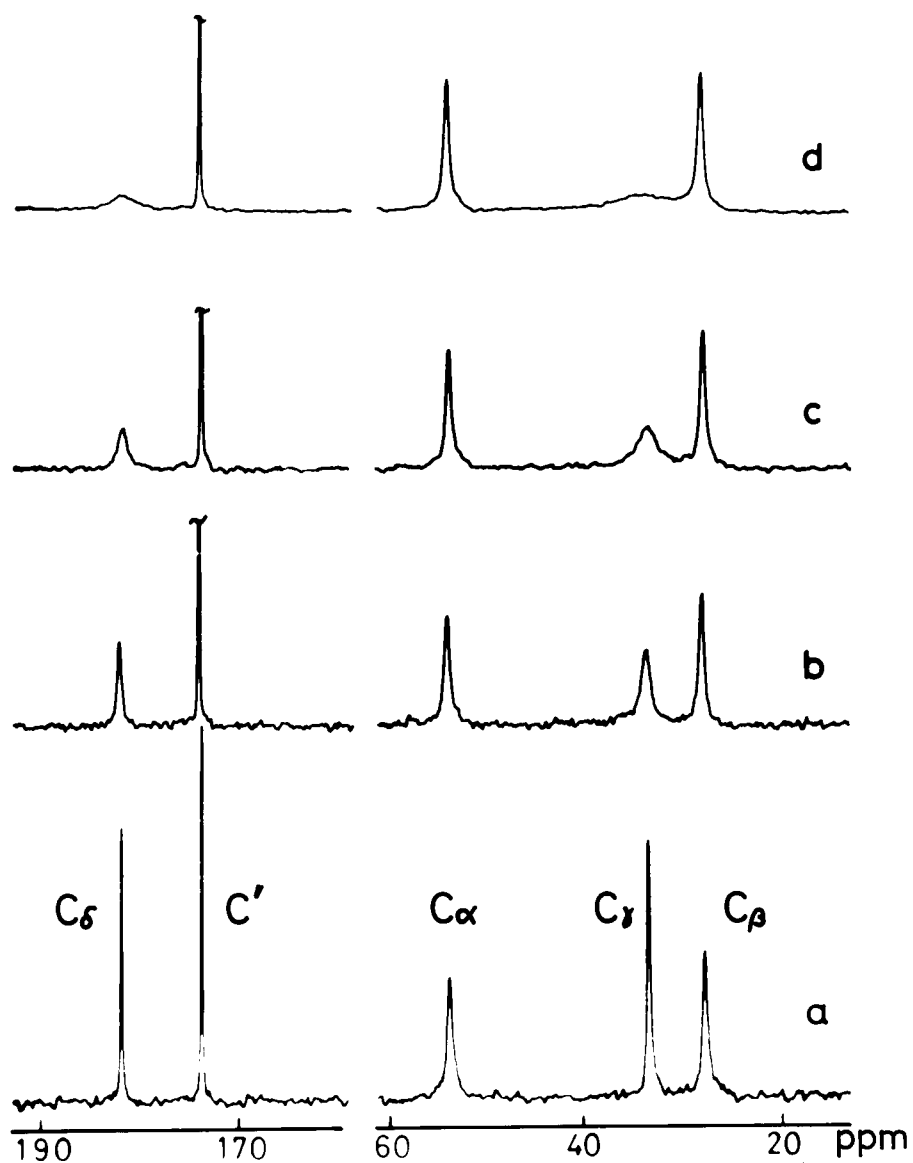


Figure IV-1. Effects of Cu(II) on ^{13}C NMR spectra of PGA (0.93 M in monomer unit) at pH 7.4 and at 300 K:
 (a) $f=[\text{Cu(II)}]/[\text{PGA}]=0$, 3,072 scans; (b) $f=4.39 \times 10^{-5}$, 3,072 scans; (c) $f=9.25 \times 10^{-5}$, 6,000 scans; (d) $f=2.41 \times 10^{-4}$, 13,000 scans. Repetition time of 90° pulses is 1.5 sec.

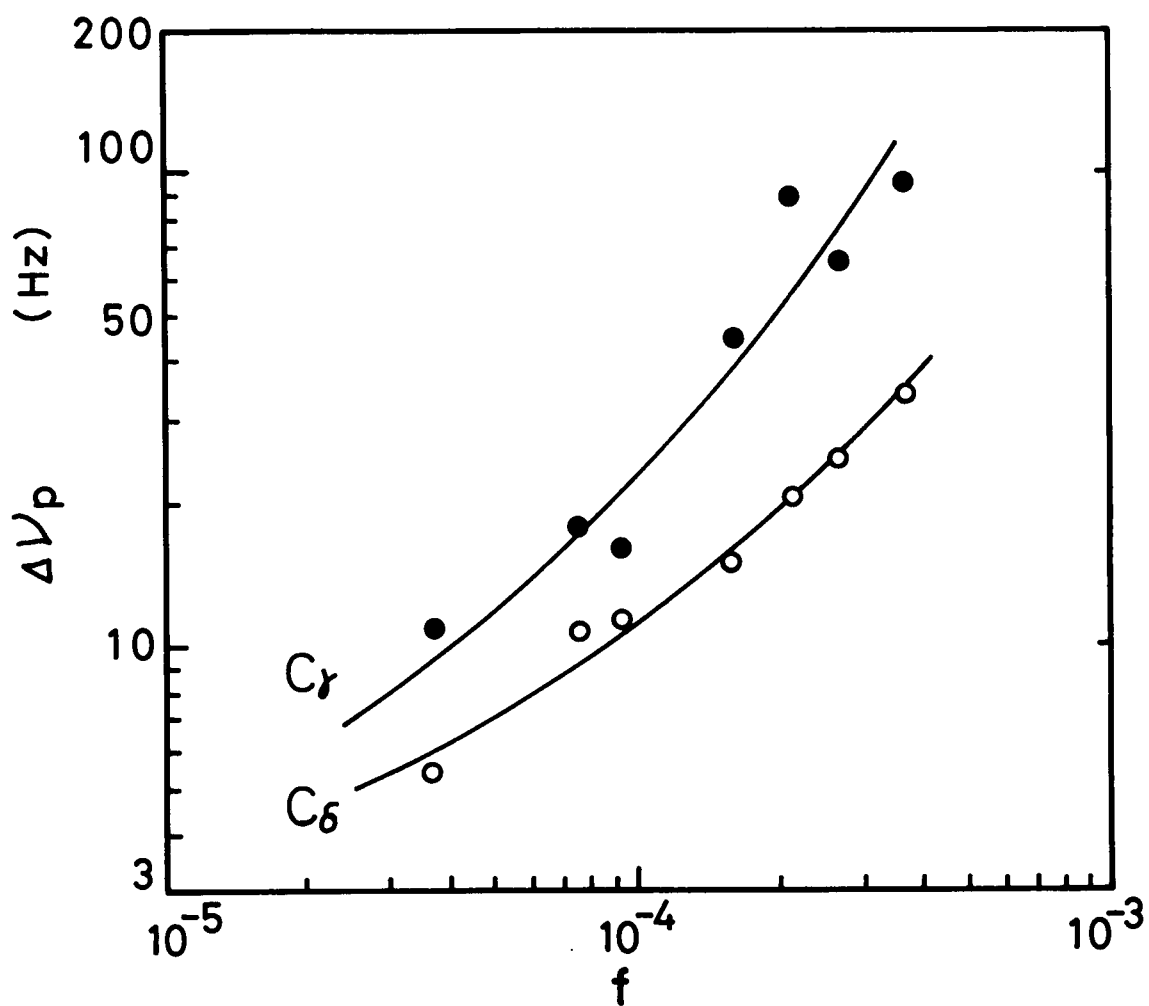


Figure IV-2. Paramagnetic broadening $\Delta\nu_p$ vs. f at 300 K.
 [PGA]=0.90-0.93 M.

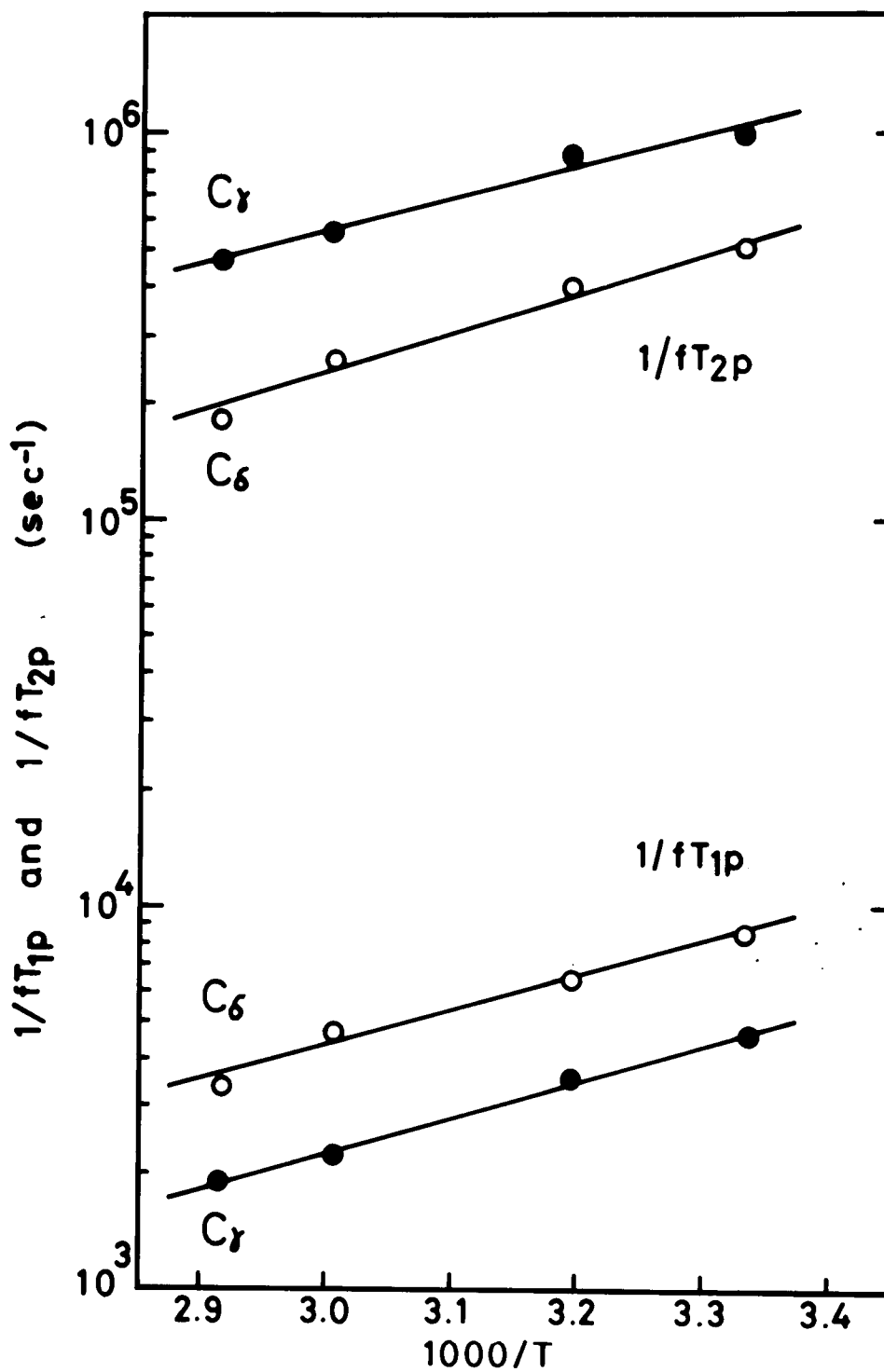


Figure IV-3. Temperature dependence of $1/fT_{1p}$ and $1/fT_{2p}$ at pH 7.4. $f=9.25 \times 10^{-5}$.

Because q and τ_e are not known in eq 4.2, it is not possible to estimate the value of the hyperfine coupling constant A . However, the ratio of A for each carbon can be evaluated from the following equation. Under the conditions of fast exchange ($\omega_I^2 \tau_c^2 \ll 1$) the combination of eq 4.1 and 4.2 yields

$$\frac{1}{T_{2p}} = \frac{7}{6} \frac{1}{T_{1p}} + \frac{fq}{4} \left(\frac{A}{h}\right)^2 \tau_e . \quad (4.3)$$

We obtained $|A(C_\gamma)/A(C_\delta)|=1.7$ and $|A(C_\beta)/A(C_\delta)|=0$ at pH 7.4 and at 300 K. These results suggest that there is a significant amount of electron spin density which is transferred from Cu(II) to the C_γ carbon, and that larger spin density is induced in C_γ than in C_δ . The presence of such larger scalar interaction demonstrates that Cu(II) is bound directly to carboxyl groups.

Under the conditions of fast exchange ($\omega_I^2 \tau_c^2 \ll 1$), T_{1p} can be rewritten as

$$\frac{1}{T_{1p}} = \frac{3fq \gamma_I^2 g^2 \beta^2}{10r^6} \tau_c . \quad (4.4)$$

In this system the g tensor does not seem to be axially symmetric and could not be determined accurately. Moreover, the spatial arrangement of the ligand nuclei with respect to the direction of the g tensor is not known. As the first approximation we use an average g value which was obtained by Takesada, et al.¹⁰

If τ_c and q are known, the distance between carbon and copper can be obtained from eq 4.4. It has been reported that τ_s is the order of 10^{-8} sec and $\tau_s \simeq \tau_e < \tau_M$ in aqueous solution at room temperature.²⁰ It was found to be $\tau_M \ll T_{2M} \simeq 10^{-6}$ sec from Figure IV-3. If we assume that the rotational correlation time of the metal-carbon vector τ_R is the same order of magnitude as the rotational correlation time of the C-H bond in metal-free PGA, τ_R^{-1} is $5 \times 10^9 \text{ sec}^{-1}$ for the C_γ carbon from eq 3.1. This yields $\tau_c^{-1} = 5 \times 10^9 \text{ sec}^{-1}$. Furthermore, we assume that all Cu(II) ions added are bound to carboxyl groups and $q=2$.²¹ On these assumptions the distance between C_γ and copper is estimated to be $3.0 \pm 1.0 \text{ \AA}$ from eq 4.4 at pH 7.4 and at 300 K. Since the rotational correlation time

of C_δ carbon is not known, we postulate that a possible upper limit of τ_c for C_δ is the same order as τ_c for C_γ . The same calculation as for C_γ carbon yields the distance between C_δ carbon and copper to be $2.5 \pm 1.0 \text{ \AA}$, which should be noted to be the maximum distance.

On the assumptions of $\tau_e = \tau_s \simeq 10^{-8} \text{ sec}$ ²⁰ and $q=2$ ²¹, the absolute value of A can be estimated from eq 4.3. The values of $|A(^{13}\text{C})/h|$ obtained are $2 \times 10^8 \text{ Hz}$ and $1 \times 10^8 \text{ Hz}$ for C_γ and C_δ carbons, respectively.

Temperature dependence of $1/T_{1p}$ reflects that of the correlation time of the tumbling motion, if the following conditions are fulfilled; the exchange is fast, the structure of the complex remains the same in the whole temperature range studied, and motions are isotropic. The activation energy E_R for the rotational motion was estimated from the slope of $1/T_{1p}$ vs. $1/T$ using eq 2.7 and 4.4 to be $E_R=5 \text{ kcal/mol}$ for C_γ and C_δ carbons. It is noteworthy that the E_R value for the complex is very close to that for metal-free PGA. This seems to indicate that although the motional freedom of PGA in the vicinity of the Cu(II) binding sites may be restricted by the binding of Cu(II), the presence of the rapid exchange of ligands reduces the rotational barrier to the same as that of metal-free PGA.

pH Dependence of ^{13}C Relaxation Rate

Figure IV-4 shows the pH dependence of ^{13}C spectra in the presence of Cu(II) at 300 K. In the lower pH region, all resonances of metal-free PGA broaden due to increasing correlation time as going from coil to helix.²² The addition of Cu(II) results in further broadening of only C_γ and C_δ resonances. This fact suggests that carboxyl groups are bound to Cu(II) even in the helix region. Cu(II) is known to induce the coil-to-helix transition.^{10-12,21} However, the concentrations of Cu(II) used in this work are too low to observe this effect.

Electron paramagnetic resonance (EPR) studies of the complex at about pH 5 have shown that Cu(II) is bound to nitrogen atoms of the backbone.^{10,21} If nitrogens are bound to Cu(II), the relaxation times of C_α and C' carbons of the backbone would be influenced. However, the present study shows that the relaxation times of the two carbons are same as those of metal-free PGA at Cu(II) concentrations studied here, indicating that Cu(II) is not bound to nitrogen atoms. This inconsistency between EPR studies and our results may be responsible for the

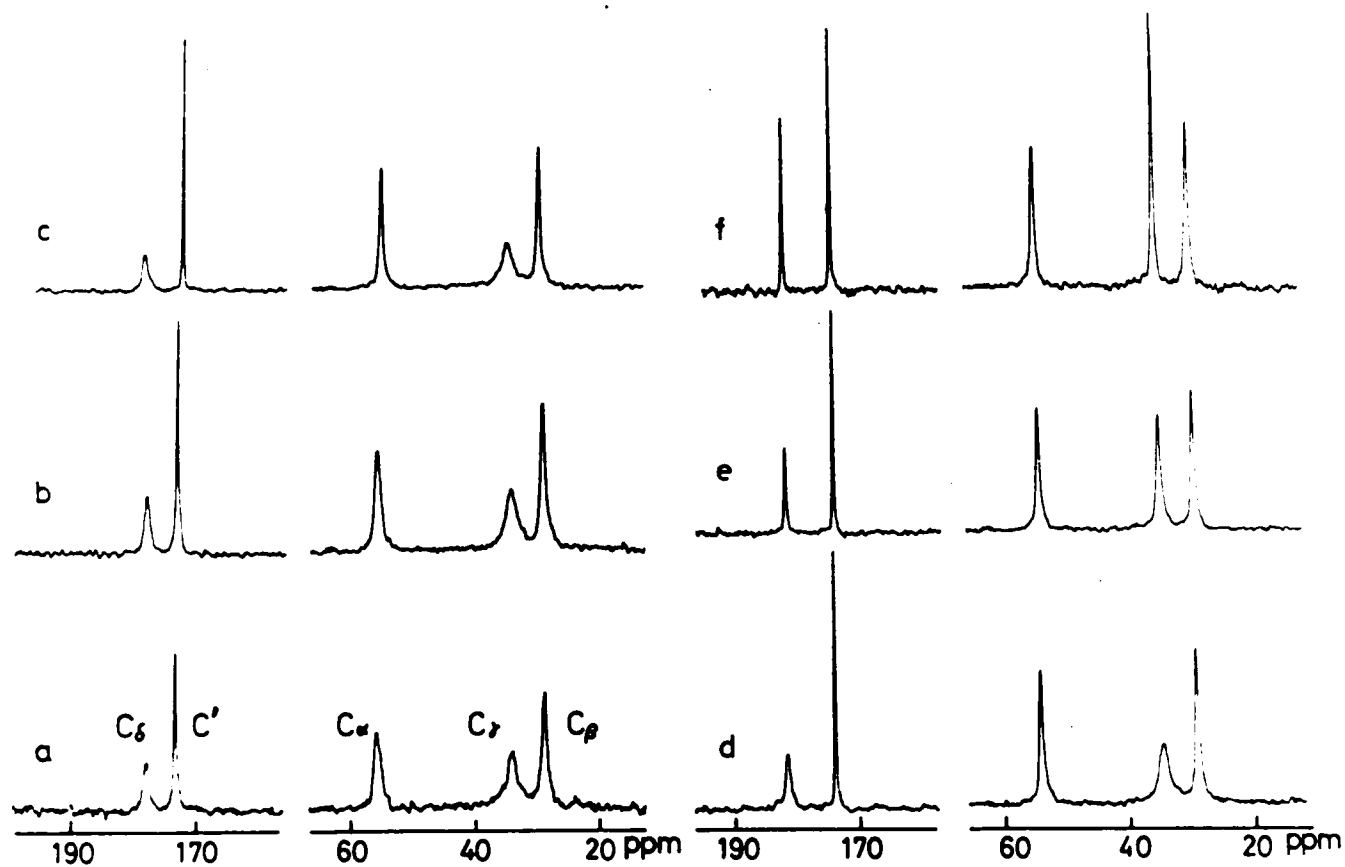


Figure IV-4. pH dependence of ^{13}C spectra of Cu(II)-PGA complex at 300 K:
 (a) pH 4.9, $f=6.9 \times 10^{-5}$, 30,000 scans; (b) pH 5.1, $f=5.4 \times 10^{-5}$,
 40,000 scans; (c) pH 5.4, $f=5.1 \times 10^{-5}$, 20,000 scans; (d) pH 7.4,
 9.3×10^{-5} , 6,000 scans; (e) pH 8.6, $f=6.9 \times 10^{-5}$, 6,000 scans;
 (f) pH 11.1, $f=6.9 \times 10^{-5}$, 3,000 scans. Repetition time of 90°
 pulses is 1.5 sec.

difference of experimental conditions; the value of f in the EPR measurements at 77 K is about 10^3 times greater than that in our NMR measurements at room temperature.

As shown in Figure IV-4, which increasing pH the peak intensities of C_γ and C_δ carbons increase. At pH 11.1 the spectrum obtained is apparently the same that of metal-free PGA in Figure IV-1 (a).

Figure IV-5 shows the pH dependence of $1/fT_{2p}$ of the complex for C_γ and C_δ carbons at 300 K. With increasing pH, values of $1/fT_{2p}$ for C_γ and C_δ carbons begin to decrease in the vicinity of pH 8 from invariable values in the lower pH region and vanish above pH 9. Values of $1/fT_{2p}$ for other carbons except for C_γ and C_δ were zero at all pH's region studied. These results indicate that carboxyl groups are released from Cu(II) at pH 7-8, and that the binding of Cu(II) to carboxyl groups does not occur in the alkaline pH region.

T_1 of Water Proton

To obtain further information on properties of the complex, we measured the spin-lattice relaxation time of water proton of the complex in 0.2 M NaCl solution. Table IV-I shows the results at pH 6.8 and at 296 K. T_1 value of water proton in Cu(II) aqueous solution is five times shorter than in PGA aqueous solution. When PGA added to Cu(II) aqueous solution, T_1 value of water proton becomes further two times shorter than that of Cu(II) aqueous solution. This is due to the fact that the correlation time of tumbling motion of water molecules bound to Cu(II) becomes longer in the presence of PGA than that in the absence of PGA because of the binding of Cu(II) to PGA. These results indicate that Cu(II) bound to PGA still holds water molecules in the first coordination sphere at this pH.

From the measurements of T_1 for aqueous solution of Cu(II), the correlation time of tumbling motion of the aquo Cu(II) complex was estimated to be 5×10^{-11} sec using eq 4.4, on the assumptions that the number of water molecules coordinated to Cu(II) is four at corners of planar square, the distance between copper and water proton is 2.77 \AA , and $\tau_M \ll T_{1M}$.²³ If the complex is octahedral, a value of 3×10^{-11} sec is obtained. The correlation time in the PGA-Cu(II)-H₂O system was also estimated in a similar way as above except for the assumption of coordination number. In the presence of PGA the number of water molecules

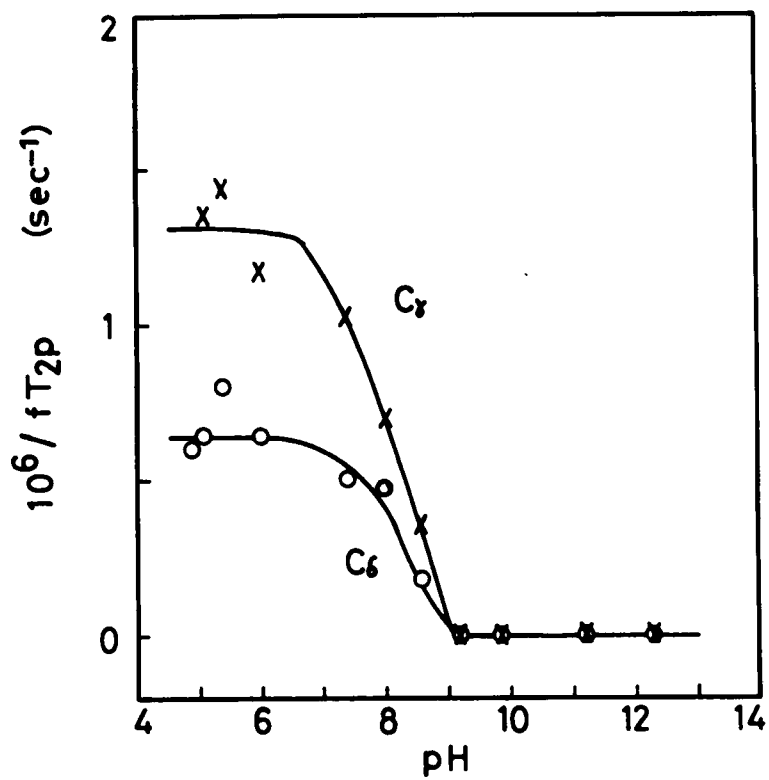


Figure IV-5. pH dependence of $1/fT_{2p}$ at 300 K.

Table IV-I. Spin-lattice relaxation times and correlation times of water proton in sec^{*}

	T_1	τ_c^{**}	τ_c^{***}
H ₂ O + PGA	2.88	-----	-----
H ₂ O + Cu(II)	0.54	5.3×10^{-11}	3.4×10^{-11}
H ₂ O + Cu(II) + PGA	0.23	2.1×10^{-10}	1.0×10^{-10}

* 0.2 M NaCl; [Cu(II)]=2.1 mM, [PGA]=69 mM; pH 6.9, 296 K.

** Assuming a tetragonal complex.

*** Assuming an octahedral complex.

coordinated to Cu(II) was assumed to be 2, because two of four coordination sites of Cu(II) are occupied by carboxyl groups of PGA in the case of tetrahedral complex.²¹ The estimation yields a value of 2×10^{-10} sec, assuming that the distance between copper and water proton is unchanged from that in the pure aqueous solution. In the case of octahedral Cu(II), as the coordination number of water molecules is assumed to be four, a value of 1×10^{-10} sec was obtained. These values obtained are summarized in Table IV-I. In the two cases the correlation times of tumbling motion are larger in the presence of PGA than in the absence of PGA. It is of interest to note that the correlation time thus obtained is approximated to be the correlation time of the tumbling motion of C_γ carbon of PGA because water molecules are bound to Cu(II) which is bound to PGA. The correlation time of tumbling motion of the complex estimated from water proton relaxation is in good agreement with the results obtained from ^{13}C nuclear relaxation of PGA

Figure IV-6 shows the pH dependence of the water proton relaxation enhancement ϵ^* for 2.1 mM Cu(II) aqueous solution at 296 K. The change of pH through the helix-coil transition region does not any effect on ϵ^* in the presence of PGA. This indicates that Cu(II) remains to bind to PGA even in the helix region, in agreement with the results of ^{13}C NMR described above. Independence of ϵ^* on pH means that the product of q and τ_c in eq 4.4 remains unchanged with pH. On the other hand, with increasing pH from neutral to alkaline, the value of ϵ^* begins to decrease in the pH region of 7-8 and vanishes in the alkaline pH region. This decrease in ϵ^* arises from the onset of releasing water molecules from the first coordination sphere of Cu(II).

Structure of Complex

In Figure IV-7 we depict schematic representations of the Cu(II)-PGA complex under the conditions of very small Cu(II) concentrations. In the neutral pH region (pH 6-8) where PGA is in the coil state, two carboxyl groups and two or four water molecules are coordinated to Cu(II) (b). In the acid region (pH 4.5-5.5) where PGA is in the helix region, carboxyl groups and water molecules remain in the first coordination sphere of Cu(II). The complex may be formed within a molecule, with coil parts of the molecule, or between molecules (a).

Hojo and coworkers showed from measurements of pH titration, visible

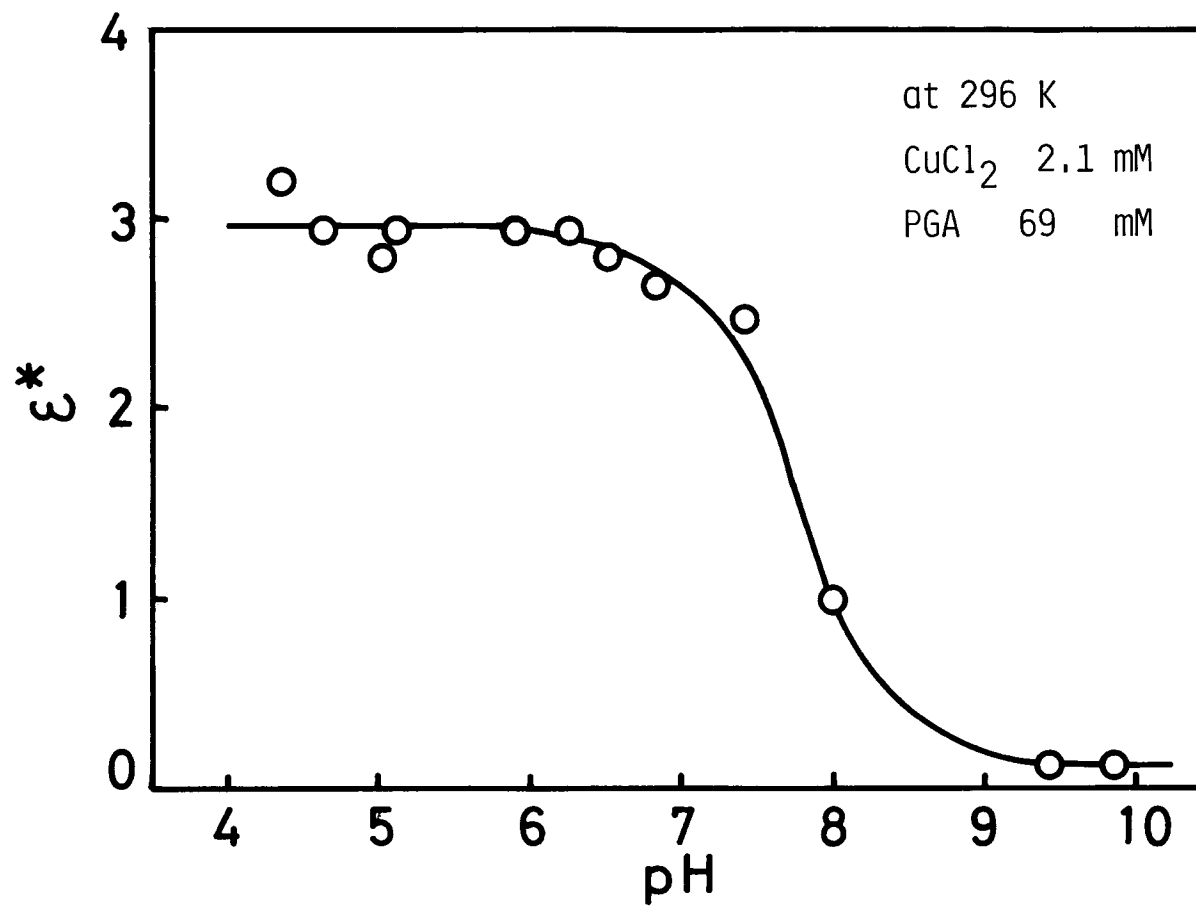


Figure IV-6. pH dependence of water-proton relaxation enhancement factor ϵ^* at 296 K: [Cu(II)]=2.1 mM, [PGA]=69 mM. All samples were prepared with 0.2 M NaCl solution.

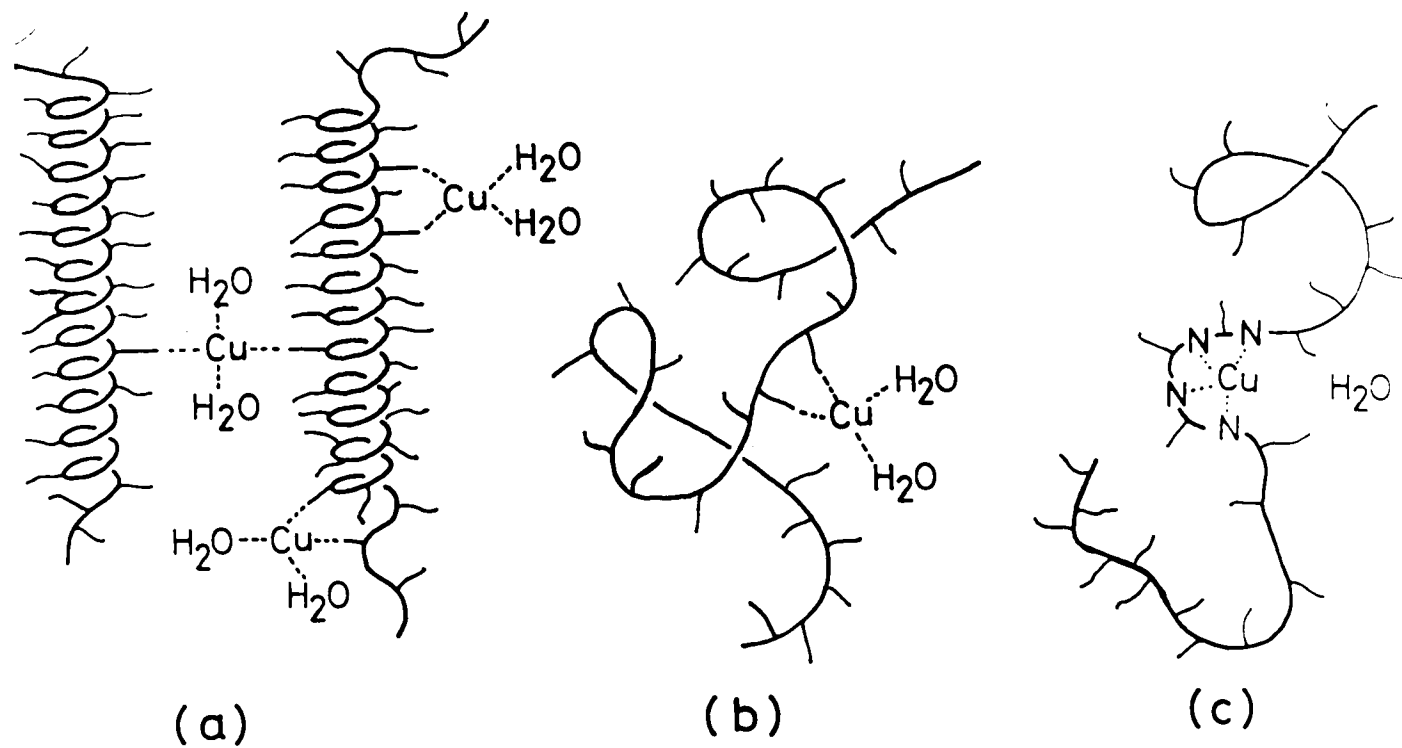


Figure IV-7. Schematic representation of Cu(II)-PGA complexes:
(a) in the acid pH region; (b) in the neutral pH region;
(c) in the alkaline pH region.

spectra, and viscosity for Cu(II) complexes with PGA, poly(L-alanine), poly(DL-alanine) that in the alkaline pH region four nitrogen atoms of the backbone are bound to Cu(II).^{24,25} Levitzki, et al., have suggested that for the Cu(II)-poly(L-histidine) complex four consecutive amide nitrogens occupy a distorted coordination square of Cu(II).⁷ The present study showed that water molecules and carboxyl groups are not bound to Cu(II) in the alkaline pH region ($\text{pH} \geq 9$). Figure IV-7 (c) shows a speculative structure of the complex at alkaline pH; only four nitrogen atoms are bound to Cu(II), and water molecules and carboxyl groups are not in the first coordination sphere of the metal ion. If nitrogen atoms are bound to Cu(II), the effect of paramagnetism should appear on ^{13}C spectrum of PGA, especially C_α and C' carbons of the backbone. However, it was not possible to observe any effect upon ^{13}C spectra. The reason for this fact is possibly as follows. The chemical exchange between the complexed and uncomplexed states is very slow, and spectra in the complexed state are too broad to be observed. Therefore, ^{13}C spectra at alkaline pH essentially consist of only the sharp resonances of uncomplexed PGA residues.

REFERENCES

1. J. Peisach, P. Aisen, and W. E. Blumberg, Eds., "The Biochemistry of Copper", Academic Press, New York, N.Y., 1966.
2. R. Malkin and Bo G. Malmstrom, *Adv. Enzymol.*, 33, 177(1970).
3. H. Irving and R. J. P. Williams, *J. Chem. Phys.*, 3192(1953).
4. M. Hatano and T. Nozawa, "Metal-Ions in Biological Systems", Vol. 5, H. Sigel, Ed., Marcel Dekker, New York, N.Y., 1976, p245.
5. I. Pecht, A. Levitzki, and M. Auber, *J. Amer. Chem. Soc.*, 89, 1587(1967).
6. M. Hatano, T. Nozawa, S. Ikeda, and T. Yamamoto, *Makromol. Chem.*, 141, 1(1971); 141, 11(1971); 141, 31(1971)
7. A. Levitzki, I. Pecht, and A. Berger, *J. Amer. Chem. Soc.*, 94, 6844(1972).
8. A. Garnier and L. Tosi, *Biopolymers*, 14, 2247(1975).
9. M. Palumbo, A. Cosani, and M. Terbojevich, and E. Peggion, *Macromolecules*, 10, 813(1977).
10. H. Takesada, H. Yamazaki, and A. Wada, *Biopolymers*, 4, 713(1966).
11. K. Fukatsu, Master thesis, Shinshu University, Ueda, 1969.
12. S. Inoue, K. Yamaoka, and M. Miura, *Bull. Chem. Soc. Japan*, 45, 1314(1972).
13. O. Iwaki, K. Hikichi, M. Kaneko, S. Shimizu, and T. Maruyama, *Polym. J.*, 4, 623(1973).
14. R. E. Wasylshen and J. S. Cohen, *J. Amer. Chem. Soc.*, 99, 2480(1977).
15. G. N. La Mar, *Chem. Phys. Letters*, 10, 230(1971).
16. R. L. Vold, J. S. Waugh, M. P. Klein, and D. E. Phelps, *J. Chem. Phys.*, 48, 3831(1968).
17. R. Freeman and H. D. W. Hill, *ibid*, 54, 3367(1970).
18. J. L. Markley, W. J. Horsley, and K. D. Klein, *ibid*, 55, 3604(1971).
19. G. G. McDonald and J. S. Leigh, *J. Magn. Resonance.*, 9, 358(1973).
20. T. J. Swift and R. E. Connick, *J. Chem. Phys.*, 37, 307(1962).
21. K. Yamaoka, T. Masujima, and S. Noji, *Polymer Preprints, Japan*, 26, 718(1977).
22. see Figure III-7 in Chapter III.
23. R. A. Bernheim, T. H. Brown, H. S. Gutowsky, and D. E. Woessner, *J. Chem. Phys.*, 30, 950(1959).

24. N. Hojo, K. Fukatsu, and T. Hayakawa, Kogyo Kagaku Zasshi (J. Chem. Soc. Japan, Ind. Chem. Sect.), 90, 823(1969).
25. N. Hojo, K. Fukatsu, T. Hayakawa, and Y. Kondo, *ibid*, 90, 827(1969).

CHAPTER V

Mn(II)-Poly(D-glutamic acid) Complex

Manganese ion was the first of metal ions used to probe the metal ion binding sites in nuclei acids¹ and enzymes.² Many subsequent applications of paramagnetic probes in the study of enzymatic mechanisms have been presented in several reviews and monographs.³⁻⁵ There are several reasons why Mn(II) has been widely applied to nuclear spin relaxation studies of biological systems:

- (1) Mn(II) is capable of activating most enzymes that normally require Mg(II) as the natural activator. Mn(II) (ionic radius 0.80 Å) and Mg(II) (0.65 Å) form similar complexes with many ligands.
- (2) Mn(II) has a labile hydration sphere ($\tau_M = 2.7 \times 10^{-8}$ sec for aquo Mn(II) at 300 K).⁶ These rapid exchange conditions permit access to structural information concerning the complexes.
- (3) Mn(II) has a large electron spin quantum number ($S=5/2$). Because the relaxation rate varies as $S(S+1)$, Mn(II) will be a more efficient "relaxer" than low-spin ions, and lower concentrations of Mn(II) may be used to effect observable relaxation.
- (4) Mn(II) has a long electron-spin relaxation time, $\tau_s \sim 10^{-9}$ sec for aquo Mn(II) complex at room temperature.⁶⁻¹⁰
- (5) Mn(II) is known to exhibit a nearly isotropic g tensor.¹¹ Mn(II) possessing half-filled electron shells has little ligand field stabilization energy and consequently will be little affected by changes in the orientation or the nature of the ligands in the complex, so that the g factor for Mn(II) may exhibit a small degree of anisotropy.

These features simplify the interpretation of the relaxation data and thereby improve the possibility of obtaining structural information.

As τ_s of Mn(II) is relatively long, EPR spectrum of the Mn(II) complex in solution is usually not difficult to observe at room temperature, so that one may obtain information on electronic structure of Mn(II) itself.

We carried out following experiments in order to obtain the detailed information concerning the interaction of Mn(II) with PGA in aqueous solution: (1) EPR measurements were made to estimate binding parameters;

(2) ^{13}C relaxation times were measured as a function of temperature at neutral pH; (3) water proton relaxation times were measured as functions of pH and temperature; (4) effect of Mn(II) upon the conformational change of PGA was studied by CD measurements. Effects of Mn(II) upon PGA was compared with those of Cu(II). This chapter is concerned with these investigations.

EXPERIMENTAL

Materials

PGA was prepared as described in the previous chapter. Analytical grade manganese(II) chloride ($\text{MnCl}_2 \cdot 4\text{H}_2\text{O}$) was purchased from Nakarai Chemicals and employed without further purification. Aliquots of MnCl_2 solution were added to PGA solution to prepare the complex. Adjustments of pH were made with 1 N NaOH and HCl. The pH was measured on a Hitachi-Horiba M-7 pH meter equipped with a combination micro-electrode (8 mm ϕ). The pH values of D_2O solution used in ^{13}C NMR measurements are direct meter readings.

^{13}C Nuclear Magnetic Resonance

All samples used for ^{13}C NMR measurements were prepared at a residual concentration of 0.83 M in 99.8% D_2O obtained from Merck. Natural-abundance proton-decoupled ^{13}C NMR spectra were obtained at 22.63 MHz using a Bruker SXP 4/100 Fourier transform spectrometer equipped with a B-NC-12 computer. A band width of 6024 Hz was used with 8 K data points. The deuterium resonance of the solvent D_2O was used for the field-frequency lock signal. The 90° pulse was 10 μsec . All measurements were carried out at controlled temperatures using a Bruker B-ST-100/700 temperature control unit. Spin-lattice relaxation time (T_1) of protonated carbons of PGA was measured by the IR method.^{12,13} Spin-spin relaxation time (T_2) was estimated from the measured line width $\Delta\nu$ by the relation of $1/T_2 = \pi\Delta\nu$. Dioxane was used as an internal standard for the reason described in the previous chapter. Chemical shift was corrected to TMS.

^1H Nuclear Magnetic Resonance

Samples used for measuring the isotropic contact shift of the water proton contain 91% (v/v) D_2O , 7% H_2O , and 2% dioxane. PGA residual concentration was 0.135 M. ^1H spectra were obtained at 90 MHz using a Bruker SXP 4/100 spectrometer with internal deuterium lock. A band width of 1000 Hz was employed with 8 K data points, using a B-NC-12 computer. The paramagnetic isotropic contact shift of the water proton was measured by the method of Led and Grant.¹⁴

It is difficult to measure directly the frequency shift of water proton signal induced by Mn(II) because of the broad signal induced also

by Mn(II). Instead it was obtained as the negative value of the frequency shift of the sharp, well-defined proton signal from the internal dioxane standard, which was observed when the signal from the internal D₂O was used as a lock signal. Under this lock system the addition of the paramagnetic ion changes the magnetic field by an amount corresponding to sum of the bulk susceptibility shift and the isotropic contact shift of the D₂O signal. This leaves the chemical shift of the H₂O signal unchanged relative to the lock when comparing samples and without paramagnetic ions, while the proton signal from the internal dioxane, which is only affected by the change in bulk susceptibility, will be shifted by an amount corresponding to the isotropic contact shift of the H₂O signal but in the opposite direction. Contrary to the H₂O signal the D₂O line is sufficiently narrow at the paramagnetic ion concentration used here to constitute a well-defined lock signal.

Samples for water proton relaxation times were prepared with redistilled and deionized H₂O in 0.2 M NaCl solution. The samples were purged with water-saturated N₂ gas for 20 min and sealed off. Measurements of water proton relaxation times were carried out at 90 MHz using a Bruker SXP 4/100 spectrometer equipped with a Bruker external stabilizer B-SN-15 by water proton lock. The 90° pulse was 8 μsec. T₁ of water proton was obtained using the Carr-Purcell 180°-τ-90°-T- pulse sequence¹⁵ generated by a Bruker pulse gated integrator. T₂ was determined using the Meiboom-Gill modification¹⁶ of a Carr-Purcell pulse sequence, 90°-τ-180°-[-τ -(echo)-τ-180°-τ-(echo)-]-.

Circular Dichroism

Circular dichroism measurements were made with a JASCO J-20 spectropolarimeter at 300 K, using path length of 1 mm. Solutions measured were the same ones used in the water proton relaxation measurements.

Electron Paramagnetic Resonance

All samples for electron paramagnetic resonance (EPR) measurements were prepared at PGA residual concentration of 85 mM for metal ion titration experiments (M-titration) and 170 mM for pH titration experiments. All solutions contain 0.2 M NaCl. A series of reference samples at the same Mn(II) ion concentration but containing no PGA were prepared. The solution was placed in a 0.75 mm i.d. quartz capillary tube.

EPR measurements were carried out on a JEOL JEX-X/K at 9.2 GHz (X-band) at room temperature.

The total amplitude of each spectrum was measured by adding peak heights of the six-peak EPR signal (see Figure V-1). The free Mn(II) concentration for each sample was calculated from the relative signal amplitude with respect to the reference sample.¹⁷

The binding parameters for the Mn(II)-PGA complex were determined using EPR technique by titrating the PGA solution with Mn(II) (M-titration).^{2,17,18} The dissociation constant K_d and the number of binding sites per PGA residue n are determined by the following equation.¹⁹

$$\frac{[\text{PGA}]_t}{[\text{Mn}]_b} = \frac{K_d}{n} \frac{1}{[\text{Mn}]_f} + \frac{1}{n}, \quad (5.1)$$

where $[\text{Mn}]_f$ and $[\text{Mn}]_b$ are the concentrations of free and bound metal ions, respectively, $[\text{PGA}]_t$ is the total PGA residual concentration. A plot of $[\text{PGA}]_t/[\text{Mn}]_b$ vs. $1/[\text{Mn}]_f$ yields values of n and K_d which can be obtained graphically.

RESULTS AND DISCUSSION

Estimation of n and K_d

The EPR spectra of Mn(II) in the absence and presence of PGA are displayed in Figure V-1. The spectrum of aquo Mn(II) complex consists of six lines of slightly different intensities and line width due to the hyperfine interaction of the electron spin with the nuclear spin ($S=5/2$). For hexaaquo Mn(II) complex the cation is in a perfectly symmetric and isotropically averaged environment, and each of the six lines is a superposition of the five electron-electron fine transitions that occurs between the six electronic energy levels. Mn(II) bound to macromolecule is always difficult to observe when free Mn(II) is present. This phenomenon has been attributed to the inability of the slow molecular motion of macromolecule to isotropically average out static distortions prevalent in macromolecule complexes resulting in an extremely asymmetric electronic environment.²⁰

When PGA is added to Mn(II) solution, the intensity of signal drastically decreases as shown in Figure V-1 (b), suggesting that Mn(II) binds to PGA. The unchanged line-shape spectrum for the Mn(II)-PGA system also suggests that the electronic environment of the metal ion is still quite isotropic, showing the absence of displaced fine structure transition due to zero field splitting.

The number of metal ion binding sites n and their dissociation constant K_d were determined by the method of M-titration at pH 7.8 and at room temperature. A solution containing 85 mM PGA was titrated with variable amount of Mn(II) solution (4-16 mM). The results are shown in Figure V-2, using eq 5.1. The plot gives a straight line, indicating that the presence of only one type of binding sites with equivalent binding constant. The average values of n and K_d obtained are 0.3 and 2×10^{-3} M, respectively. The value of n means that about three residues of ten residues of PGA are able to bind to one metal ion.

Estimation of $q(H_2O)$ and $A(H_2O)$

If $\tau_M^{-2} \gg T_{2M}^{-2}$ and $\Delta\omega_M^{-2}$, eq 2.11 can be reduced to

$$\Delta\omega = fq\Delta\omega_M, \quad (5.2)$$

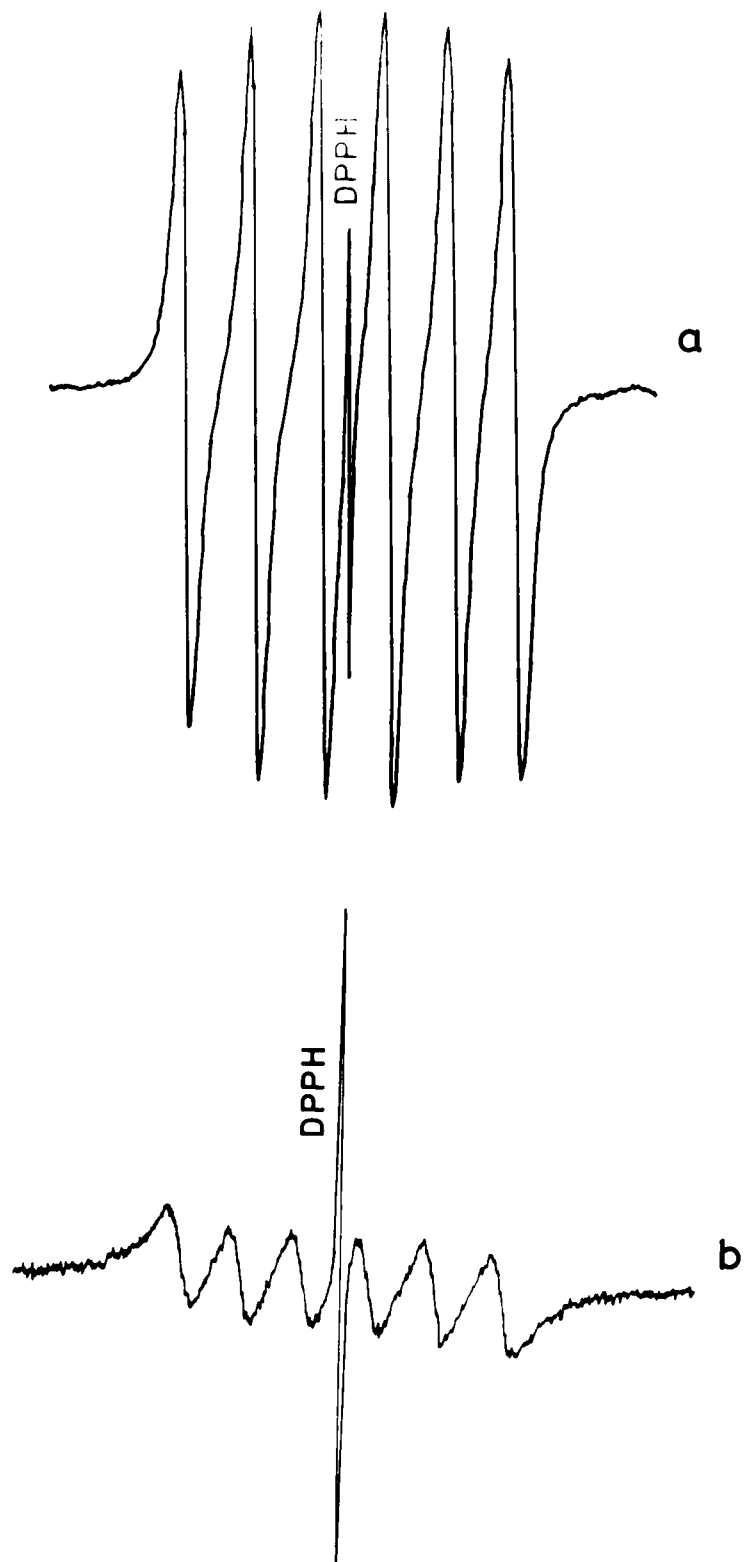


Figure V-1. EPR spectra of Mn(II) (8.3 mM) at room temperature and at pH 7.0: (a) [PGA]=0 mM; (b) [PGA]=170 mM. All samples were prepared in 0.2 M NaCl solution. DPPH (2,2-diphenyl-1-picrylhydrazyl) was used as an external reference.

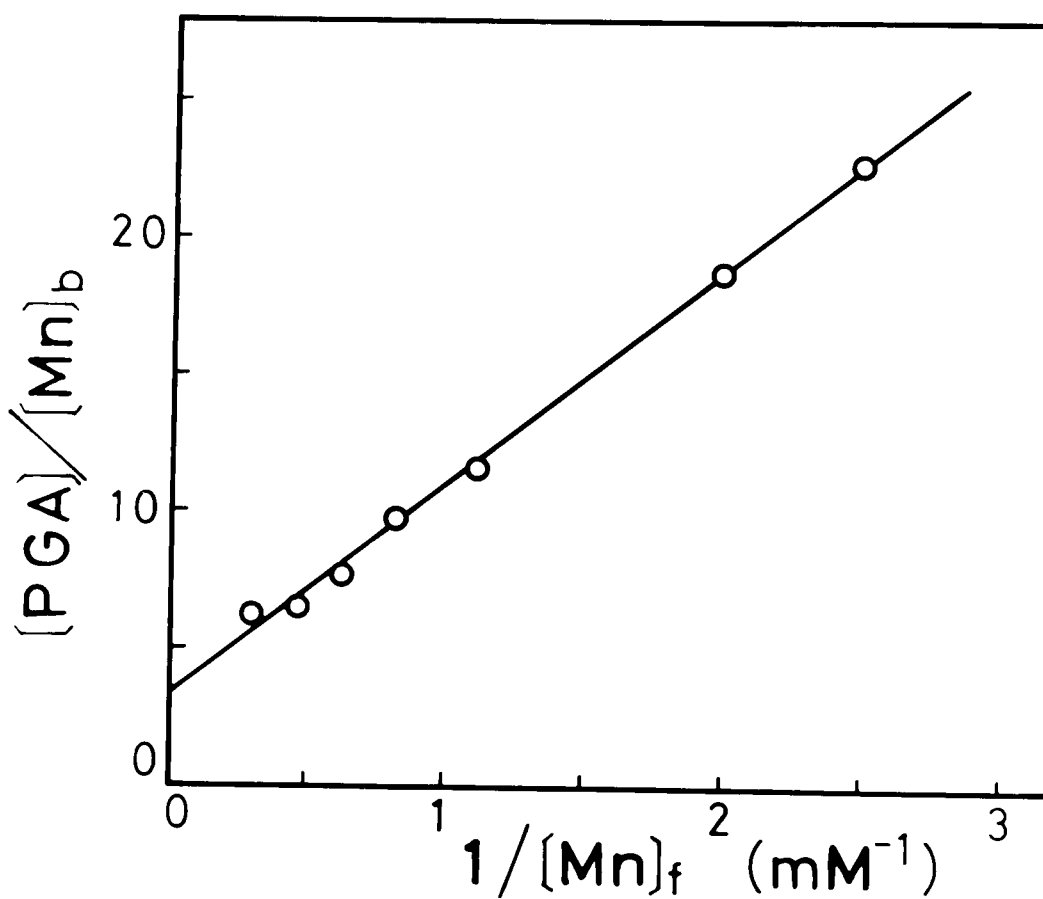


Figure V-2. Hughes and Klotz plot of the data obtained from an EPR titration experiment: $[PGA]=85 \text{ mM}$, $[Mn(II)]=4\text{-}16 \text{ mM}$.

which has the Curie law temperature dependence according to eq 2.1. The simple Curie law exhibited by the isotropic contact shift of water protons is only compatible with eq 2.11. The electron-water proton hyperfine coupling constant $A(\text{H}_2\text{O})$ was obtained from the contact shift data for the protons in the absence of PGA presented in the upper curve of Figure V-3. A value of A/h was estimated to be 6.5×10^5 Hz for $f=2.0 \times 10^{-4}$ and $q(\text{H}_2\text{O})=6$. The contact shift of water proton decreased by the addition of PGA as shown in lower curve of Figure V-3. This indicates that the first coordination sphere of Mn(II) is partly occupied by PGA molecules. Using the value of $A(\text{H}_2\text{O})/h$ obtained above and $f=2.1 \times 10^{-4}$, the number of coordinated water molecules to Mn(II), $q(\text{H}_2\text{O})$, was found to decrease from 6 to 3.7 ± 0.2 upon the addition of PGA. Thus PGA residues of 2.3 ± 0.2 are bound to Mn(II). In view of the charge compensation it appears reasonable to assume that each Mn(II) on an average binds two PGA residues and four water molecules.

^{13}C Nuclear Magnetic Resonance

Figure V-4 shows ^{13}C NMR spectra of PGA in the absence and presence of Mn(II) at pH 7.1 and at 304 K. This figure illustrates the selective broadening of ^{13}C resonances, particularly, the carboxyl carbon C_δ .

It is found that upon the addition of a trace of Mn(II) C_δ , C_γ , and C_β resonances of the side chain show broadenings, and that C_α and C' resonances are not affected at Mn(II) concentrations studied. These observations indicate that there is a specific interaction of Mn(II) with the carboxyl group of the side chain of PGA. Paramagnetic induced shifts were not able to be observed beyond broadening for any resonances.

Figure V-5 shows the temperature dependence of $1/fT_{2p}$ for C_δ , C_γ , and C_β carbons and that of $1/fT_{1p}$ for C_γ carbon. It is apparent that each relaxation rate decreases with increasing temperature. This result indicates that T_{1p} and T_{2p} are controlled by T_{1M} , T_{2M} , respectively, rather than T_M , i.e., T_{1M} , $T_{2M} \gg T_M$ in eq 2.12 and 2.14 (fast exchange). For C_γ carbon the relation of $T_{1p}/T_{2p} \gg 1$ holds in all temperature range studied, indicating that the scalar relaxation is dominant in T_{2M} , while T_{1M} is dominated by the dipolar relaxation. In this case the paramagnetic broadening no longer shows the dependence of r^{-6} in eq 4.2.

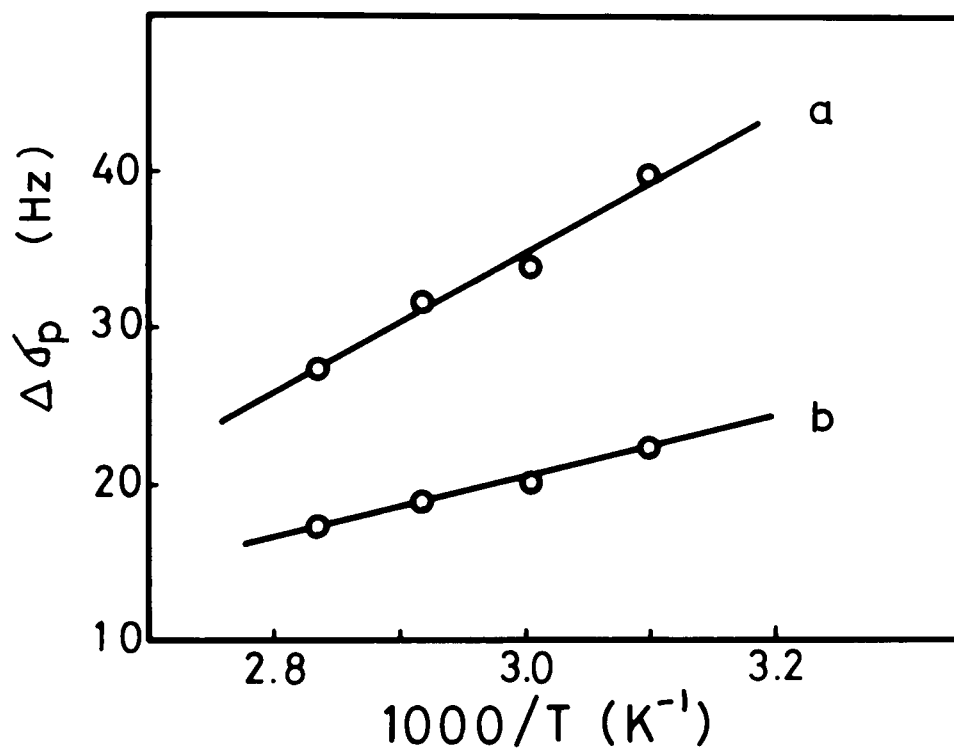


Figure V-3. Temperature variation of the isotropic contact shift of water proton at pH 7.0: (a) $[Mn(II)]=11$ mM; (b) $[Mn(II)]=11$ mM, $[PGA]=136$ mM.

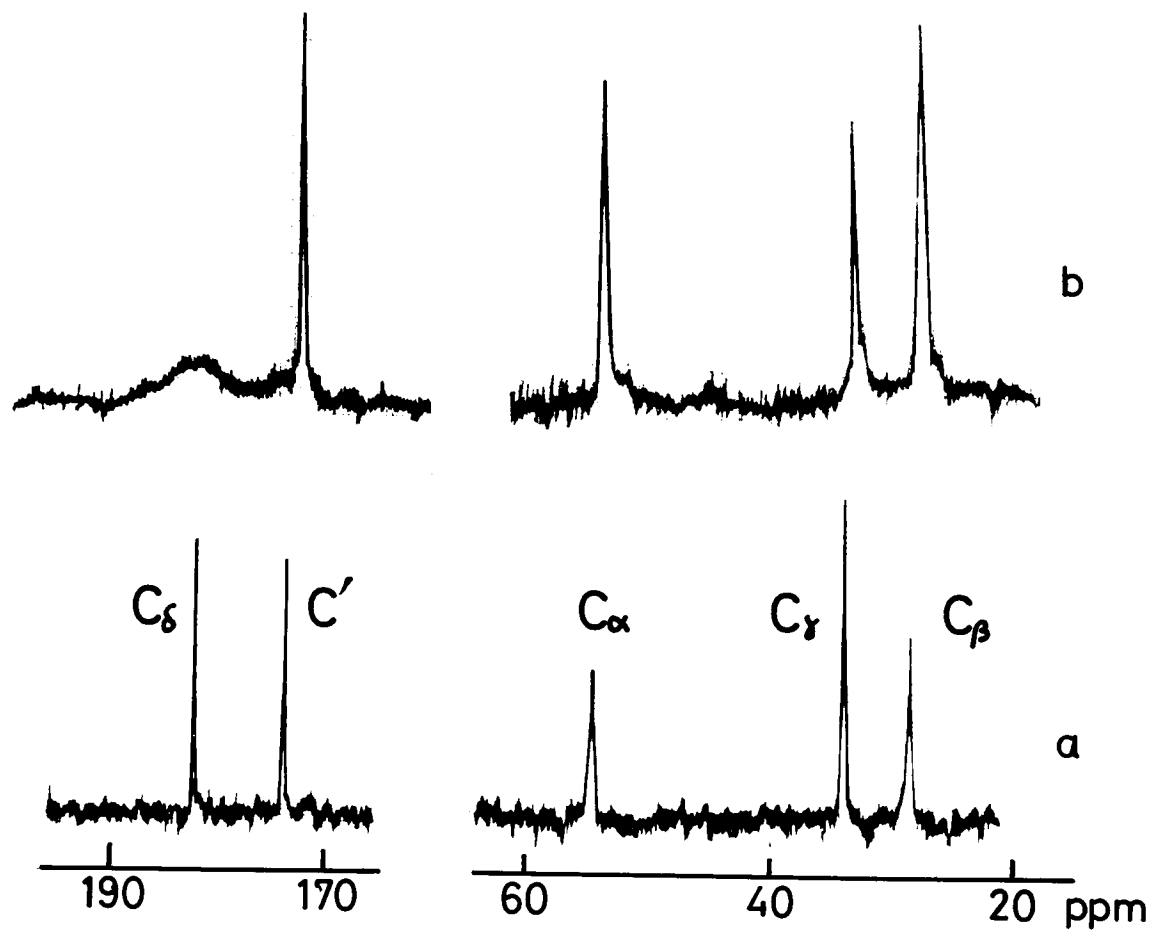


Figure V-4. Effect of Mn(II) on ^{13}C NMR spectra of PGA (0.83 M in monomer unit) at 304 K: (a) PGA only; (b) $f = [\text{Mn}]/[\text{PGA}] = 2.44 \times 10^{-4}$.

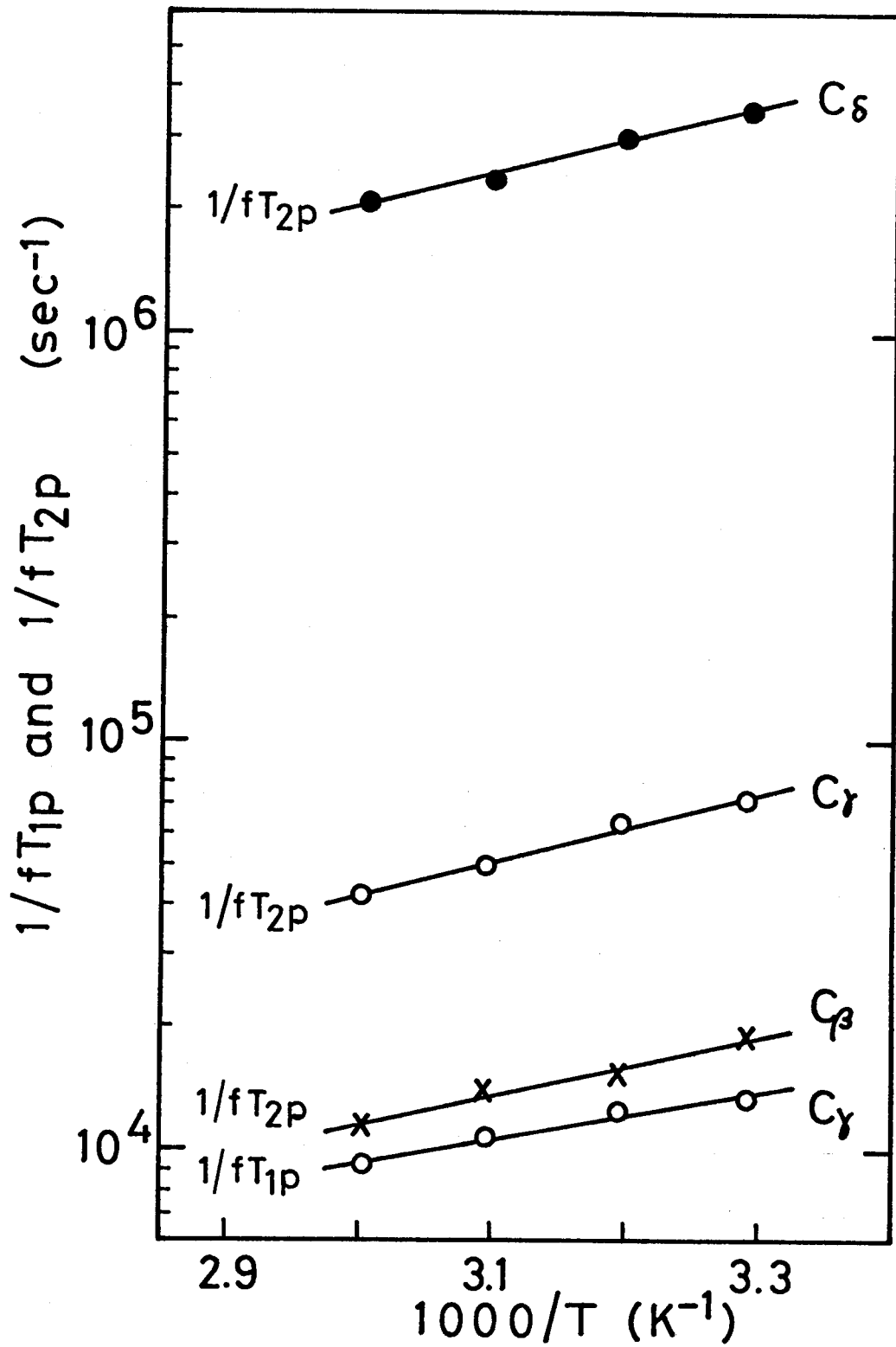


Figure V-5. Temperature variation of $1/fT_{1p}$ and $1/fT_{2p}$ at $f=5.17 \times 10^{-4}$.

Under the conditions of fast exchange ($T_{1M} \gg \tau_M$ and $\omega_I^2 \tau_c^2 \ll 1$) eq 4.1 can be reduced to

$$\frac{1}{T_{1p}} = \frac{7fq}{2} \frac{\gamma_I^2 g^2 \beta^2}{r^6} \tau_c \quad (5.3)$$

The distance between carbon atom and manganese ion can be evaluated from eq 5.3 if τ_c is known. It was found from Figure V-5 to be $\tau_M \ll T_{2M} \simeq 6 \times 10^{-7}$ sec at 304 K. For complexes of Mn(II) τ_e is nearly equal to the electron spin relaxation; $\tau_e = \tau_s \simeq 10^{-9}$ sec.⁶⁻¹⁰ If the rotational correlation time of the metal-carbon vector is roughly approximated to be the same order of magnitude as the rotational correlation time of the C-H bond in metal-free PGA, then τ_R at 304 K is evaluated to be 1.6×10^{-10} sec for C_γ carbon from eq 3.1. This value therefore yields $\tau_c^{-1} = \tau_R^{-1} = 6.3 \times 10^9$ sec⁻¹. Furthermore we assume $q(\text{PGA})=2$. On these assumptions the distance between C_γ carbon and manganese was estimated to be $3.3 \pm 1.5 \text{ \AA}$ from eq 5.3 at pH 7.1 and at 304 K. The same calculation yields a value of $> 3.5 \pm 1.5 \text{ \AA}$ as the distance between C_β and Mn(II).

Under the conditions of $T_{1M}, T_{2M} \gg \tau_M$ and $\Delta\omega_M^2 \ll (T_{2M} \tau_M)^{-1}$, the combination of eq 4.1 and 4.2 yields

$$\frac{1}{T_{2p}} = \frac{7}{6} \frac{1}{T_{1p}} + \frac{35fq}{12} \left(\frac{A}{h}\right)^2 \tau_e \quad (5.4)$$

Only the ratio of A for each carbon can be evaluated from this equation, since the accurate value of τ_e is not known. Using the observed values of T_{2p}, T_{1p}, f , and $q=2$, we obtain $|A(C_\beta)/A(C_\gamma)|=0.3$ and $|A(C_\alpha)/A(C_\gamma)|=0$ at pH 7.1 and at 304 K. These results suggest that there is small amount of electron spin density which is transferred to C_β from Mn(II). If we assume very roughly $\tau_e \simeq 10^{-9}$ sec,⁶⁻¹⁰ $|A(C_\gamma)/h|=10^5$ Hz and $|A(C_\beta)/h|=10^4$ Hz are obtained. It is of interest to note that unpaired spin density induced on C_γ carbon is much smaller for Mn(II) than for Cu(II) as shown in Chapter IV.

Water Proton Relaxation Rate

Figure V-6 shows the temperature dependence of $1/T_{1p}$ and $1/T_{2p}$ of

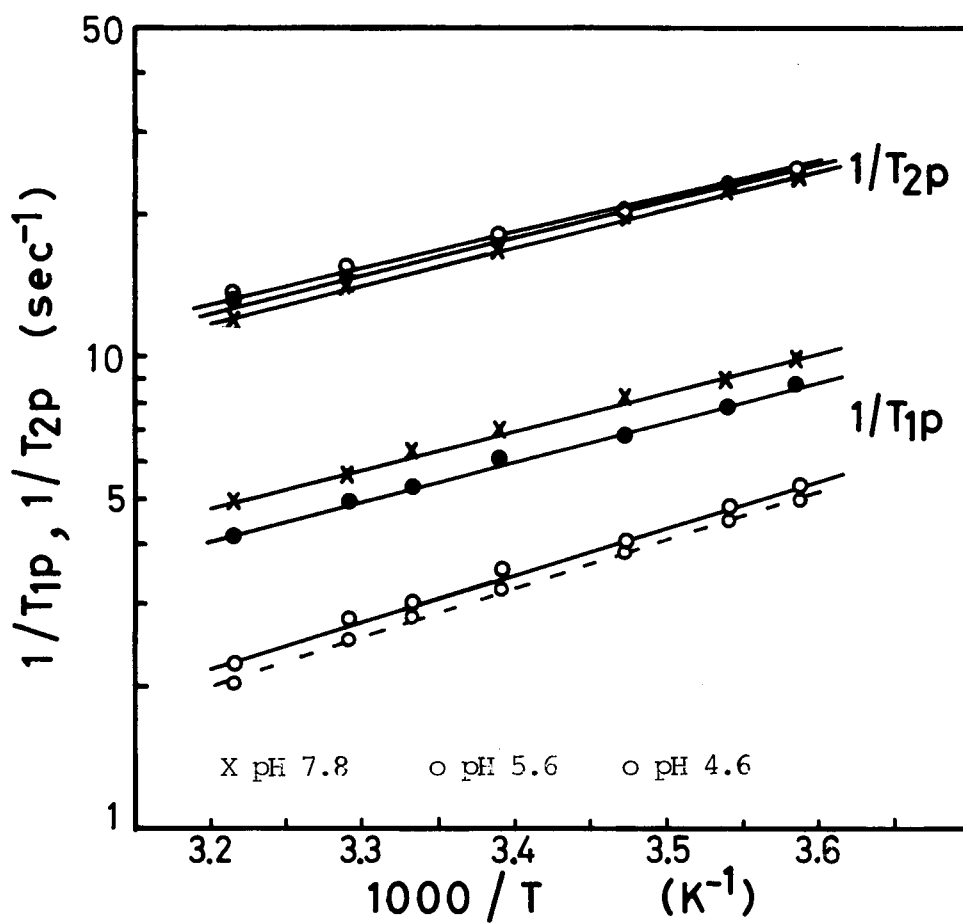


Figure V-6. Temperature variation of $1/T_{1p}$ and $1/T_{2p}$ of water proton: $[Mn(II)]=0.52$ mM, $[PGA]=10.2$ mM. The dotted line represents the variation of aquo Mn(II). All samples were prepared in 0.2 M NaCl solution.

water proton of the Mn(II)-PGA-H₂O system at several pH's. The values of $1/T_{1p}$ for aquo Mn(II) are plotted together in Figure V-6. A comparison of the data indicates that in both cases of the presence and absence of PGA relaxation rates behave in quite same way: these values vary linearly with temperature. The value of $1/T_{1p}$ of the Mn(II)-PGA complex is larger than that of aquo Mn(II) complex. These results imply that the correlation time of tumbling motion of water molecules bound to Mn(II) is larger in the presence of PGA than in the absence of PGA because of the binding of Mn(II) to PGA, and that Mn(II) bound to PGA possesses water molecules in the first coordination sphere.

In all pH region studied, both relaxation rates monotonously decrease with increasing temperature. This fact tells us that the system is in the fast exchange limit, that is, $T_{1M}, T_{2M} \gg \tau_M$ in eq 2.12 and 2.14. The value of T_{1p}/T_{2p} is larger than unity and is about 2.4 in all temperature range studied. In the fast exchange limit, the fifty-fifty contribution to T_{2M} from dipolar and scalar interactions yields $T_{1p}/T_{2p}=2.33$. Thus, the observed ratio greater than 2.33 indicates that the dipolar term is not the dominant contribution to T_{2M} , but the scalar relaxation is dominant.

Comparisons of the Mn(II)-PGA complex with the hexaaquo Mn(II) are now made in Table V-I at pH 7.8 and at 300 K. There are six water molecules in the first coordination sphere of the metal ion in the case of aquo Mn(II), while for the Mn(II)-PGA complex the number of hydration decrease to four. Here, an average value of 2.87 Å was assumed for the Mn(II)-water proton distance in computing the parameters in Table V-I.²² The distance between the water proton and the Mn(II) has been reported to be 2.815-2.923 Å.²¹ Under the conditions of fast exchange, the correlation time of water proton for the Mn(II)-PGA complex was calculated to be 1.1×10^{-10} sec from eq 5.3 using $q(H_2O)=4$ and $r=2.87$ Å. This value of 1.1×10^{-10} sec is larger than that in the absence of PGA. The best-fit activation energy E_R was 3.7 kcal/mol using eq 2.7, assuming that the value of q does not change in the temperature range studied.

Using values of $A(H_2O)$ and q obtained above, a value of τ_e was estimated to be 4.2×10^{-9} sec at 300 K from eq 5.4. As $\tau_e^{-1} \ll \tau_c^{-1}$, τ_c is equal to the correlation time of tumbling motion of the complex τ_R in all temperature range studied. Assuming that τ_s in the Mn(II)-PGA complex is the same as in the aquo Mn(II) complex, the value of τ_M of 5×10^{-9} sec at 300 K

Table V-I. Comparison with parameters for water molecules in PGA-Mn(II) and hexaaquo Mn(II) complexes at 300 K and at pH 7.8

	PGA-Mn(II)-H ₂ O	Mn(II)(H ₂ O) ₆
τ_R (sec)	1.1×10^{-10}	3×10^{-11} *
E_R (kcal/mol)	3.7	4.5 *
τ_M (sec)	5×10^{-9} ***	2.5×10^{-8} *
E_M (kcal/mol)	6	7.5 *
q(H ₂ O)	4	6
A(H ₂ O)/h (Hz)	6.5×10^5	6.3×10^5 **

* Reference 23.

** Reference 9.

*** See the text.

can be obtained from eq 2.6. The temperature dependence of τ_M gave $E_M = 6$ kcal/mol. The value of E_M obtained is close to the value for the aquo Mn(II). This suggests that water molecules can readily exchange between the first coordination sphere of Mn(II) bound to PGA and the bulk solvent.

As the coordination number of q is not known at each pH, we can not estimate the thermodynamic and kinetic parameters about the Mn(II)-PGA complex in the present study. However, as will be described below, since Mn(II) is released from PGA with decreasing pH, the values of these parameters will approach to those of the aquo Mn(II) complex.

pH Dependence of Complex

In Figure V-7 the water-proton relaxation enhancement factor ϵ^* is plotted against pH at 300 K. The value of ϵ^* is a constant of 2.2 above pH 6. With decreasing pH, ϵ^* sharply decreases and approaches to unity. This fact suggests that the coordination number of water molecules per Mn(II) changes from four to six, that is, PGA does not bind to Mn(II) at all, and that the correlation time of water molecule for Mn(II)-PGA complex decreases to that of the aquo Mn(II) complex.

CD measurements at 222 nm were carried out at 300 K. The experimental conditions are same as the measurements of ϵ^* . The results are shown in Figure V-8 against pH. With decreasing pH, $[\theta]_{222}$ increases indicating that the conformation of PGA in aqueous solution containing Mn(II) changes from coil to helix. The helix-coil transition region was not affected by the presence of Mn(II) at least at concentrations studied here.

The fraction of free Mn(II) existing in the Mn(II)-PGA-H₂O system is plotted against pH in Figure V-9. The concentration of free Mn(II) was measured by EPR method. There is little free Mn(II) in the system above pH 6. With decreasing pH, the fraction of free Mn(II) increases. This fact indicates that Mn(II) is released from PGA at acid pH.

These results obtained lead to the following conclusions. Mn(II) is bound to the carboxyl groups of PGA in neutral pH region. When pH decreases, Mn(II) is released from the carboxyl groups and consequently the concentration of free Mn(II) increases. This fact is in contrast with that in the Cu(II)-PGA complex. In Mn(II)-PGA complex, PGA changes its conformation from coil to helix with decreasing pH as in the absence of Mn(II).

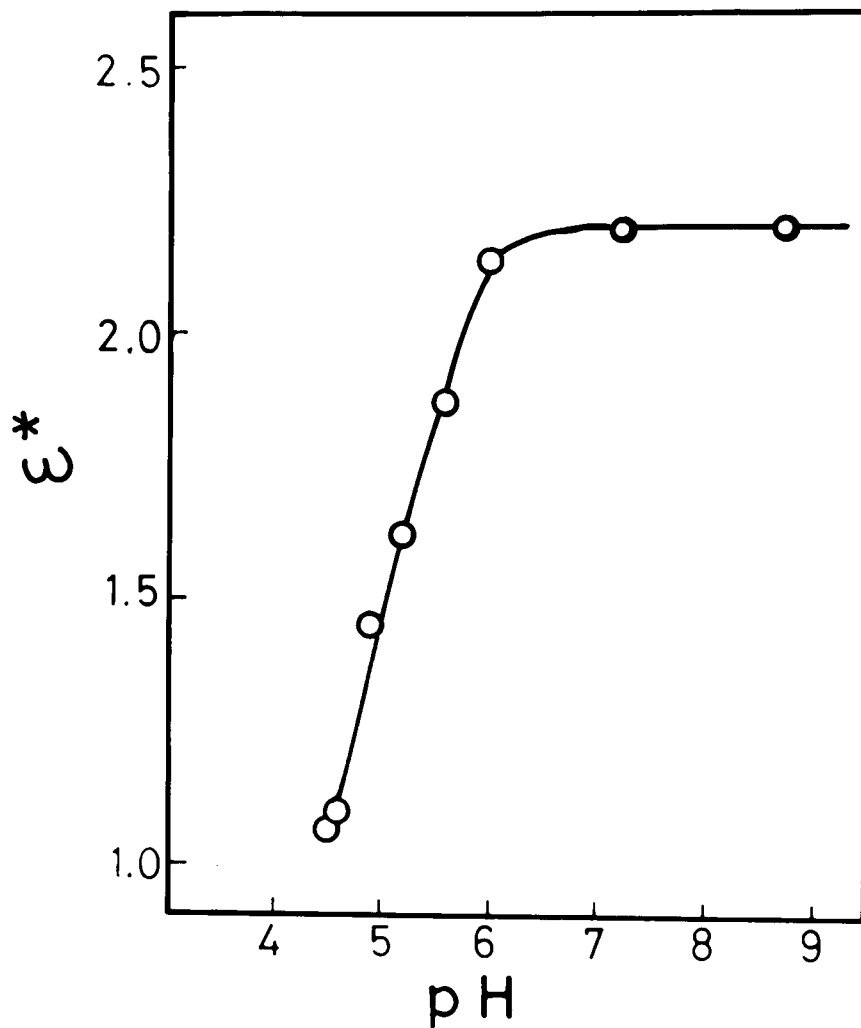


Figure V-7. pH dependence of ϵ^* at 300 K: $[\text{Mn(II)}]=0.52$ mM, $[\text{PGA}]=10.2$ mM. All samples were prepared in 0.2 M NaCl solution.

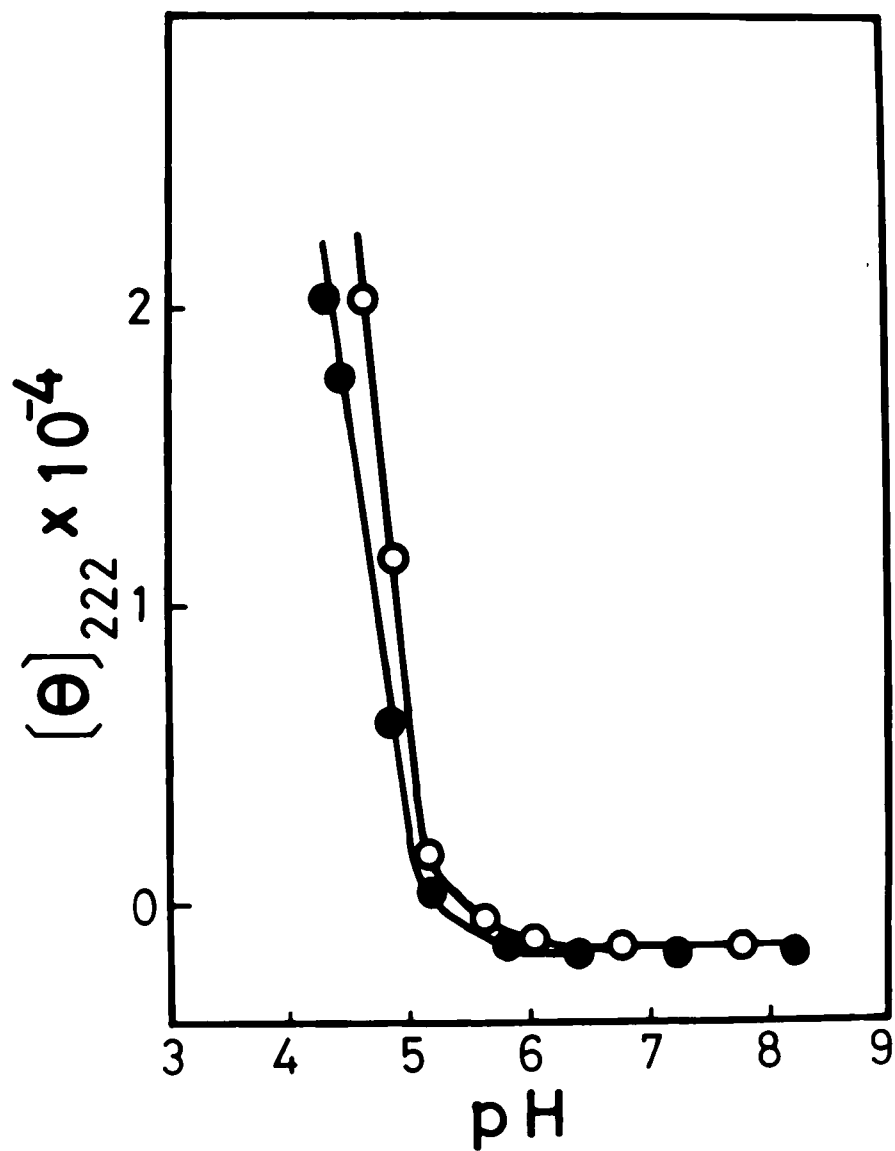


Figure V-8. pH dependence of $[\theta]_{222}$ at 300 K:
 (o) poly(D-glutamic acid) + Mn(II);
 (●) poly(D-glutamic acid) only.
 All samples were same as shown in Figure V-7.

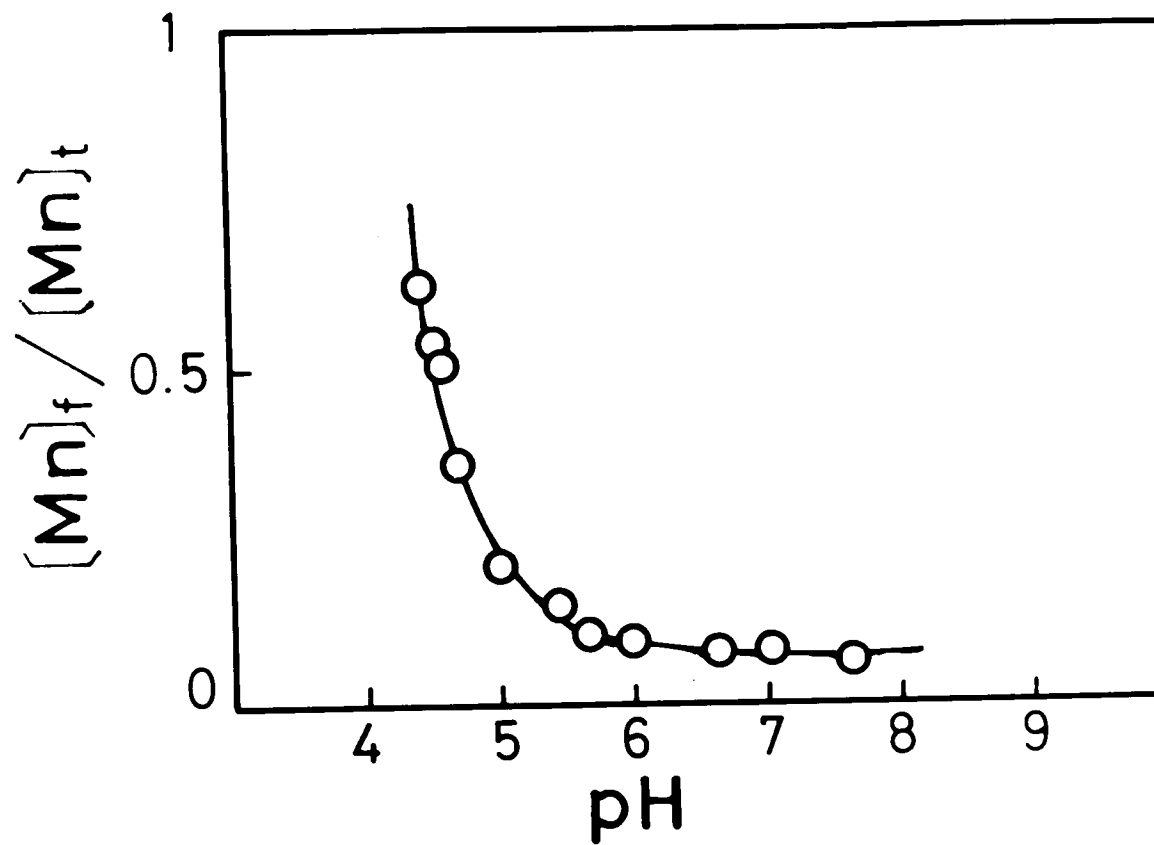


Figure V-9. pH dependence of the free manganese ion for Mn(II)-PGA complex at room temperature: $[Mn(II)] = 8.3 \text{ mM}$, $[PGA] = 170 \text{ mM}$.

REFERENCES

1. J. Eisinger, R. G. Shulman, and B. M. Szymansky, *J. Chem. Phys.*, 36, 1721(1962).
2. M. Cohn and J. R. Leigh, *Nature*, 193, 1037(1962).
3. A. S. Mildvan and M. Cohn, *Adv. Enzymol.*, 33, 1(1970).
4. R. A. Dwek, "Nuclear Magnetic Resonance in Biochemistry", Clarendon Press, Oxford, 1973, chapter 9-11.
5. K. Wüthrich, "NMR in Biological Research", North-Holland, Amsterdam, 1976, chapter 6.
6. T. J. Swift and R. E. Connick, *J. Chem. Phys.*, 37, 307(1962).
7. M. Tinkham, R. Weistein, and A. F. Kip, *Phys. Rev.*, 84, 848(1951).
8. R. S. Codrington and N. Bloembergen, *J. Chem. Phys.*, 29, 600(1958).
9. Z. Luz and R. G. Shulman, *ibid*, 43, 3750(1965).
10. A. R. Peacocke, R. E. Richards, and B. Sheard, *Mol. Phys.*, 16, 177(1969).
11. B. R. McGarvey, *Transition Met. Chem.*, 3, 89(1966).
12. R. L. Vold, J. S. Waugh, M. P. Klein, and D. E. Phelps, *J. Chem. Phys.*, 48, 3831(1968).
13. R. Freeman and H. W. D. Hill, *ibid.*, 54, 3367(1970).
14. J. J. Led and D. M. Grant, *J. Amer. Chem. Soc.*, 97, 6962(1975).
15. H. Y. Carr and E. M. Purcell, *Phys. Rev.*, 94, 630(1954).
16. S. Meiboom and D. Gill, *Rev. Sci. Instrum.*, 29, 688(1958).
17. M. Cohn and J. Townsend, *Nature*, 173, 1090(1954).
18. A. S. Mildvan and J. L. Engle, *Methods Enzymol.*, 26, 654(1972).
19. T. R. Hughes and I. M. Klotz, "Methods of Biochemical Analysis", Vol III, D. Glick, Ed., Interscience Publishers Inc., New York, N.Y., 1956, p265.
20. G. H. Reed and M. Cohn, *J. Biol. Chem.*, 245, 662(1970).
21. H. Montgomery, R. V. Chastain, and E. C. Lingafelter, *Acta. Crystallogr.*, 20, 731(1966).
22. J. Reuben and M. Cohn, *J. Biol. Chem.*, 245, 6539(1970).
23. N. Bloembergen and L. O. Morgan, *J. Chem. Phys.*, 34, 842(1961).

CHAPTER VI

Co(II)- and Ni(II)-Poly(D-glutamic acid) Complexes

Differing from Mn(II) and Cu(II), some paramagnetic ions such as Co(II), Ni(II), Fe(II), low spin Fe(III), and lanthanide ions except for Gd(III) have short τ_s (10^{-12} - 10^{-13} sec) in aqueous solution at room temperature.¹ EPR signals of these ions are very broad, and these ions have little effect on the NMR line width and cause large paramagnetic shift of ligand nuclei. In the system containing these ions the correlation time τ_c is no longer determined by τ_R . Instead, τ_c is determined by τ_s . So far, paramagnetic shift observed for the complexes of Co(II) and Ni(II) have provided information concerning the electronic structure of ligand, rather than the dynamic properties of the complex.²

McDonald and Phillips have used Co(II) as a paramagnetic probe to improve the resolution in the higher field region of the ^1H NMR spectrum of lysozyme.³ It has been observed that some resonances are shifted to higher field, some to lower field. The magnitude of the shifts are quite different for different resonances, and the Co(II)-induced shifts increase with increasing Co(II) concentration. They have shown that the binding sites of Co(II) and the structure of the metal environment. Iwaki, et al., have suggested the binding sites of Co(II) and Ni(II) for PGA in the neutral pH region from the results of ^1H NMR.⁴

Of particular interest is transfer mechanism of unpaired electron spin density. Taking account of the large contribution of the carbon orbitals to the electron-spin containing molecular orbitals of the paramagnetic complex and in view of the difference between the gyromagnetic ratios of ^{13}C and ^1H , it would be expected that ^{13}C NMR measurements provide unique information about electron-spin delocalization in the paramagnetic system.²

In this chapter we will focus on ^{13}C chemical shift and line width of the Co(II)-PGA and Ni(II)-PGA complexes in aqueous solution which were measured as functions of metal concentration, temperature, and pH in order to compare with the results of ^1H NMR measurements.

EXPERIMENTAL

PGA was prepared as described in Chapter III. Analytical grade $\text{CoCl}_2 \cdot 6\text{H}_2\text{O}$ and $\text{NiCl}_2 \cdot 6\text{H}_2\text{O}$ purchased from Nakarai Chemicals were used without further purification. Aliquots of the metal solution were added to PGA solution to prepare the complex. Adjustments of pH were made with DC1 obtained from Merck. The pH was measured on a Hitachi-Horiba M-7 pH meter equipped with a combination micro-electrode (8 mm ϕ). The pH value is direct meter reading.

Natural-abundance proton-decoupled ^{13}C NMR spectra were obtained at 22.63 MHz using a Bruker SXP 4/100 spectrometer equipped with a B-NC-12 computer. A band width of 6024 Hz was used with 8 K data points. Solvent D_2O was served as the internal lock. All measurements were carried out at controlled temperatures using a Bruker B-ST-100/700 temperature control unit. Dioxane was used as an internal standard. Chemical shift was corrected to TMS. Spin-spin relaxation time (T_2) was estimated from the line width $\Delta\nu$ by the relation of $1/T_2 = \pi\Delta\nu$. A 90° pulse used was 9.5 μsec .

RESULTS AND DISCUSSION

^{13}C NMR spectra of PGA are shown in Figure VI-1 against Co(II) concentration at pH 7.1 and at 304 K. The bottom spectrum is the one of PGA in the absence of Co(II). It is apparent that the addition of Co(II) causes shift and broadening of ^{13}C resonances, especially of C_δ and C_γ resonances, and that shift and broadening markedly depend on the metal ion concentration. The effect of addition of Ni(II) is shown in Figure VI-2. It is obvious that for the Ni(II)-PGA system C_δ and C_γ resonances broaden at smaller f as compared with the Co(II)-PGA system. These results obtained are apparently caused by unpaired electron spin of Co(II) and Ni(II). It is reasonable to assume that these metal ions form complexes with PGA. The carboxyl groups of the side chain are participated to form the complex at metal concentrations studied.

Figure VI-3 shows the metal ion concentration dependence of paramagnetic shift of the Co(II)-PGA system. With increasing f ($[\text{Co(II)}]/[\text{PGA}]$), all the resonances shift downfield in the order of $\text{C}_\gamma > \text{C}_\delta > \text{C}_\beta > \text{C}_\alpha, \text{C}'$. These paramagnetic shifts vary linearly with f . Paramagnetic shifts are also found to be more effective at pH 7.1 than at pH 4.7-4.8. This result is due to the difference in conformation and/or the degree of ionization of the carboxyl group. It is clear that even in the helix state Co(II) interacts with the carboxyl groups of PGA. In Figure VI-4 is shown the paramagnetic broadening $\Delta\nu_p$ for C_γ and C_δ resonances, showing the linear variation of f . It is difficult to observe the broadening for C_α and C' at Co(II) concentration studied.

In Figure VI-5 is shown the paramagnetic shift against f for C_β , C_γ , and C_δ resonances. Since C_γ resonance markedly broadened and further addition of Ni(II) made the observation of the paramagnetic shift of C_γ difficult due to the severe broadening, only one point of f was shown in the figure. For C_α and C' any paramagnetic shift could not be observed at Ni(II) concentration used. C_β and C_δ resonances shift downfield, while C_δ shifts upfield. Observed paramagnetic shift is also a linear function of f .

Iwaki, et al.,³ have shown from ^1H NMR measurements that Co(II) interacts the carboxyl group of the side chain as well as the amide group of the backbone. Although the metal concentration used in this study is lower than in ^1H NMR study, results of ^{13}C NMR obtained here do not

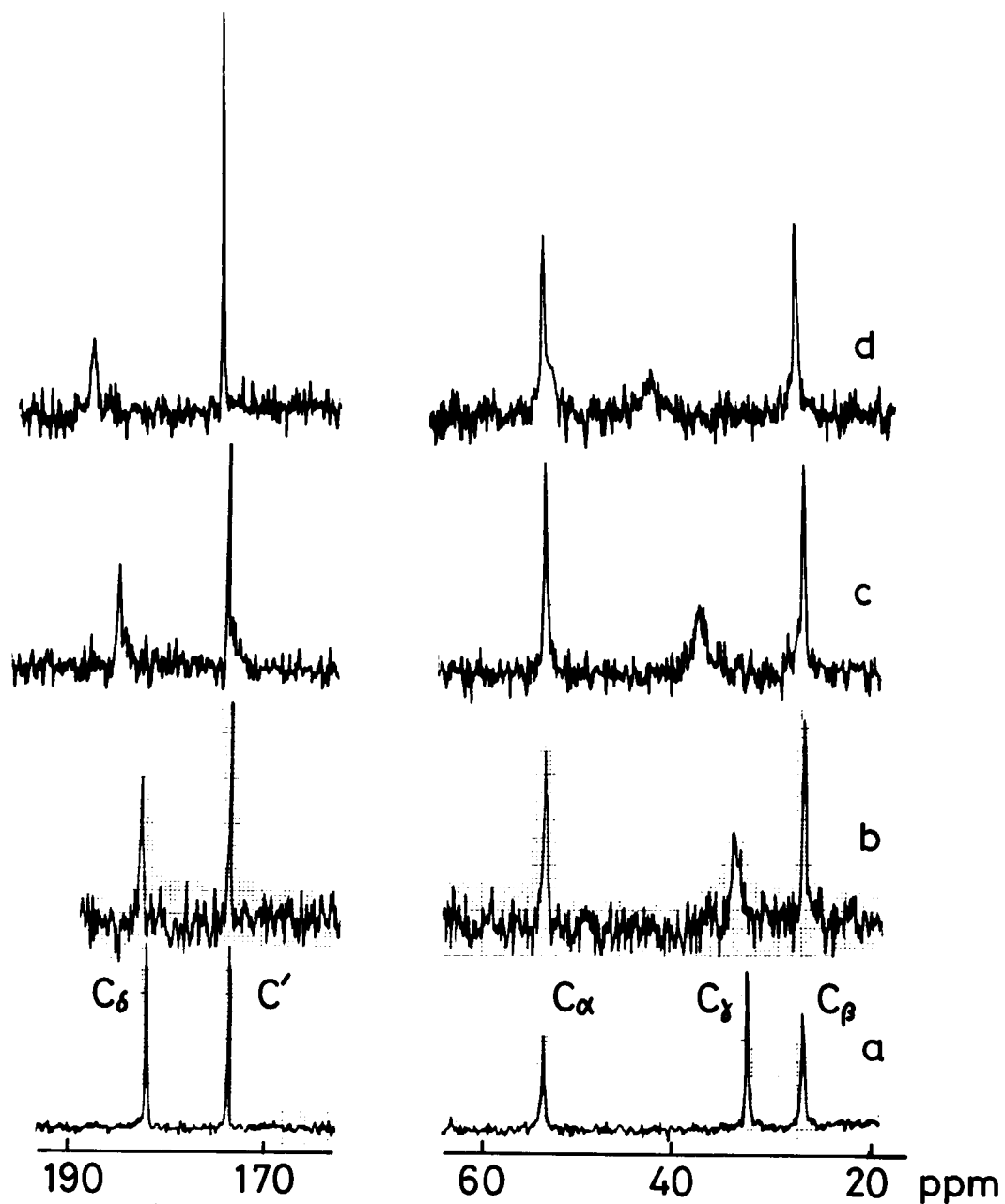


Figure VI-1. Effect of Co(II) on ^{13}C NMR spectra of PGA (0.83 M in monomer unit) at 304 K and at pH 7.1: (a) $f=[\text{Co(II)}]/[\text{PGA}]=0$; (b) $f=3 \times 10^{-3}$; (c) $f=8 \times 10^{-3}$; (d) $f=1.5 \times 10^{-2}$.

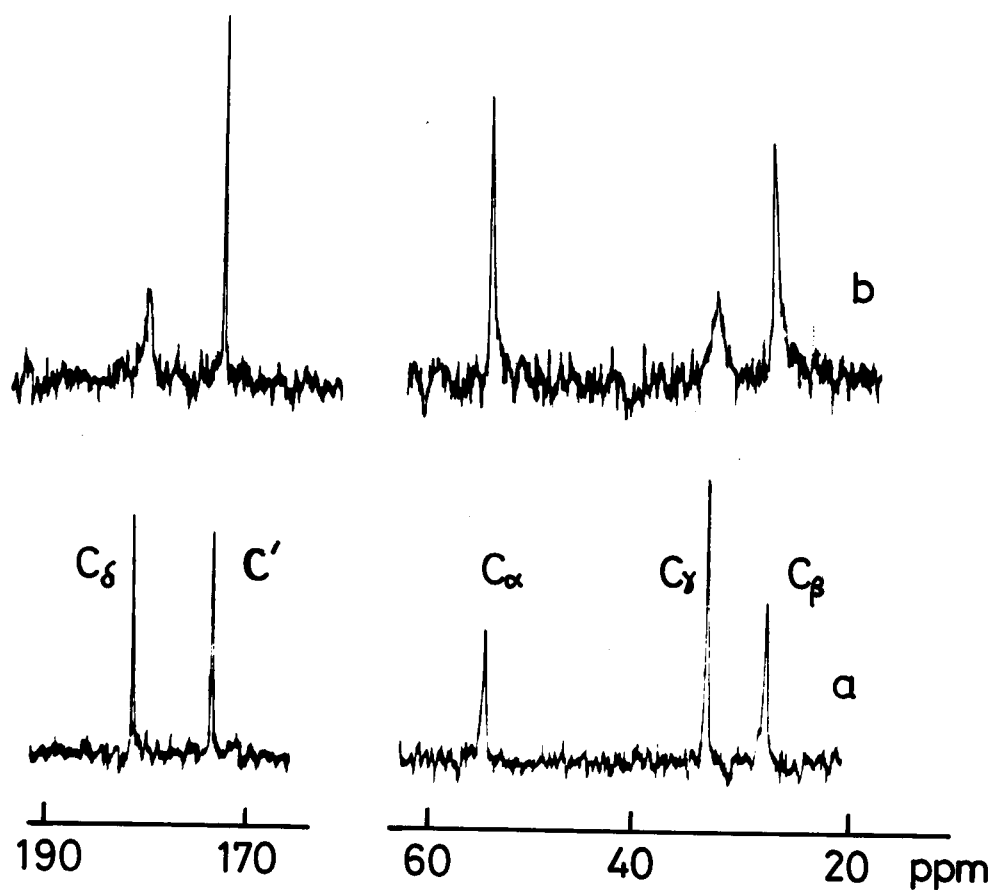


Figure VI-2. Effect of Ni(II) on ^{13}C NMR spectra of PGA (0.83 M in monomer unit) at 304 K and at pH 7.1: (a) PGA only; (b) $f = [\text{Ni(II)}]/[\text{PGA}] = 8.1 \times 10^{-4}$.

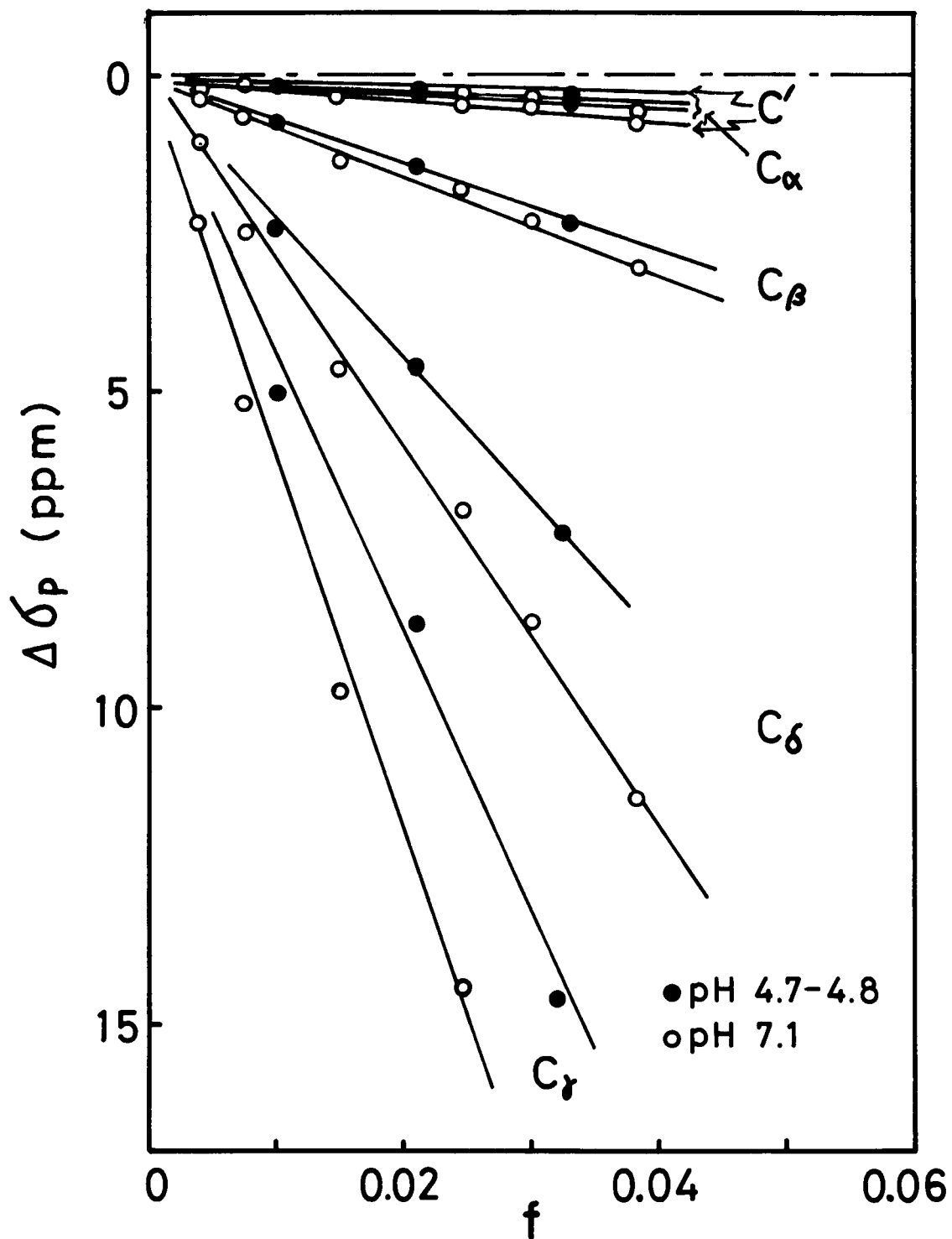


Figure VI-3. Concentration variation of paramagnetic shift $\Delta\sigma_p$ for Co(II)-PGA complex at 304 K. $f = [\text{Co(II)}]/[\text{PGA}]$. The positive value of $\Delta\sigma_p$ means lower field shift.

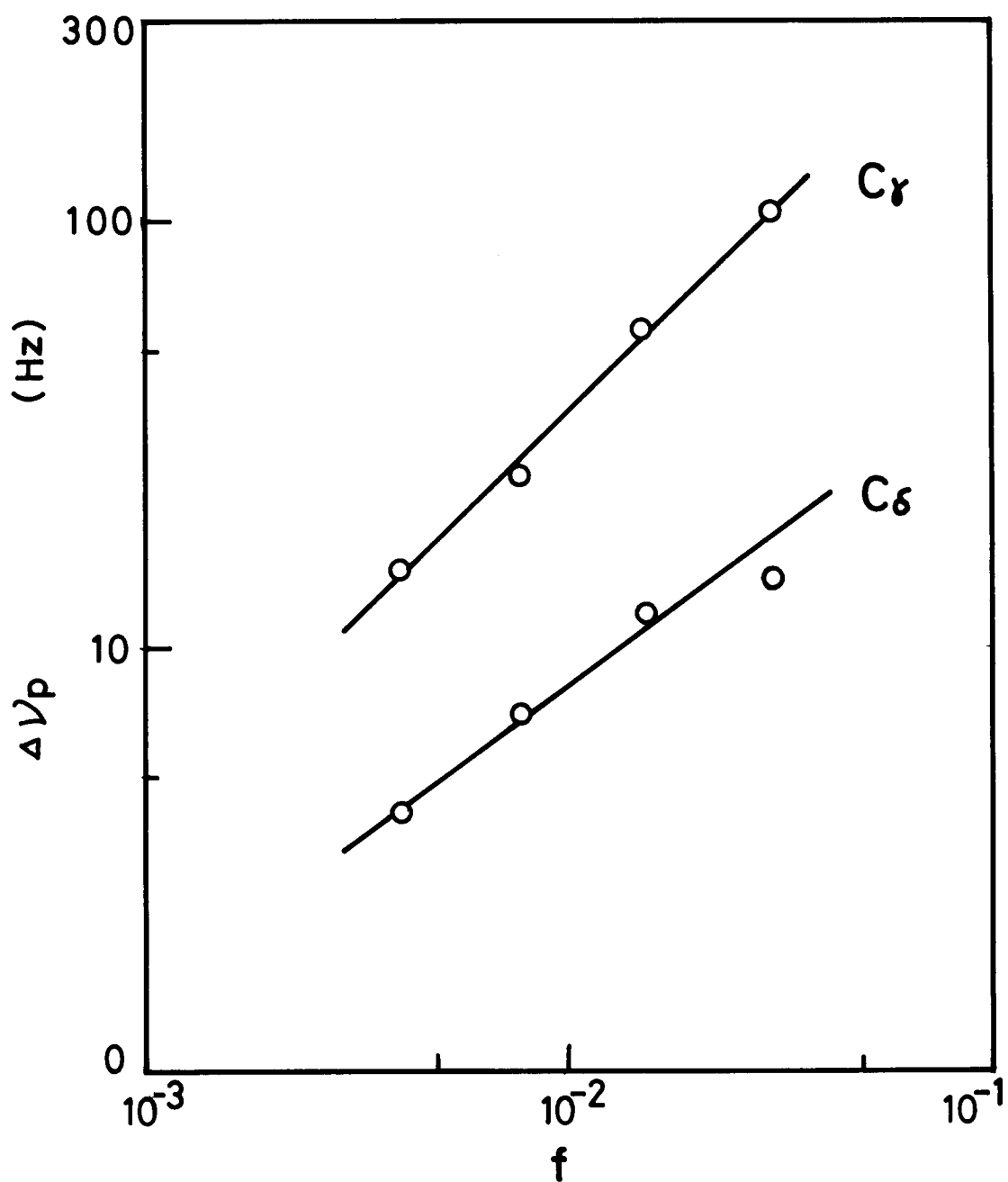


Figure VI-4. Concentration variation of paramagnetic broadening $\Delta\nu_p$ for C_γ and C_δ carbons at 304 K and at pH 7.1.

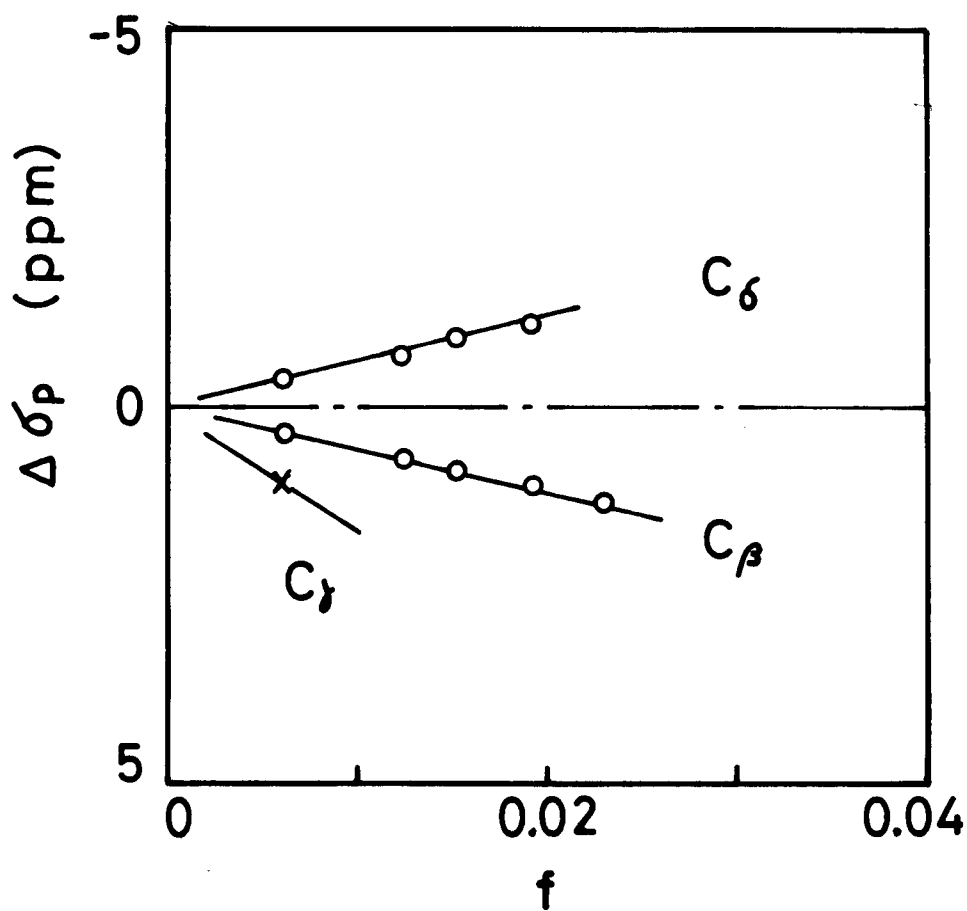


Figure VI-5. Concentration variation of paramagnetic shift $\Delta\sigma_p$ for Ni(II)-PGA complex at pH 7.1 and at 304 K. $f=[\text{Ni(II)}]/[\text{PGA}]$. The positive value of $\Delta\sigma_p$ means lower field shift and the negative value upper field shift.

show the evidence that the metal ion binds to the amide nitrogen atom of the backbone.

As paramagnetic shifts vary with f and two separate resonances from the complexed and uncomplexed states are not able to simultaneously observed, the chemical exchange between the two sites occurs and the exchange rate is so fast as compared with an NMR time scale.

Figure VI-6 and VI-7 show the temperature dependences of the observed paramagnetic shift for Co(II) and Ni(II), respectively. Figures show that the observed shifts for both complexes increase with increasing temperature. These results are in good agreement with those of ^1H NMR.³ As only a single peak is observed for all the resonances and $1/T_{2p}$ values decrease with increasing temperature, one may obtain that $\Delta\omega_M \tau_M < 1$ and $T_{2M} > \tau_M$. These conditions reduce eq 2.11 to its simplest form

$$\Delta\omega = fq\Delta\omega_M . \quad (4.1)$$

The temperature dependence of observed shift $\Delta\omega$ therefore arises from that of $\Delta\omega_M$.

As shown in Chapter II, the paramagnetic shift consists of the contact and pseudo-contact shifts. Both shifts are proportional to the reciprocal of temperature (Curie's law). Results obtained here are in contrast to the temperature dependence of Curie's law. This fact suggests that the chemical equilibrium between the complexed and uncomplexed states shifts to direction of formation of the complex with increasing temperature.⁴ The paramagnetic shifts observed for the Ni(II)-PGA system may be contact shift, for pseudo-contact interaction should be negligible for octahedral Ni(II) complexes which have the orbitally nondegenerate ground state.⁵⁻⁷ The downfield shifts of C_γ and C_δ carbons suggest that unpaired electron spin is delocalized on the ligand via σ -orbitals of PGA residue, since spin polarization effects are expected to attenuate rapidly with increasing distance from the metal ion.⁸ The upfield shift of C_δ carbon suggests that the position of C_δ acquires a net negative electron spin density via a spin polarization mechanism⁹ which overwhelms the effect of the direct delocalization of positive electron spin from Ni(II).¹⁰

For the octahedral Co(II) complex, in general, observed paramagnetic shift is mainly due to the pseudo-contact interaction rather than the

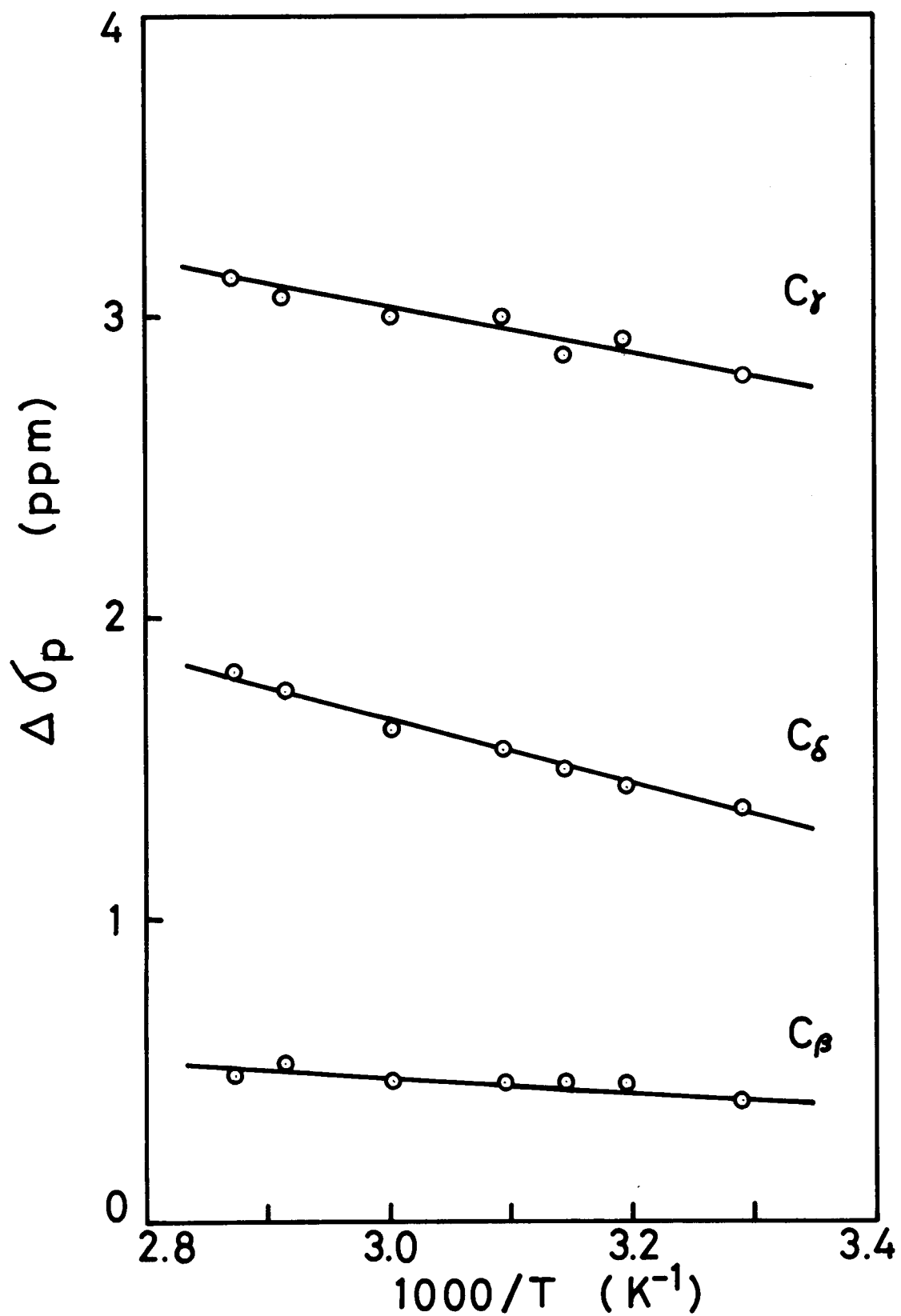


Figure VI-6. Temperature variation of paramagnetic shift for Co(II)-PGA complex at pH 7.1. $f=5.2 \times 10^{-3}$.

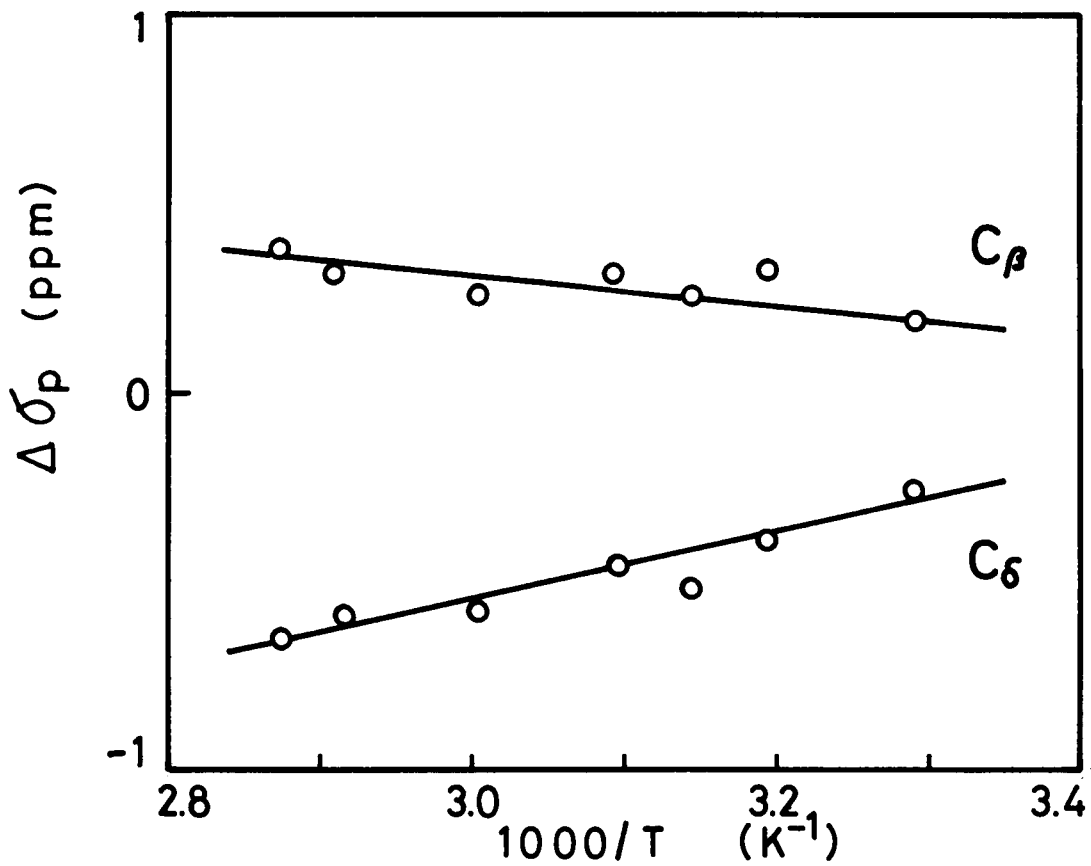


Figure VI-7. Temperature variation of paramagnetic shift for Ni(II)-PGA complex at pH 7.1. $f=8.1 \times 10^{-4}$.

contact interaction. In some cases it is possible to separate these two contributions from observed shift.¹¹ Since the geometric factor $(3\cos^2\theta-1)/r^3$ and the anisotropy of g factor cannot be evaluated for the Co(II)-PGA system, it is not possible to separate the two. It is, however, of interest to note that observed shift is larger for C_γ than for C_δ . This fact may imply that more positive spin density is localized in C_γ carbon rather than in C_δ carbon.

REFERENCES

1. T. J. Swift and R. E. Connick, *J. Chem. Phys.*, 37, 307(1962).
2. G. N. La Mar, W. D. Horrocks, Jr., and R. H. Holm, Eds., "NMR of Paramagnetic Molecules", Academic Press, New York, N.Y., 1973.
3. C. C. McDonald and W. D. Phillips, *Biochem. Biophys. Res. Comm.*, 35, 43(1969).
4. O. Iwaki, K. Hikichi, M. Kaneko, S. Shimizu, and T. Maruyama, *Polymer J.*, 4, 623(1973).
5. H. M. McConnell and R. E. Robertson, *J. Chem. Phys.*, 29, 1361(1958).
6. J. P. Jesson, *J. Chem. Phys.*, 47, 1482(1967).
7. Z. Luz and S. Meiboom, *J. Chem. Phys.*, 40, 1058(1964); 40, 1066(1964).
8. J. A. Happe and R. L. Ward., *J. Chem. Phys.*, 39, 1211(1963).
9. D. Lazdius and M. Karplus, *J. Chem. Phys.*, 44, 1600(1966).
10. C. E. Strouse and N. A. Matwiyoff, *Chem. Commun.*, 439(1970).
11. W. D. Horrocks, Jr., reference 2, chapter 4.

CHAPTER VII

Conclusion

The pH and temperature dependences of chemical shift, T_1 , T_2 , and NOE were measured for poly(D-glutamic acid)(PGA) complexes with paramagnetic metal ions such as Cu(II), Mn(II), Co(II), and Ni(II) in aqueous solution.

As described in Chapter III, the ^{13}C chemical shift, relaxation times, and NOE demonstrated a reasonable detailed picture of the conformation and motion of PGA in the absence of a paramagnetic ion. C_α and C' resonances shift upfield in conjunction with the helix-to-coil transition, while C_β , C_γ , and C_δ resonances move downfield with the ionization of the carboxyl group. T_1 and NOE of protonated carbons increase in company with the helix-to-coil transition. This is interpreted in terms of a decrease in correlation time of tumbling motion caused by the onset of fast segmental motion. As going away from the backbone, correlation times of the side chain carbons progressively decrease, showing the presence of fast internal reorientation.

It was found in Chapter IV that ^{13}C and water proton relaxation times provided information about the structure and dynamics of the Cu(II)-PGA complex. In the pH region of 4.9 to 8 relaxation times of C_γ and C_δ are reduced upon the addition of Cu(II), while those of C_α , C_β , and C' are not influenced. Paramagnetic relaxation rates of C_γ and C_δ decrease with increasing temperature, indicating the fast exchange. The scalar relaxation is dominant to line broadening, suggesting that a significant amount of electron spin density is transferred from Cu(II) to C_γ . Above pH 9 paramagnetic effect for ^{13}C nuclei was not observed. The water proton relaxation rate is markedly enhanced by the addition of Cu(II) at acid pH, but diminished at alkaline pH. These results indicate that carboxyl groups and water molecules are bound to Cu(II) at $\text{pH} \leq 8$, while these two are excluded from Cu(II) at $\text{pH} \geq 9$.

In Chapter V, the structure and dynamics of the Mn(II)-PGA complex were described on the basis of ^{13}C and water proton relaxation times, EPR, and CD measurements. In the neutral pH region the carboxyl groups and water molecules are bound to Mn(II), but the chemical exchange

between complexed and uncomplexed states is fast. An electron spin was found to spread over to C_{β} from Mn(II). Parameters for ligand water molecules of the complex were compared with those for the aquo Mn(II). With decreasing pH Mn(II) is released from the carboxyl groups, and PGA changes its conformation from coil to helix. Water-proton relaxation enhancement reflects the conformational change of PGA in the case of Mn(II), while it does not in the case of Cu(II).

It was demonstrated in Chapter VI that ^{13}C paramagnetic shifts provided qualitative information of the structure of the Co(II)- and Ni(II)-PGA complexes. The addition of the metal ions caused remarkable paramagnetic shift and broadening of C_{γ} and C_{δ} , leading to a conclusion that the carboxyl groups participate to form the complex at neutral and acid pH's. Paramagnetic shifts of both complexes show the temperature dependence opposite to Curie's law, suggesting that chemical equilibrium shifts to the direction of formation of the complex.

The present study demonstrates the feasibility of using NMR of ^{13}C and water proton nuclei in the paramagnetic complexes of macromolecules to achieve information on the structure and dynamics in solution.